Estimating productivity in habitat-forming seaweeds

Jo Randall
BSc (Hons)

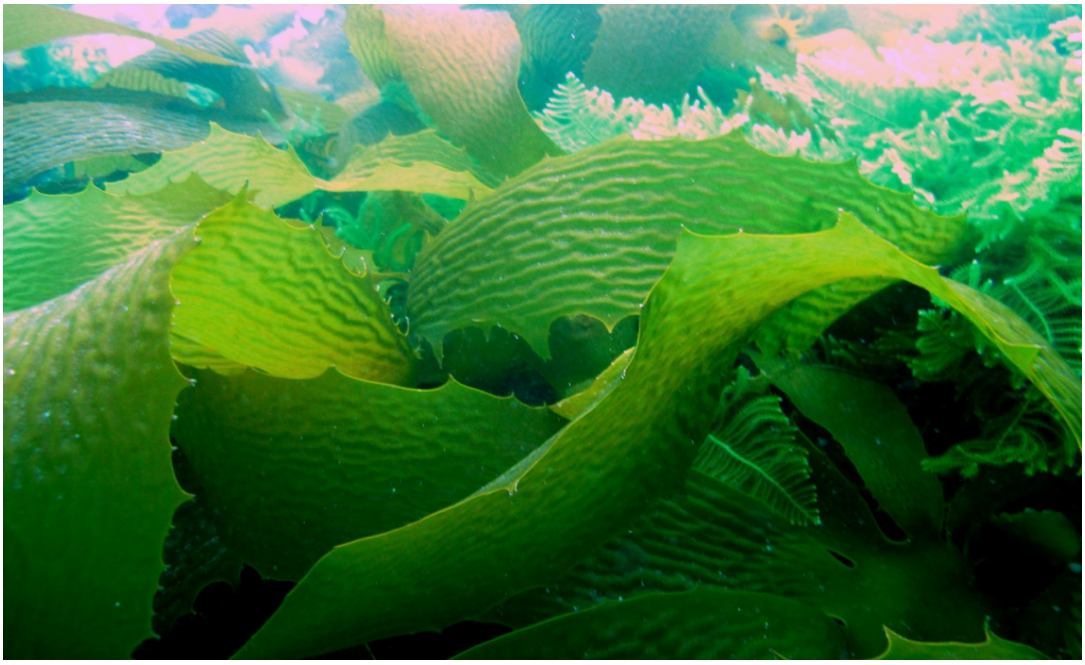

Submitted in fulfilment of the requirements for the
Degree of Doctor of Philosophy in Life Sciences
and
Doctorat en Sciences de l'Ingénieur et Technologie

LISAcoustics
Environmental Hydroacoustics Lab

Institute for Marine and Antarctic Studies (IMAS), **University of Tasmania**
Environmental Hydroacoustics Laboratory (EHL), **University of Brussels**

April 2018

This page intentionally left blank

Declarations

Statement of originality

This thesis contains no material that has been accepted for a degree or diploma by the Universities or any other institution. The work contained in this thesis, except where otherwise acknowledged, is the result of my own research.

Signed: Jo Randall

Date: 20/05/2018

Statement of authority of access

This thesis may be available for loan and limited copying in accordance with the Copyright Act 1968.

Signed: Jo Randall

Date: 20/05/2018

Abstract

Macroalgal beds provide the ecological foundations for most shallow reef ecosystems in temperate environments. With distinctive canopies primarily of brown laminarian algae (northern hemisphere), or laminarian or fucalean algae (southern hemisphere), in many areas these habitats are at risk from human activity. Overexploitation, pollution, and other effects of coastal activities have resulted in significant habitat loss in coastal ecosystems, and human-induced climate change is now seen as a major threat to ecosystem health in marine systems. Understanding the impact of climate change is particularly important for habitat-forming ecosystem engineers like kelps, as these species form the basis of hierarchically organised communities and play a fundamental role in determining community structure and ecological processes.

South eastern Australia has experienced increases in marine temperatures at nearly four times the global average, and there is now evidence that, in some locations, macroalgae communities are retreating in a manner consistent with ocean warming. Successful management of marine systems requires understanding ecosystem processes, particularly the patterns and magnitude of production. Macroalgal communities often show relatively low resistance to disturbance, yet rapid recovery once disturbances are removed, hence they are generally highly dynamic in response to environmental perturbations. As a result, macroalgae are likely to play an increasingly important role in buffering the short term/dynamic effects of climate change on temperate reef communities.

Knowledge of the productivity of seaweed-dominated temperate reef systems is largely a synthesis from studies conducted over small spatial scales utilising a variety of methods that generally measure different characteristics of both individual seaweeds and collectively. As a result of the diversity of measurement methods, estimates of gross primary productivity (GPP), production potential, and macroalgal biomass for temperate reefs are numerous and variable. This can lead to challenges for ecologists attempting to amalgamate research findings to facilitate long-term, broad-scale perspectives or compare short-term research between spatially separated communities. However, to date there has been relatively little research to compare measurement approaches and quantify differences in productivity estimates across the different techniques.

The present research provides a unique investigation into some of the techniques and methodology involved in measuring primary productivity in marine systems, particularly kelp forests, using the macroalgae *Ecklonia radiata, Phyllospora comosa* and *Macrocystis pyrifera* as study species. The work is based on both field and laboratory exploration of productivity measurements and associated parameters. *In situ* measurements of primary productivity (diel oxygen modelling, benthic oxygen

exchange chambers) or PSII electron transport (PAM fluorometry) are compared, and the possibility of using acoustics as a means of quantifying oxygen production at large scales is explored, as has already been applied in seagrass beds. This thesis also provides an in depth investigation of the effect of variability in sampling methodology with regards to interpretation of PAM fluorometry-derived parameters.

Chapter 2 investigates the acoustic properties of *Ecklonia radiata*. The density, sound speed and resulting adabiatic compressibility of *E. radiata* tissue were investigated in the laboratory. Four methods were developed and trialled to determine the intrinsic sound speed of *Ecklonia radiata* tissue based on measurement of the time of flight of an ultrasonic pulse, while compressibility was calculated from density measurements. The results show that *Ecklonia radiata* sound speed and density are higher, and compressibility lower, than that of seawater. Properties varied according to size and tissue type and the variation likely reflected differences in cell type, packing and structure as well as the concentrations of alginates and other carbohydrates. These are important considerations for acoustic propagation and the results provide valuable inputs for future acoustic work.

Chapter 3 focuses on the acoustic modelling of different scenarios of primary production in a shallow water rocky reef environment of Fortescue Bay (Canoe Bay), Tasmania, where *E. radiata* dominates the canopy. In February 2012, the environment was continuously probed by acoustic signal transmission and monitored by a comprehensive set of oceanographic sensors with the aim to assess the potential for acoustics to quantify excess oxygen production in bubble form. Ray-theory acoustic modelling results indicate that ecologically-significant void fractions of oxygen in the canopy layer from production would be clearly seen in diel variation of propagation features such as the energy decay rate of the medium impulse response. The model can then be used to invert empirical data for retrieving void fraction. However, comparative analysis of part of FORTES 12 data and model suggests that no large excess of bubbles was produced by photosynthesis under the present environmental conditions, in contrast to earlier observations made in seagrasses. As a result, the use of acoustics as a means of measuring primary productivity in kelp could not be further explored during the course of this research.

Chapter 4 provides a unique comparison of the estimates of photosynthetic O_2 production rates in an *Ecklonia radiata* dominated community using three different measurement methods: diel oxygen GPP models, benthic oxygen exchange chambers, and electron transport rate from PAM fluorometry which is usually interpreted as a measure of production potential. All three methods were run concurrently *in situ* in Fortescue Bay, Tasmania. The first diel oxygen model was fitted to *in situ* measures of dissolved oxygen (DO) in the environment and demonstrated a good fit, however, a consequence of this approach is that large variation in oxygen production was predicted at low PAR levels. A second model was created which utilised an explicit relationship between DO production and PAR, but it

didn't represent DO at the surface as well as the first model. Importantly, the two models indicate similar daily production rates of the seaweed bed (all species combined) that are ~ 2 times that predicted for the kelp alone based on incubations in the benthic chambers and scaling for the average size of adult kelp sporophytes and their population density. Oxygen evolution from incubation of sporophytes in benthic chambers and PAM fluorometry derived electron transport rates showed similar patterns, but the results indicate that the latter method may overestimate potential photosynthesis. The results suggest that diel oxygen modelling, benthic oxygen exchange chambers and PAM fluorescence can all provide good indications of productivity in shallow water marine environments. However, care must be taken in interpretation of results as each method differs in the type of productivity estimates it provides. As a direct measure of total seaweed production per unit area of reef, estimates from models based on empirical measures of environmental DO have much to recommend them.

Chapter 5 details a final analysis investigating the effects of diurnal, seasonal and latitudinal variability in ambient light on PAM-derived parameters, as well as possible effects associated with depth, within- and between-alga variation in PSII performance, and latitudinal effects unrelated to the light climate. This research was based on field measurements undertaken in Tasmania, Western Australia and New South Wales, Australia in both summer and winter during 2012 and 2013, focussing on *Ecklonia radiata, Macrocystis pyrifera* and *Phyllospora comosa*. Photosynthetic characteristics of all species were highly dependent on the time of day, depth, latitude/region, season, and part of the thallus from which measurements were taken. Patterns dependent on time-of-day, depth and thalli placement varied with season and/or geographic region, and the nature of these patterns varied between species. It is clear from this work that efforts to standardise approaches to taking measurements of seaweeds using PAM fluorometry will be essential if measurements are to be compared meaningfully across studies.

The key findings of this thesis are: (1) a first determination of the acoustic properties of *E. radiata* tissue which enable the development of scattering models to interpret scientific echosounder data collected in kelp beds; (2) a Gaussian beam/finite element beam code (Bellhop) with detailed environmental input and a huge number of beams can predict the acoustic character of a shallow water rocky reef and bubble layers with low-frequency effective sound speed; (3) the model allows prediction of the acoustic energy decay rates due to various scenarios of ecologically-relevant photosynthetic O2 production rates; (4) day vs night acoustic measurement and model data comparisons challenge void fraction predictions made from well-established measurements and methods; (5) diel oxygen modelling, benthic oxygen exchange chambers and PAM fluorescence can all provide good indications of productivity, however, understanding the limitations of each method is essential when interpreting the results as the measurements they provide are not directly comparable;

and (6) applying a consistent sampling methodology is a key consideration when planning research utilising PAM fluorometry as diurnal, seasonal, and latitudinal variability, as well as effects associated with depth and within- and between-alga variation in PSII performance will have significant impact on PAM-derived parameters. The results of this work give valuable insight into the advantages and disadvantages involved with several main techniques currently utilised to measure production of macroalgal/seagrass beds, and the challenges faced by ecologists attempting to interpret results and compare research between methods and across studies. Last but not least, this study provides important and relevant information on the potential use of acoustics as a future means of determining productivity of benthic habitat on large scales in marine environments. The work presented herein will assist in both development and interpretation of future study of productivity in marine systems.

Contents

List of Tables

List of Figures

Acknowledgements

I am very grateful to have received great support from my research organisations, the Institute for Marine and Antarctic Studies (IMAS), the University of Tasmania (UTAS), the Environmental Hydroacoustics Laboratory (EHL), and Universite libre de Bruxelles (ULB). This research would also not have been possible without the financial assistance from a number of funding bodies including the Australian National Network in Marine Science (ANNiMS), Australian Research Council (ARC), the Office of Naval Research Global - Office of Naval Research (ONR), and Brussels Institute for Research and Innovation (INNOVIRIS).

This thesis would not have been possible without the assistance and encouragement of a large number of people. I am sincerely grateful to all who have helped me along the way, but the following deserve special thanks:

I thank my chief UTAS supervisor Craig Johnson for providing me with the opportunity, funding and support to undertake the significant amount of fieldwork and travel required to achieve the objectives of this thesis. Furthermore, I acknowledge his vision, efforts and persistence in maintaining momentum and guidance in an often-challenging multidisciplinary project.

My chief ULB supervisor Jean-Pierre Hermand has provided endless support in navigating an international research project between two research institutions. The valuable input, time and expertise have been important. I am also thankful for the remarkable research opportunities afforded me throughout this experience, and his love of sharing fine gastronomy.

To my co- supervisor Jeff Ross, thank you for the technical and field support and providing "hands on" assistance in times of need. I am particularly grateful for your words of wisdom and clarity in times of difficulty, and for the more than one occasion where you have rescued me in a fieldwork "emergency". I also thank Simon Wotherspoon for his assistance in creating underwater environmental models.

The tremendous field effort demanded by this thesis would not have been possible without the assistance of many divers, surface attendants and boating crew who frequently withstood challenging conditions, long hours and demanding requests. In particular, I thank Robert Perry and Pearse Buchanan who braved many late nights and cold early mornings with no complaint. Acknowledgement also goes to Adam Stephens and Simon Talbot (IMAS) for field support. Thanks to my fellow PhD monkey Emma Flukes for fieldwork assistance, emotional support, and answers to my sometimes stupid and often repetitive questions.

I would also like to acknowledge the incredibly important role of my family in allowing me to undertake postgraduate study. To my parents, Wendy and Tim: thank you for amazing practical and emotional support, as well as the never-ending offers of home-cooked meals. There are too many things to list. Mostly, thank you for the constant belief that all the hard work, sacrifices and sleepless nights would eventually result in the submission of this thesis. Thanks Martha and Evan for the love and offers of refuge. I give thanks also to my very patient, tolerant and supportive friends, who have clung to the hope that they would eventually get their friend back.

Finally, special thanks to Chris for his understanding, and to Pingu for a newborn's patience.

Statement of co-author contributions

Chapters 2-6 of this thesis have been prepared as scientific manuscripts for submission to peer reviewed journals. In all cases the design and implementation of the research, data analysis, interpretation of results and manuscript preparation was the responsibility of the candidate but was carried out in consultation with supervisors and other specialist contributors. These contributors are outlined for each chapter below.

Chapter 2: Prof. Jean-Pierre Hermand (primary supervisor ULB) contributed conceptual and practical knowledge in addition to practical assistance with experimental work. Prof. Craig Johnson (primary supervisor UTAS) and Dr. Jeff Ross (co-supervisor) provided practical assistance and the manuscript was improved by feedback from both. Marie-Elise Ernould assisted with practical knowledge of techniques and review of ultrasound interpretation.

> *Manuscript published as: Randall, J., Hermand, J-P., Ernould, M-E., Ross, J. and Johnson, C.(2014). Measurement of acoustic material properties of macroalgae (Ecklonia radiata), Journal of Experimental Marine Biology and Ecology, 461, 430-440.*

Chapter 3: Prof. Jean-Pierre Hermand provided conceptual and practical knowledge of acoustic propagation modelling and underwater acoustic theory, as well as development of the modelling and processing of the empirical acoustic data. Prof. Craig Johnson and Dr. Jeff Ross contributed practical knowledge of temperate reef environments and productivity, in addition to manuscript improvements.

Chapter 4: Prof. Craig Johnson and Dr. Jeff Ross contributed to the conceptual and practical knowledge of seaweed environments and primary productivity in these systems as well as assistance with fieldwork, data analysis and interpretation. Dr Simon Wotherspoon assisted with the creation of the dissolved oxygen models. Prof. Jean-Pierre Hermand contributed to the conceptual theory and interpretation.

Chapter 5: Prof. Craig Johnson contributed conceptual and practical knowledge on temperate reef productivity and experimental design, analysis and interpretation. Dr Emma Flukes assisted with practical and theoretical knowledge of PAM fluorometry techniques and interpretation of data. Associate Prof. Thomas Wernberg and Dr. Thibaut de Bettignies provided practical knowledge and advice with respect to *Ecklonia radiata,* including assistance with data interpretation and manuscript revision.

> *Manuscript submitted for review as: Randall, J., Flukes, E., Wernberg, T., de Bettignies, T. and Johnson CR. Space-time variability in in situ PAM fluorometry measures in three key habitat-forming macroalgae.*

Chapter 6: Prof. Craig Johnson provided conceptual and practical knowledge on kelp productivity dynamics, measurement and management needs.

Jo Randall, IMAS, University of Tasmania	Candidate
Prof. Jean-Pierre Hermand, EHL, University of Brussels	Author 1
Marie-Elise Ernould, Laborelec Research Center, Belgium	Author 2
Dr. Jeff Ross, IMAS, University of Tasmania	Author 3
Prof. Craig Johnson, IMAS, University of Tasmania	Author 4
Dr Simon Wotherspoon, IMAS, University of Tasmania	Author 5
Dr. Emma Flukes, IMAS, University of Tasmania	Author 6
Ass. Prof. Thomas Wernberg, UWA Oceans Institute, University of Western Australia	Author 7
Dr Thibaut de Bettignies, UWA Oceans Institute, University of Western Australia	Author 8

We the undersigned agree with the above stated "proportion of work undertaken" for each of the above published (or submitted) peer-reviewed manuscripts contributing to this thesis:

Signed:

Candidate (*Jo Randall*)	18/05/2018
Author 1 (*Prof. Jean-Pierre Hermand)*	18/05/2018
Author 2 *(Marie-Elise Ernould)*	06/10/2016
Author 3 *(Dr. Jeff Ross)*	20/10/2016
Author 4 *(Prof. Craig Johnson)*	18/05/2018
Author 5 *(Dr. Simon Wotherspoon)*	12/10/2016
Author 6 *(Dr. Emma Flukes)*	02/10/2016
Author 7 *(Ass. Prof. Thomas Wernberg)*	12/10/2016
Author 8 *(Dr. Thibaut de Bettignies)*	16/10/2016

Chapter 1 General Introduction

Kelp beds and primary production

The temperate coastline of Australia covers more than 8000 km including extensive areas of rocky reef dominated by canopy-forming macroalgal species (*Ecklonia radiata*, *Phyllospora comosa* and *Macrocystis pyrifera*) (Bennett et al., 2016; Marzinelli et al., 2015; Wernberg et al., 2011). With distinctive canopies, primarily of laminarian algae (northern hemisphere) or laminarian and fucalean algae (southern hemisphere), kelps are the foundation species of shallow temperate reef systems (Steneck, Johnson, 2013) and are among the most productive ecosystems on earth (Mann, 1973a). These species function as habitat-forming ecosystem engineers (Jones et al., 1996) and play a dominant role in ecological processes and the determination of community structure.

Human activity has resulted in significant habitat loss in coastal ecosystems (Jackson, Sala, 2001), and anthropogenic climate change is now seen as a major threat to marine ecosystem health (Richardson, Poloczanska, 2008; Wernberg et al., 2011). Climate change is predicted to increase the importance of ecosystem engineers in maintaining healthy ecosystems because of their capacity to mitigate some environmental stressors (Bruno et al., 2003; Russell, Connell, 2005; Russell et al., 2009; Wernberg et al., 2011). As a result, macroalgae are likely to play an increasingly important role in buffering the effects of climate change on temperate reef communities.

South eastern Australia has experienced increases in marine temperatures at nearly four times the global average (Johnson et al., 2011; Ridgway, 2007), and there is now evidence that, in some locations, macroalgae communities are retreating in a manner consistent with long term ocean warming (Johnson et al., 2011; Wernberg et al., 2011; Wernberg et al., 2016). Macroalgal communities often show low resistance to disturbance, but often recover rapidly once disturbances are removed, and thus tend to be very dynamic in response to environmental perturbations (Dayton, 1985; Kennelly, 1987; Tegner, Dayton, 1987) which provides for consistency in ecological functioning.

Primary production of marine macroalgae is arguably one of the most important elements of ecological function to consider on temperate reefs. Management requires a clear understanding of patterns of spatial and temporal variation in photosynthetic parameters (Urban et al., 2017). However, knowledge of the productivity of these systems is largely an amalgamation from studies conducted over small spatial scales and using a variety of methods that generally measure different characteristics both individually and collectively (IMOS, 2017). As a result of the diversity of

measurement methods, estimates of primary productivity for temperate reefs are numerous and inconsistent (Schreiber, 2004a). This can lead to challenges for ecologists attempting to synthesise research findings to produce long-term, broad-scale perspectives or compare short-term research between spatially separated communities. Additionally, there is a paucity of research comparing measurement techniques and quantifying differences in productivity estimates across different methods.

Measuring primary production or production potential

Traditionally, the most broadly used method of measuring primary productivity in aquatic ecosystems used diel changes in "free water" oxygen to calculate rates of production and respiration (Cole et al., 1998; Gelda, Effler, 2002; Lauster et al., 2006; Suggett et al., 2003). Although first applied in coral reef systems (Sargent, Austin, 1949) the diel oxygen method (DOM) became widely established after work by the Odum brothers in the 1950s broadened the application from coral reef metabolism to river and lake systems (Odum, 1956; 1957; Odum, Odum, 1955). The technique has now been extensively used in a range of aquatic ecosystems (e.g.,Cole et al., 1998; Gattuso et al., 1993; Hanson et al., 2003; Kemp, Boynton, 1980; Smith, Key, 1975; Staehr et al., 2010; Van de Bogert et al., 2007).

DOM models estimate gross primary productivity (GPP) from changes in dissolved oxygen measurements over time, factoring in ecosystem respiration (estimated from night time decline in dissolved oxygen), exchange of O_2 from the atmosphere (generally modelled as a function of the concentration gradient between water and atmosphere with a wind-derived coefficient), and vertical and horizontal advection (Staehr et al., 2010). Technological development of sensors has made it easy to continuously and precisely measure DO concentrations and relevant physical and chemical parameters, allowing for detailed description of temporal variability and calculation of metabolism. However, although there are clear advantages to the method (not least its simplicity), questions remain about the extent to which free-water measurements actually represent whole-system metabolism (Coloso et al., 2008; Lauster et al., 2006; Van de Bogert et al., 2007). In particular, consideration must be given to assumptions associated with advection, quantification of the air-water exchange, and respiration (Staehr et al., 2010).

The use of benthic chambers is another method used widely to measure photosynthetic rates in macroalgae. The method involves enclosing (usually) entire individuals in chambers and measuring changes in dissolved oxygen (O_2) or carbon dioxide (CO_2). The design of data-logging oxygen exchange devices enables *in situ* measurements of the initial slope (α) of the irradiance-dependent O_2 evolution curve, the rate of maximum photosynthesis, irradiance where α intercepts the maximum rate of photosynthesis under light saturation (P_{max}), and respiration rates in the dark (Chalker et al., 1985; Cheshire et al., 1995; Cheshire et al., 1996b). Since respiration can also be measured, the technique allows determination of both net and gross primary productivity over periods of 24 hours. Using this

oxygen evolution apparatus, primary productivity and photosynthesis has been measured in macroalgae (Cheshire et al., 1997; Longstaff et al., 2002), seagrass (Ralph, Burchett, 1995), invertebrate symbioses (Cheshire et al., 1997; Hoegh-Guldberg, Jones, 1999), and turf algal assemblages (Klumpp, McKinnon, 1989; Westphalen, Cheshire, 1997). This technique allows controlled measurement of the primary productivity of an individual or assemblage (e.g. in the case of filamentous turfing species) of interest, however, the need to enclose the algae inside a chamber substantially limits scale. Some species (e.g. turf algae) cannot be individually separated due to their small size and other large species (such as *Macrocystis pyrifera*) can only be sampled in tissue segments.

Other open system techniques exist, most notably the 'Eddy Covariance' method (Berg et al., 2003). This approach relies on measuring vertical water column velocity and O_2 concentration in a ~ 1 cm^3 volume located 5 to 30 cm above the benthos. The underlying assumption is that all O_2 transported vertically toward or away from the benthos is facilitated by turbulent motion, hence the vertical flux can be derived from these two variables (Berg, Huettel, 2008). However, a number of challenges remain, including deployment considerations as well as requirements on sensor response time (McGinnis et al., 2011). Most notably, technology constraints and microelectrode breakages mean that deployments are relatively short, thereby limiting the scalability of productivity estimates (Glud et al., 2010). This technique has thus far been successful in measuring O_2 flux over relatively simple habitats in less dynamic habitats, such as sheltered soft sediment and seagrass habitats.(Berg, Huettel, 2008; Glud et al., 2010; Long et al., 2015). Moreover, flux estimates using this approach have been limited to small space and time scales. Thus, at this point in time the dynamical physical environment in which most macroalgal systems occur, and the desire to estimate production over meaningful ecological space (metres to 100s m) and time (days) scales precludes the application of this approach for this purpose.

A relatively recent but now widely used non-invasive method to monitor the functional state of photosynthetic organisms in real-time is Pulse Amplitude Modulation (PAM) fluorometry, which measures chlorophyll (Chl) *a* fluorescence associated with photosystem II (Rosenqvist, van Kooten, 2003) as a measure of photosynthetic potential. PAM fluorometry has been used to assess the physiology of macroalgae *in situ* under varying environmental conditions (Edwards, Kim, 2010; Franklin, Badger, 2001; Kim, Garbary, 2006; Longstaff et al., 2002). Fluorescence emission recordings can provide estimates of a number of different photosynthetic characteristics which indicate different aspects of an organism's photophysiology (Ralph, Gademann, 2005). Traditional methods of assessing kelp productivity directly measure net rates of photosynthesis such as using benthic chambers to measure oxygen evolution and/or CO_2 uptake (e.g. Hatcher, 1977; Hatcher et al., 1977; Suggett et al., 2003) or using lateral extension (e.g. Hanelt, Nultsch, 1991; Mann, 1972). In contrast, fluorescence measurements assess several properties of the photosynthetic apparatus

(Schreiber, 2004b) and thus, theoretically, provide a deeper understanding of the processes and potential limiting mechanisms. However, *in situ* underwater measurements apply only to a very small area of tissue and not to the whole individual.

PAM fluorometers use three different lights to manipulate the photosynthetic apparatus (specifically the chlorophyll *a* molecule), which in turn emits different quantities of fluorescence (see Ralph, Gademann, 2005). Various photosynthetic parameters can be derived from the subsequent fluorescence recordings. Electron transport rate (ETR) or, when an absorbance factor is not used, relative electron transport rate (rETR), is measured at increasing light intensities to produce rapid light curves (RLCs). Curves fitted to raw rETR data enable derivation of the saturating light intensity (*Ek*), maximum electron transport rate or photosynthetic capacity (rETRmax), and light harvesting efficiency of photosynthesis (see Falkowski, Raven, 1997). Collectively these parameters have been used as a measure of potential photosynthetic performance. Electron transport rate (ETR) in particular, has been found to relate closely to photosynthetic activity as measured by CO_2 uptake or oxygen evolution (Beer et al., 1998). Hence, PAM fluorometry is often interpreted as a comparable method of measuring photosynthetic performance, or at least potential photosynthetic performance, with the benefit of providing virtually instantaneous (90 second) measurements.

PAM fluorometry measurements are strongly influenced by the plants ambient light history (Schreiber, 2004b; Schreiber et al., 1997; White, Critchley, 1999), therefore estimates of photosynthetic performance may vary substantially depending on diurnal cycles and/or the sun's position in the sky at the time when measurements are made. This is due to short term changes in photoprotective mechanisms (such as xanthophyll pigments) and longer term cycles (e.g. changes in other pigment concentrations) as a response to irradiance. Variation in the spectral quality and quantity of irradiance with depth results in additional variation in irradiance which may cause individuals in shallow water to demonstrate different patterns in photosynthetic responses (diurnal or seasonal) than those in deeper water (Edwards, Kim, 2010; Ekelund et al., 2008).This applies both to species where individuals occur over a range of depths, and to species where the thallus or fronds of an individual may span several metres through the water column. In the latter scenario, individual algae are exposed to a range of irradiances at different points across their structure, and measurements of photosynthetic performance may yield different values depending on the position at which they are taken (Nielsen et al., 2006; Silva et al., 1998). In addition, self-shading can also create within-thallus differences in ambient light climate.

The ways in which all of these factors affect photosynthetic performance may vary in both direction and/or magnitude with latitude, as a result of selection or differential up-regulation of genes (i.e. phenotypic plasticity). Physiological performance of macroalgae has been shown to vary latitudinally due to acclimation and adaptation by means of compensatory mechanisms at various biochemical

levels (Davison, Davison, 1987; Flukes et al., 2015b; Raven, Geider, 2003; Wernberg et al., 2010). Indeed, *Ecklonia radiata* and *Phyllospora comosa* in Australia have been shown to vary in their response (growth, pigment content and tissue chemistry) to changes in temperature and nutrient concentrations depending on their latitudinal point of derivation (Flukes et al., 2015b; Suggett et al., 2003). Hence, the effects of depth and/or thallus sampling position on photosynthetic measurements may vary between regions. Additionally, latitudinal variation in the magnitude of diurnal light cycles may lead to regionally dependent seasonal effects of the time of day at which measurements are made.

Consequently, appropriate interpretation of studies using PAM fluorometry to measure (potential) photosynthetic performance must consider patterns of diurnal, seasonal, and latitudinal variability in ambient light. The effects that these factors have on PAM parameters, as well as possible effects associated with depth, within- and between-alga variation in PSII performance, and latitudinal effects unrelated to the light climate, are all potentially important considerations when using this technique and interpreting the results.

Can acoustics be used to measure production in kelp beds?

Another much more recent method showing promise as a potential means of measuring primary productivity in aquatic environments over a range of space and time scales is underwater acoustics. Acoustic imaging is generally used in marine environments to create habitat and bathymetry maps and characterise the benthic biotic layer (Komatsu et al., 2002; Komatsu et al., 2003; Lucieer, 2008). However, exploratory research in seagrass meadows (Hermand, 2003; Hermand et al., 1998) gives promising results for expanding the use of acoustics to measure primary production. In seagrass meadows (*Posidonia oceanica*) patterns in the amount of oxygen in the water column in both dissolved and gaseous form follow pronounced diurnal cycles (Hermand, 2003; Hermand et al., 1998), and variability in acoustic propagation is correlated with this diurnal productivity cycle. This acoustic variation can be mainly attributed to gas bubble production (Hermand, 2003; Hermand et al., 1998). While dissolved oxygen in the environment has no measurable effect on the transmitted acoustic signal, the gas bubbles have a profound effect in decreasing sound speed or on scattering sound (depending on frequency) and can therefore potentially provide information on photosynthetic parameters. Acoustics therefore has the potential to detect oxygen microbubbles that would not be detected by instruments measuring dissolved oxygen.

Measuring benthic production in shallow water marine environments using acoustics involves tracking changes in sound propagation characteristics over time with the ultimate goal of quantifying the volume of oxygen bubbles formed in the macroalgal canopy. However, many factors, including water temperature, salinity, and current fields in the water column, as well as the sea surface conditions and the bottom material properties also affect the propagation of sound. They need to be taken into account in processing the acoustic signal as an inverse problem to derive estimates of

bubble production or the so-called void-fraction in the water column. Acoustic models applied to estimating kelp production must take into account sound interacts with the macroalgal canopy but also with outcropping rocks, the benthic sediment layer and underlying bedrock. Understanding the frequency-dependent acoustic behaviour is essential to match prediction and measurement in solving the acoustic inverse problem.

Although work regarding the use of acoustics to measure productivity in marine systems is in its infancy, the technique holds particular interest given the potential to allow integration of productivity measurements over large scales. In addition, most research concerning productivity in macroalgal and seagrass communities uses measurement of dissolved oxygen to estimate oxygen production. Given the likelihood that substantial proportions of the oxygen produced may, in fact, be in gas form, there is a risk that marine ecologists are substantially underestimating productivity in coastal environments when using traditional techniques. Early research in this area, limited to seagrass communities, has indicated substantial bubble production (Hermand, 2003; Hermand et al., 1998). However, the high productivity of macroalgae (among the highest of any ecosystem (Cebrian, 1999) indicates that oxygen microbubbles formed through photosynthesis may well be present in the water column over temperate reefs, depending on different factors such as temperature-dependent oxygen solubility and water stirring at the boundary layer. Hence, acoustics needs to be evaluated as a potential new tool to assess the functioning of seaweed dominated temperate reefs.

This Thesis

The research presented here attempts to provide a comprehensive analysis of three of the most widely used methods of measuring primary productivity or production potential in macroalgae (and seagrasses), in addition to exploratory research into the use of acoustics as a means to quantify oxygen production by macroalgae at large scales. The work contained in this thesis was based on both field and laboratory experiments using the macroalgae *Ecklonia radiata* (Laminariales)*, Phyllospora comosa* (Fucales)*,* and *Macrocystis pyrifera* (Laminariales) as study species. These canopy-forming macroalgae on shallow temperate reefs in Australia beyond the wave-washed *Durvillaea potatorum* zone (Steneck, Johnson, 2013), and play important functional roles as ecosystem engineers (Jones et al., 1996) and in regulating ecological processes and community structure.

Ecklonia radiata (Laminariales) is the key habitat-forming kelp in southern Australia, with a larger depth (4−75+ m) and latitudinal (27.5−43.5 °S) range than any other canopy-forming macroalga (Steinberg, Kendrick, 1999). *Ecklonia radiata* has a single stipe bearing a flattened blade with distinct lateral fronds, and grows to 0.7−1.3 m in height (Wernberg et al., 2003b). *Phyllospora comosa* (Fucales) is a large brown fucoid alga restricted to southeastern Australia from Robe (South Australia) to Port Macquarie (NSW) where it dominates the shallow high wave-energy zone from 0-5 m (Campbell et al., 2014). This species grows to ~0.5−3 m in length, and has a short stipe bearing

multiple primary branches. *Macrocystis pyrifera* (Laminariales), the largest of the brown algae, historically grows from 5−45 m in depth from the benthos to the surface and forms dense beds in nutrient-rich waters along the inshore subtidal reefs of southeast South Australia, Victoria and Tasmania, although it is now largely restricted to southern Tasmania. Each individual comprises several fronds arising from a holdfast and branching three or four times from near the base, with blades developing at irregular intervals along the frond, and with a single pneumatocyst at the base of each blade.

Firstly, a field experiment was run over two weeks during the Austral summer in February, 2012 in Fortescue Bay, Tasmania. During this period environmental variables were continuously monitored, together with 24 hour recording of an active sound source received at positions within a dense, shallow-water *E. radiata* forest. Benthic oxygen exchange chambers were deployed at the site for 24 hour periods during the experiment to measure oxygen exchange in individual *E. radiata.* Concurrent diurnal PAM fluorometry measurements were taken to obtain estimates of saturating light intensity (*Ek*), maximum electron transport rate or photosynthetic capacity (rETRmax), and light harvesting efficiency of photosynthesis. In addition, diel changes in "free water" dissolved oxygen were recorded to allow synthesis of GPP models aimed at calculating rates of primary production and respiration for the macroalgal bed as a whole.

Secondly, as essential input parameters to numerical models that will enhance habitat mapping by means of scientific echosounders and enable the development of inverse methods to extract ecologically-relevant information from acoustic signals propagated in kelp beds, the acoustic properties of *E. radiata* tissue were investigated in the laboratory. As is the case for most marine organisms, there is a paucity of information available on the acoustic properties of macroalgae and those of *Ecklonia radiata* were unknown when the present work was undertaken. The most important inputs to acoustic models are density and compression wave speed, or the ratios of these parameters to those of the surrounding seawater, in addition to compressibility. These properties were measured in the laboratory using a variety of methods, mostly based on ultrasound.

A ray-based model (Bellhop) was developed for the acoustic measurement setup at Fortescue Bay using detailed environmental information for two periods coinciding with the experiment, chosen to compare contrasting diurnal productivity periods. This was analysed together with experimentally observed propagation features measured for these periods with the aim to assess the potential for acoustics to quantify oxygen production in the environment. The results of the Bellhop model show that significant proportions of productivity in gas form in the macroalgal canopy would markedly influence the received acoustic signals on the four hydrophones. However, analysis of the experimental acoustic data concluded that the modelled bubble layers were not present during the experimental period. As a result, the use of acoustics as a means of measuring primary productivity

could not be further explored during the course of this research, and analysis of the field experiment focused on comparison of measures of productivity using the diel oxygen model method, oxygen exchange chambers, and PAM fluorometry.

A final investigation focussed in greater detail on the effects of diurnal, seasonal and latitudinal variability in ambient light on PAM parameters, as well as possible effects associated with depth, within- and between-alga variation in PSII performance, and latitudinal effects unrelated to the light climate. This research was based on field measurements undertaken in Tasmania, Western Australia and New South Wales (Australia) in both summer and winter during 2012 and 2013. Work focussed on *Ecklonia radiata, Macrocystis pyrifera,* and *Phyllospora comosa*, as three key habitat-forming species of macroalgae in the temperate coastal rocky reef environment of Australia. The effect of sampling methodology with regards to interpretation of PAM measures was explored, and recommendations suggested for the application of PAM fluorometry methodology in future ecological research.

The components of this thesis are arranged as follows:

Chapter 2 details the laboratory investigation of the density, sound speed and resulting compressibility of *E. radiata* tissue, with sound speed measured by four methods developed using ultrasonic testing (UT) equipment.

Chapter 3 focuses on the development and results of Bellhop beam-tracing model for predicting the acoustic response of a kelp forest environment at Fortescue Bay, Tasmania, for periods of low and high productivity as well as model-data comparison.

Chapter 4 provides a comparison of a diel oxygen model, benthic chamber oxygen evolution and PAM fluorometry to compare measurements and quantify differences in productivity estimates across the different techniques.

Chapter 5 details the effects of diurnal, seasonal and latitudinal variability in ambient light on PAM parameters, as well as possible effects associated with depth, within- and between-alga variation in PSII performance, and latitudinal effects.

Chapter 6 is the General Conclusion, which as the final chapter of this thesis, provides discussion of the integrated results of this research and implications for past, present, and future studies involving measurement of primary productivity in coastal marine environments.

This research provides a unique investigation into the techniques and methodology involved in measuring primary productivity in marine macroalgal systems. The results of this work give valuable insight into the advantages and disadvantages involved with several main-stream techniques currently

utilised in macroalgal (and seagrass) research, and the challenges faced by ecologists attempting to interpret results and compare research between methods. This study provides important and distinctive information on the potential use of acoustics as a future means of determining productivity and interpretation of future studies of macroalgal productivity in marine systems.

Readers should note that the thesis has been prepared with chapters formatted as a series of standalone journal articles now submitted to international peer-reviewed scientific journals. As a result there is, of necessity, a degree of repetition between chapters, particularly in the Introduction section. While this is unavoidable, it has been kept to a minimum as much as possible.

Chapter 2 Measurement of acoustic material properties of macroalgae (*Ecklonia radiata*)

2.1 Abstract

Temperate macroalgal forests are among the most productive ecosystems in the world. Acoustic propagation measurements have been used to monitor primary production over broad spatial scales (10^1—10^3 m) in seagrass meadows, and work is in development to assess the application of acoustics for measuring aggregate production in kelp beds and forests. In addition, scientific echosounders have been used routinely for mapping these benthic habitats and, in some cases, identify dominant species. Further advances in these areas require the development of species-specific acoustic models. However there is little knowledge of the acoustic properties of macroalgae, in part because measuring sound speed in large macroalgae is challenging due to their complex morphology. In this study four different methods are developed and trialled to determine the intrinsic sound speed of *Ecklonia radiata* tissue based on measurement of the time of flight of an ultrasonic pulse, while compressibility is calculated from density measurements. Direct methods involved lengths of stipe and tightly packed stacks of macroalgae blade tissue. Indirect methods focused on an entire intact macroalga submerged in seawater, and a homogenate solution containing seawater and blended blade tissue. Blade tissue showed a density contrast (relative to seawater) of 1.23 and a sound speed contrast of 1.0374 for the stacks. The homogenate solution gave a sound speed contrast of 1.0424. Stipe tissue density and sound speed were lower. Density contrast was 1.04 and sound speed contrasts were 1.0179 (SD=0.0025) and 1.0064 (SD=0.0032) depending on the sample. Whole macroalgae had age- and size-dependent densities with an average density contrast of 1.11 (SD=0.09) and showed an average sound speed of 1572.8 m/s (17.8 ˚C) and contrast of 1.0404 (SD=0.015). Compressibility was higher in stipe than blade tissue, with $3.924e^{-10}$ Pa^{-1} and $3.982e^{-10}$ Pa^{-1} for stipes and $3.209e^{-10}$ Pa^{-1} and $3.180e^{-10}$ Pa^{-1} for blade in stacks and homogenate respectively. The results show that *Ecklonia radiata* sound speed and density are higher, and compressibility lower, than that of seawater. This is likely related to high concentrations of alginate, and other structural and storage carbohydrates in the macroalgae, and thus may vary seasonally. The differences between tissue types found for all properties reflect the morphology and anatomy of this macroalga, with tightly condensed chloroplast cells in blade tissue and loosely packed structural cells in the stipe. This research provides essential input parameters to numerical models that will enhance acoustic habitat mapping and allow the development of acoustic inverse methods. This may enable the estimation of aggregate primary

production over large spatial scales in temperate kelp habitats, thus informing their future management.

2.2 Introduction

Marine ecosystem services are critical for human welfare with an estimated worth to the global economy of trillions of dollars each year (Costanza et al., 1997). Macroalgal forests with distinctive canopies, primarily of brown laminarian algae (northern hemisphere) or laminarian or fucalean algae (southern hemisphere), dominate the coastal reefs of the world's temperate marine habitats (Steneck, Johnson, 2013). They are among the most productive ecosystems on earth and provide essential structure for associated organisms including marine mammals, fish, crustaceans and molluscs (Steneck, Johnson, 2013). However, obtaining precise and accurate measurements of primary production aggregated across entire assemblages of algae and over ecologically meaningful spatial scales (10^0—10^5 m) is difficult, and acoustic techniques emerge as a method to consider (Hermand, 2003; Hermand et al., 1998). South eastern Australia has experienced increases in marine temperatures at nearly four times the global average (Johnson et al., 2011; Ridgway, 2007), and there is now evidence that, in some locations, macroalgae communities are retreating in a manner consistent with ocean warming (Johnson et al., 2011; Wernberg et al., 2011). Therefore, estimating primary production across assemblages at ecologically relevant scales is important to quantify ecosystem functioning and services and for monitoring change in macroalgae forests in the face of climate change and other significant anthropogenic stressors (Steneck et al., 2002).

Successful management of marine systems requires robust understanding of ecosystem process and, therefore, suitable tools for monitoring in space and time. However, monitoring changes in abundances and in ecosystem functioning (including primary production) is challenging at meaningful scales. Recent studies have utilised satellite and aerial imagery to map changes in coverage in both seagrass (Ferwerda et al., 2007; Fletcher et al., 2009) and macroalgal (Mount, 2005; Tyberghein et al., 2012) habitats over time, and acoustic imaging is increasingly being used in marine environments to create habitat and bathymetry maps and characterise the benthic biotic layer (Komatsu et al., 2002; Komatsu et al., 2003; Lucieer, 2008). Many studies have shown that seaweed provides a high degree of acoustic backscatter compared to other benthic substrata (Seaman et al., 2000). However, numerical models that relate material properties of the macroalgae to acoustic propagation and scattering are needed to infer target and ecological parameters and improve acoustic image formation, as well as to assist in species classification.

Exploratory research in seagrass meadows (Hermand, 2003; Hermand et al., 1998) gives promising results for expanding the use of acoustics to measure primary production. Photosynthesis in *Posidonia oceanica* increases the amount of oxygen in the water column in both dissolved and gaseous forms.

Although the dissolved oxygen has no measurable effect on the transmitted acoustic signal, the gas bubbles do have a profound effect due to sound speed decrease or scattering depending on frequency and can therefore provide information on photosynthetic parameters. Variability of the acoustic propagation in this seagrass community is correlated with the diurnal productivity cycle, and can be largely attributed to gas bubble production. While investigation of the use of acoustics to measure production in marine systems has thus far been limited to seagrass communities, the high productivity of macroalgal beds suggests that acoustics might also be usefully applied to measure and monitor productivity of these assemblages (Hermand et al., 2013).

Measuring benthic production in shallow water marine environments using acoustics involves tracking changes of propagation characteristics over time with the ultimate goal of quantifying the volume of oxygen bubbles formed in the macroalgal canopy. However, many factors, including the temperature, salinity and current fields in the water column as well as the sea surface conditions and the bedrock material properties affect the propagation of sound. In order to identify the part of the signal indicative of microbubbles these components must first be 'stripped' from the total signal (the acoustic inverse problem). In kelp forests acoustic models must, in addition to these factors, incorporate those related to the presence of a macroalgal canopy overlying the bed rock. Understanding the frequency-dependent acoustic behaviour of kelps and other seaweeds is essential to match prediction and measurement in resolving the acoustic inverse problem .

The temperate coastline of Australia covers more than 3000 km on which are extensive areas of rocky reef dominated by *Ecklonia radiata* (Wernberg et al., 2011). The ability to track changes in production associated with recent contractions of *E. radiata* communities or other changes in the marine environment is important in the context of climate change. As is the case for most marine organisms, there is a paucity of information available on the acoustic properties of macroalgae. The most important inputs to acoustic models are density and compression wave speed, or the ratios of these parameters to those of the surrounding seawater, in addition to compressibility . Several studies have investigated these material properties in marine organisms, for example zooplankton (Smith et al., 2010; Warren, Smith, 2007), copepods and euphausids (Chu, Wiebe, 2005; Greenlaw, Johnson, 1982; Smith et al., 2010), and more recently seagrass (Wilson et al., 2010; Wilson, Dunton, 2009). Recent research investigated the acoustic properties of macroalgae species with and without pneumatocysts (gas filled floats) using various models of macroalgae and water (Wilson et al., 2013), but there is no published information regarding direct measurement of sound speed in macroalgae.

For modelling the acoustic propagation in a shallow water kelp environment, the density, sound speed and resulting adabiatic compressibility of *E. radiata* tissue were investigated in the laboratory. Sound speed was measured by four methods developed using ultrasonic testing (UT) equipment.

2.3 Materials and Methods

2.3.1 Macroalgae transport and treatment

Measurements were undertaken in Tasmania, Australia, and Brussels, Belgium. All samples were collected from Fortescue Bay, Tasmania (-43.12574 S, 147.96068 E). For measurements in Tasmania eighteen intact macroalgae (ranging in mass from ≅ 40—800 g fresh weight) were collected in May 2012. Individuals were transported in seawater, and on arrival at the laboratory remained submerged with aeration until measurements were taken (< 12 hours). For transport to Brussels, five mature, average sized (≅ 500 g, ≅ 80 cm length) individual *E. radiata* were collected in June, 2012. Each macroalga was cut from a position just above the holdfast, leaving the main part of the alga intact. Individuals were transported moist in a cooled unit to Brussels. On arrival, algae were submerged in a tank of oxygenated artificial seawater (ASW; salinity 35, Instant Ocean Sea Salt) for 24 h prior to commencing experiments. Although the samples were not able to be tested for photosynthetic capacity on arrival in Brussels, it was assumed that as photosynthesis itself was not being measured (just acoustic properties), visual analysis was sufficient. This procedure was repeated in November, 2012, with the transport of five stipes, each separated from holdfast and blades.

2.3.2 Tissue density measurements

Initial density values (May 2012) were calculated from mass measured with an electronic balance, and volume determined by immersion in a graduated cylinder. Measurements were taken of whole individual algae, excluding the holdfast, after removal of excess moisture with paper towel. The density of blade and stipe tissues was also measured in macroalgae transported to Brussels using the methods as outlined above, however, for these measurements blade and stipe tissue were measured separately. The blades of four macroalgae were combined to estimate blade density, and five stipes were measured together to estimate stipe density. The density contrast (g) was calculated as

$$g = \frac{\rho_a}{\rho_w} \qquad (1)$$

where ρ_a and ρ_w are the densities of algae and seawater, respectively. The density of seawater was taken as 1.026 g/cm^3.

2.3.3 Seawater sound speed measurement

For the indirect methods that involved a volume fraction of ASW collected from the storage bath, the introduction of air bubbles by the aeration system will have a large effect on sound propagation, including sound speed and signal transmission (Povey, 1997). Even a small amount of undissolved air

will decrease sound speed in water (e.g. 0.1 ppm will reduce sound speed by ≅1.34 m/s). However, removal of dissolved oxygen may affect macroalga cell contents by altering chemistry and hastening degradation / decomposition. To determine the point at which bubbles are removed while preserving dissolved oxygen content, measurements were taken from samples of water subject to a vacuum for a range of time periods (Figure 2.1). Results showed that after 15 seconds under vacuum the dissolved oxygen content of the water began to decrease rapidly, and no bubbles were visible. Consequently, all seawater was vacuumed for a period of 15 seconds to remove gas bubbles without significantly affecting the dissolved oxygen content.

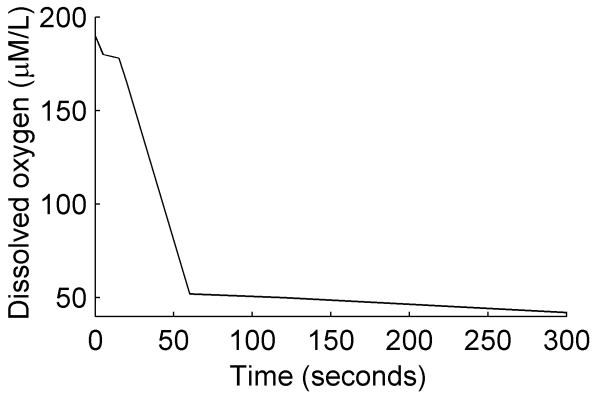

Figure 2.1: Dissolved oxygen concentration after vacuuming for different time periods. Note the steep decline after 15 seconds indicating where gas bubbles are removed and vacuuming begins to take out dissolved oxygen.

The sound speed of the ASW was then measured in the Plexiglas vessel (200 x 200 x 200 ±0.02 mm, internal dimensions 192 x 192 x 192 ±0.02 mm) which was also used for two indirect measurements of algae sound speed in seawater (Figure 2.2). The vessel dimensions were measured with high precision digital callipers (associated error 0.02 mm, resolution 0.01 mm). Measurements were repeated at temperatures of 16.5 °C, 17.2 °C, 18.1 °C and 18.4 °C using ultrasonic probes with nominal frequencies of 2 MHz and 6 MHz in reflection mode (where the pulse reflected from the Plexiglas/air interface at the back face is received back at the emitting transducer). The specifications of all transducers used in measurements are given in Table 2A.

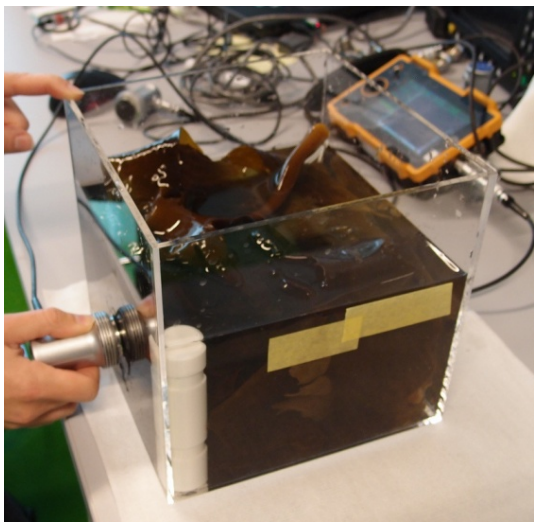

Figure 2.2: Plexiglas vessel used for sound speed measurements in artificial seawater, here containing macroalga and temperature sensor (white).

2.3.4 Tissue sound speed measurements

Macroalgae present unique challenges in the investigation of acoustic properties due to their complex morphology. Blades of *E. radiata* (and other laminarians) are characteristically thin, typically 1—2 mm, in contrast to other species, such as bull kelp (*Durvillaea potatorum*), which can develop blades with thickness >5 mm. Blade thickness varies depending on the age of the tissue, the particular part of the thallus, time of year (Lobban, Harrison, 1994) and environmental characteristics that correlate with water motion (e.g. depth and exposure). Thus it is difficult to obtain relatively uniform segments of sufficient size within which to measure sound speed with ultrasonic contact probe. Methods used in studies of other biological material, such as direct laboratory measurement of whole organisms (Warren, Smith, 2007) and *in situ* measurements of large, highly-concentrated aggregations (Chu, Wiebe, 2005), are not appropriate for the measurement of sound speed in *E. radiata*. Here, four different methods are proposed to determine sound speed using reflection and transmission modes (where an emitted pulse is received on a separate transducer after travelling through a medium).

Indirect measurements in seawater

Two indirect methods in this study measured travel time with known (accurately measured) volumes of macroalgae in seawater using standard pulse-echo techniques (Povey, 1997). In the first, a single macroalga (including stipe) was placed in the water-filled Plexiglas vessel. The method hereafter referred to as 'submerged alga' (Hermand, Randall, 2015) involves measuring the two-way (reflection) travel time of an ultrasonic pulse through a pathway containing a known volume of tissue and comparing it to the travel time in seawater alone. A transducer with a nominal frequency of 2 MHz, a focal width of 2.9 mm and a small beam divergence (angular measure of the increase in beam

diameter or radius with distance from the optical aperture) was used (Table 2A). A comparable method (using transmission mode) was used to measure sound speed in krill (Foote, 1990).

The macroalga was nearly entirely submersed in the vessel, with accurate measurements of the water level obtained before and after the addition of the macroalga. A multitude ($3\,e^{03}$) of pulse-echo measurements were recorded whilst displacing the macroalga in the vessel by slow movements of rotation about the stipe axis and small translations in all directions. The precise volume of macroalga in the direct path was expected to vary as the beam intersects different pieces of tissue, depending on the position and orientation of the macroalga. These movements were randomized as much as possible so that the measurements scanned across the entire volume along a multitude of radials. The extracted travel times were expected to vary as the volume of tissue in the path varied about the known ratio (0.08) of total macroalgae volume to the total water volume in the vessel. The average of the travel time values is expected to yield an accurate estimate of sound speed for a known volume ratio provided the macroalga is manoeuvred randomly in the vessel.

The second indirect method involved preparing a homogenate (or dense suspension) of seawater (750 ml) and blade tissue (850 ml). The blade tissue from four macroalgae was homogenized in a commercial blender for approximately five minutes and then vacuumed for approximately fifteen minutes to remove all air bubbles or pockets. Sound speed was determined from measured reflection mode travel time through the homogenate (poured into the vessel) using a nominal frequency of 2 MHz (Table 2A). An effective medium acoustic model was used, based on propagation in multiphase materials as proposed by Wood (Wood, 1932) and developed by Urick (Urick, 1947). Provided that the acoustic wavelength is larger than the characteristic size of the mixture components and the mixture is homogeneous, the effective sound speed of the mixture can be calculated from the material properties of the components. Ultrasound measurements were undertaken shortly after blending and vacuuming to prevent potential vertical settling according to mixture component density. After blending visual inspection was unable to distinguish individual particles giving an estimated particle size of <0.1 mm. With a wavelength in seawater of 0.75 mm it was assumed that the model could be applicable despite the high concentration of alga tissue in the homogenate.

The effective sound speed c_{eff}, in the mixture, which is also the sound speed measured, is given by Urick's equation (Urick, 1947)

$$\frac{1}{c_{\text{eff}}^2} = \left[\sum_{\text{i}} \phi_{\text{i}} \kappa_{\text{i}}\right] \left[\sum_{\text{i}} \phi_{\text{i}} \rho_{\text{i}}\right] = \left[\sum_i \frac{\phi_{\text{i}}}{c_i^2 \rho_i}\right] \left[\sum_{\text{i}} \phi_{\text{i}} \rho_{\text{i}}\right], \qquad (2)$$

where κ_{i} , c_i , ρ_{i} , and ϕ_{i} represent the compressibility, sound speed, density and volume fraction of material or component *i* in the homogeneous mixture. If, as was the case in this study, the sound speed

of the mixture is known (measured), an unknown input parameter can be determined if all other inputs are known. In this instance, given the measured density of blade tissue, its intrinsic compressibility can be obtained from the sound speed measured in the homogenate. The intrinsic sound speed (c) of the tissue can then be calculated as

$$c = \sqrt{\frac{1}{\kappa\rho}}, \qquad (3)$$

where κ and ρ are compressibility and density of the macroalga respectively. The compressibility values for seawater were calculated using the GSW Oceanographic Toolbox (McDougal, Barker, 2011) for given temperature and salinity.

Direct measurements on the samples

The intrinsic sound speed (ultrasonic velocity) of stipe and blade tissues was also measured directly. Two-way travel time was measured along the longitudinal axis of stipe segments from both ends to assess reproducibility (Figure 2.3A). The two longest segments available (184.50 ±0.10 mm and 224.90 ±0.10 mm) were used and were then repeatedly cut into smaller lengths. The sound speeds were then measured on each smaller segment to increase confidence in the accuracy of the measurements. Care was taken to cleanly cut each segment perpendicular to the axis to ensure good acoustic coupling with the contact probe, beam steering in the longitudinal direction, and vertical-incidence reflection at the tissue-air interface of the opposite cut. The segments were held straight in a grooved guide, and ultrasonic gel couplant applied to the stipe end in contact with the transducer (Figure 2.3B). Lengths were ascertained with the digital callipers. Because length measurements could potentially be dependent on pressure applied by the callipers themselves, stipe lengths were also measured by ruler and high-resolution photographs (with no parallax error) taken for later visual inspection.

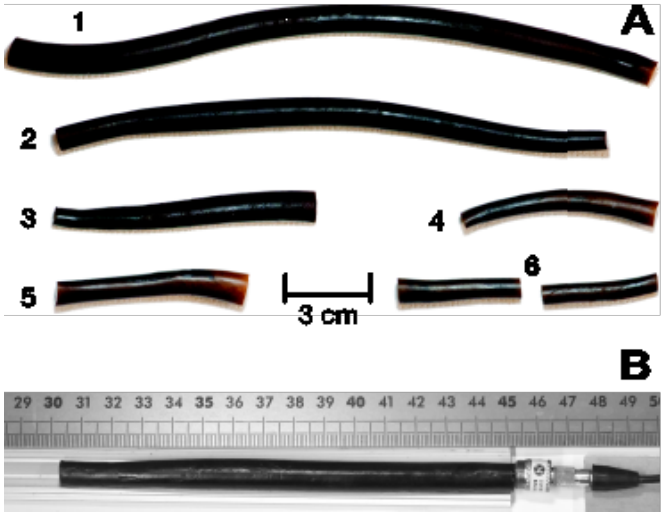

Figure 2.3: Stipe segments from laboratory experiments showing (A) the two samples from which direct measurements of sound speed were taken and (B) stipe 2 in grooved rule with ultrasonic contact probe.

Transducers with small piezoelectric elements were chosen to fit the small diameter (≅10 mm) of the stipe segments. Measurements were repeated using small-diameter (6.35 mm) transducers with nominal frequencies of 2.25 MHz, 5 MHz and 10 MHz and suitable beam characteristics (Table 2A). Some measurements were not possible due to attenuation depending on length and frequency. For stipe 1, five different lengths were used ranging from 184.50 ±0.10 mm to 50.68 ±0.10 mm, with an average diameter of 8.96 (SD=0.15) mm (17 measurements), and for stipe 2, a total of 14 lengths were measured ranging from 224.90 ±0.10 mm to 55.17 ±0.10 mm, with average diameter of 10.72 (SD=0.06) mm (60 measurements). Since sound speed in wet tissue is expected to depend on temperature, this parameter was monitored continuously, both in the seawater vessel holding the stipes and in the air near the ultrasonic testing apparatus using self-recording devices. Due to time spent handling the material out of water (≅two hours) during the first day's measurements it was assumed that stipe temperature was at equilibrium with ambient air temperature. On the second day, the stipe segments were repeatedly immersed in the seawater vessel in between the measurements so that temperature and moisture content in the stipes would remain the same as in the vessel.

For direct measurement of sound speed in blade material, stacks were constructed by layering blade tissue horizontally and binding the material together with cotton thread (Figure 2.4A). These measurements were made in transmission mode. Each stack contained blades from two independent algae. The stacks measured 39.43 ±0.10 mm and 39.27 ±0.10 mm in thickness, with ≅50−60 blade pieces per stack. To prevent entrapment of gas between blades, each stack was constructed whilst submerged in seawater. The stacks were then vacuumed in air in a separate vessel for ~6 minutes to remove air bubbles between the blade layers, the binding tightened and the stack again submerged in

seawater. The length of the acoustic path was deduced from the distance between transducer faces measured directly with points placed at the rear edge of the transducers (Figure 2.4B) to account for the compression of the stack during the measurement due to the small pressure applied. One-way travel time through each stack was measured. Sound speed measurements of each tissue type were taken at different temperatures and corrected to a temperature of 18 ˚C. Due to the high water content of macroalgae tissue (≅70—90% for some species of brown seaweeds (Horn, 2000)), sound speed in the tissue was expected to vary with temperature as does sound speed with temperature in seawater. Therefore, for each 1 ˚C of variation from 18 ˚C among samples, the sound speed was adjusted by 3.0 m/s (TEOS-10) (McDougal, Barker, 2011).

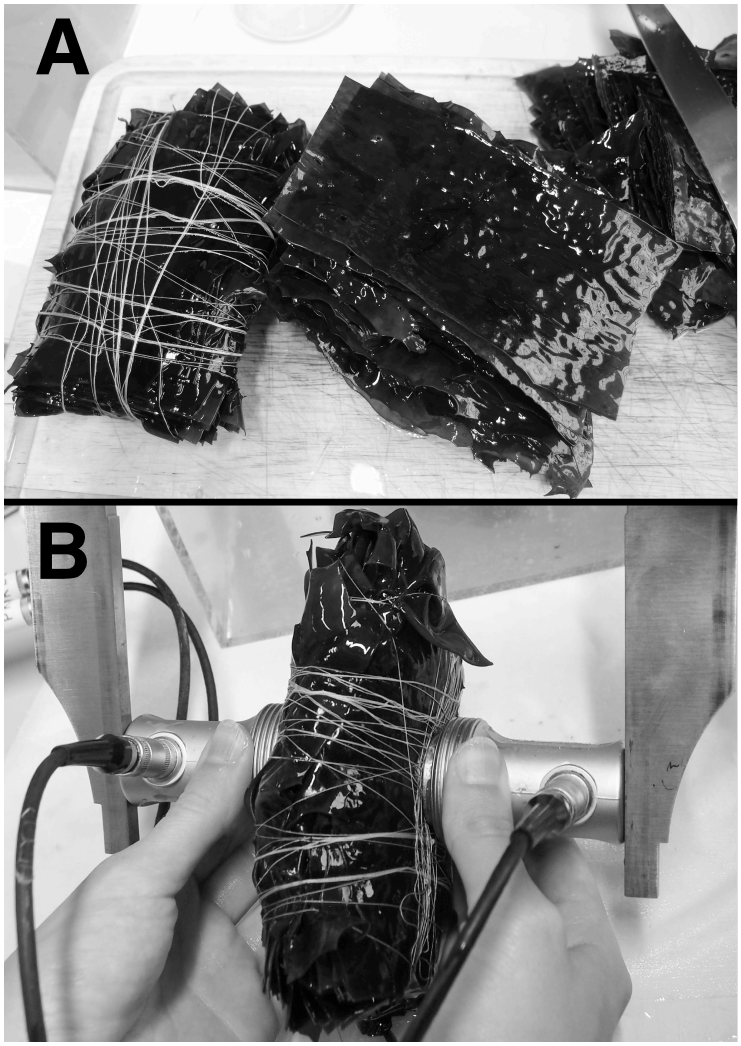

Figure 2.4: Blade material from which (A) blade stacks were bound with cotton and (B) cotton bound stack showing placement of transducers and callipers.

For all methods sound speed contrast (h) was calculated as the ratio of sound speed in the macroalgae medium to sound speed in seawater for the temperature at the time of measurement, according to

$$h = \frac{c_a}{c_w}, \qquad (4)$$

where c_a and c_w are sound speed in macroalgae and seawater, respectively.

2.3.5 Compressibility

Compressibility is the inverse of the bulk modulus of a substance, which measures resistance to uniform compression. Compressibility was calculated as

$$\kappa = \frac{1}{{c_a}^2 \rho_a}, \qquad (5)$$

where κ, c_a and ρ_a are respectively compressibility (Pa^{-1}), sound speed (m/s) and density (g/cm^3) of the macroalgae tissue.

2.4 Results

2.4.1 Algae density

Macroalga density increased with absolute size (Figure 2.5; adjusted R^2= 0.49, $F_{1,16}$=15.59, p=0.0001). Average density was 1.14 ±0.01 g/cm^3 (SD=0.005), with a range of 0.34 g/cm^3. The average volumes of whole alga and stipe were 280 cm^3 and 20 cm^3, respectively. The stipe tissue had a density of 1.07 ±0.01 g/cm^3, giving a lower density contrast (ratio of density to that of seawater) than that of blade tissue and whole macroalgae (Table 2.1). Blade tissue showed a higher density and density contrast than that of whole macroalgae.

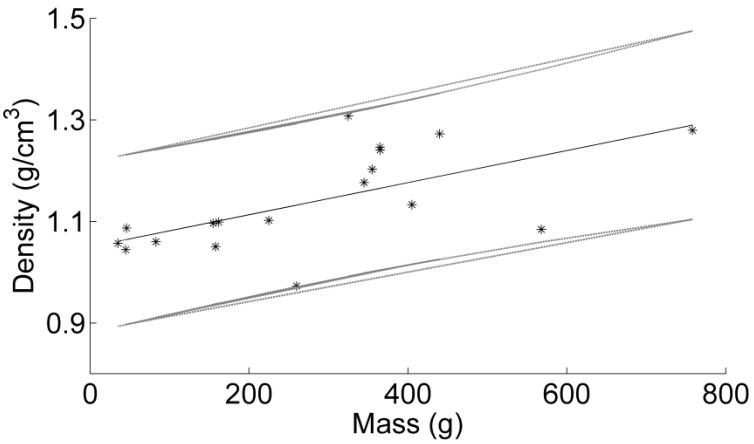

Figure 2.5: Relationship between total macroalga mass and density for whole *Ecklonia radiata* individuals measured in Tasmania (adjusted R2= 0.49, F=(16,15.59), p=0.0001). Dotted lines indicate 95% confidence intervals.

Table 2.1: Density and density contrast of *Ecklonia radiata* measured according to tissue type. Mean values and standard deviation (in parentheses) are indicated. These measurements were respectively made in May, November and June, 2012. Note for stipe and blade tissue measurements were taken with tissue of all individuals combined so no standard deviation is available.

Location	Tissue	Sample size	Volume (ml)	Mass (g)	Density (g cm^{-3})	Density contrast (g)
Tasmania	Whole alga	18			1.14 SD=0.10	1.11 SD=0.09
Brussels	Stipe	5	114 ±1	122.0 ±0.1	1.07 ±0.01	1.04 ±0.01
Brussels	Blade	4	850 ±8	1075.0 ±0.2	1.26 ± 0.01	1.23 ±0.01

2.4.2 ASW sound speed

The artificial seawater (ASW) gave sound speeds slightly higher than those given by the Thermodynamic Equation of Seawater - 2010 (TEOS-10) (McDougal, Barker, 2011) (Figure 2.6). Calculations were based on pulse-echo time of flight measurements (Povey, 1997) with the acoustic path length measured with high accuracy (±0.02 mm). For an acoustic path length of 384.00 mm, an error of 0.10 mm translates as a potential error in sound speed of ≅1.6 m/s, and this may have contributed to the observed differences in sound speed. This could potentially result in error in estimates of macroalga tissue sound speed derived using either the 'homogenate' or the 'submerged' alga method of ≅2 m/s. Given that this error is so small, we used the Thermodynamic Equation of Seawater to calculate temperature dependent sound speed in ASW when using the 'homogenate' or the 'intact macroalga in ASW' methods.

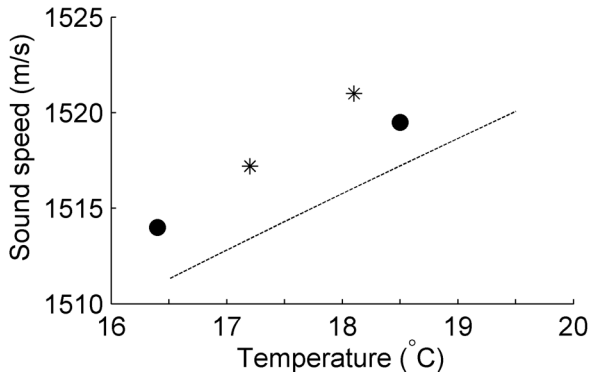

Figure 2.6: Sound speed measured in artificial seawater at 2 MHz (crosses) and 6 MHz (circles) and sound speed calculated using explicit TEOS-10 (dashed line).

2.4.3 Tissue sound speed

For the first indirect method of submerged intact alga, an average sound speed of 1572.8 ± 3.6 m/s (SD=21.2 m/s) was obtained for the whole alga which includes both stipe and blades (16.9 ˚C) (Hermand, Randall, 2015). The error assumes a possible error in volume fraction of 0.002. The corresponding sound speed contrast is 1.0404 (SD=0.0139). For the second method based on the homogenate of blade tissue and ASW, an effective sound speed of 1548.1 m/s was measured. According to Urick's equation (Equation 2), given a measured tissue volume fraction of 53 (±1) %, a measured tissue density of 1.26 ±0.01 g/cm^3 and a predicted sound speed in ASW at 22.6 °C, the resulting sound speed and contrast of the blade tissue at the same temperature are 1589.3 ±3.7 m/s and 1.0424, respectively. As only one homogenate was created (from blades of four macroalgae), no standard deviation is available on this estimate.

For the two direct methods, results varied according to tissue type. Both blade stacks gave sound speeds of 1574.0 m/s (at 18.5 ˚C), which correspond to a sound speed contrast of 1.0374 (SD=0.0032). Assuming a distance measurement error of 0.10 mm (larger than the accuracy of the callipers used) a potential error in sound speed for the blade material of 4.0 m/s is calculated, corresponding to a potential error in sound speed contrast of 0.0026.

The different lengths of stipe 1 gave a sound speed ranging from 1547.7 m/s to 1562.3 m/s with an average of 1557.9 ±1.3 m/s (SD=4.1 m/s) (Figure 2.7A). The ambient air temperature over the period of measurements (from right to left in the graphics) increased from 23.0 °C to 23.8 °C which represents an increase of ASW sound speed of ≅2.5 m/s. Assuming, due to water content of the macroalgal cells, that the temperature effect on sound speed in the tissue is similar to temperature effects on sound speed of seawater, this 2.5 m/s increase was considered negligible compared to the observed variation in stipe sound speeds and an average temperature of 23.4 °C was taken as the reference for sound speed contrast (1.0179 (SD=0.0025)).

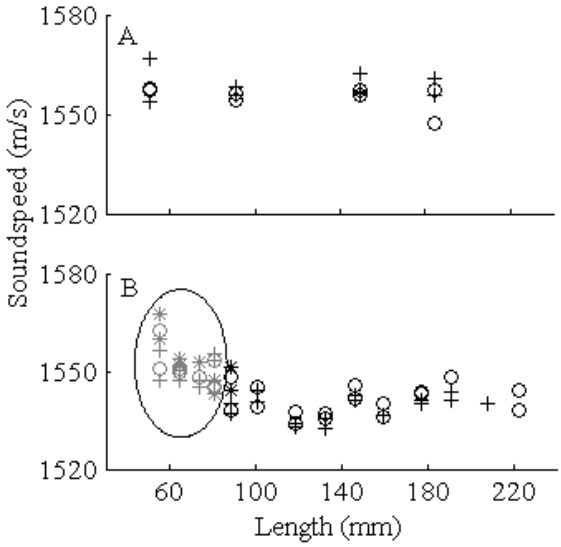

Figure 2.7: Sound speed of stipe material as a function of cut length from stipe 1 (A) and stipe 2 (B). The period of measurement runs from right to left in the graphics. Crosses, circles and stars indicate 2.25 MHz, 5 MHz and 10 MHz frequency. Stipe 1 measurements were taken at 23.4 ˚C and stipe 2 measurements at 18.8 ˚C, causing the main differences in sound speed between stipes. Note increasing trend of sound speed for segment lengths less than 80 mm in stipe 2. Circled values (B) indicate values excluded from analysis due to lack of temperature control within the alga tissue.

Sound speeds in stipe 2 ranged from 1532.9 m/s to 1567.7 m/s. Values were mostly independent of segment length until the stipe was cut to ≅88 mm (Figure 2.7B). Over the range of remaining segment lengths sound speed continued to increase with decreasing length of the segment (from right to left in the graphics). Due to constant handling these smaller segments were not re-submerged in the seawater in the manner in which larger segments were, and due to their small size and constant handling were likely to have increased in temperature over the measurement period. This likely resulted in their temperature becoming closer to the (warmer) air temperature, which would directly affect sound speed measurements. Given lack of temperature control for these segments the corresponding measurements were excluded from further analysis.

Water (ASW) temperature over the period of stipe 2 measurements (where stipe segments were continually re-submerged for temperature control) averaged 18.7 ˚C with a range of ±0.3 ˚C. This range corresponds to a seawater sound speed increase of ≅1 m/s, which again is negligible compared to the range of sound speed values estimated. This temperature average was, therefore, taken as stipe temperature for all measurements. The average sound speed after exclusion of the smaller stipe

segments was 1540.2 ±1.0 m/s (SD=4.6 m/s) corresponding to a contrast of 1.0064 (SD=0.0032) (Table 2.2).

Table 2.2: Sound speed and contrast of the different *Ecklonia radiata* tissue types obtained with the different measurement methods. Ultrasonic probe nominal frequency, sample temperature and sample size are given. The methods indicated by * used additional artificial seawater. ** denotes volume fraction of alga in method. Stipe SD is from all segments, and error calculated from average length. The results are compensated for temperature in Table 3. The stipe results were obtained in November, 2012 while the others in June, 2012. For blade, both stacks gave identical values. Only one homogenate was processed so standard deviation is not applicable.

Material	Frequency (MHz)	Temperature (˚C)	Sample size	Size	Sound speed c (m/s)		Sound speed contrast h	
Submerged alga*	2	17.8	1	1 alga	1572.8 ±3.6	SD=21.2	1.0404 ±0.0013	SD=0.0139
				**0.080 ±0.002				
Stipe 1	2.25, 5	23.4	17 segments	51—184 mm	1557.9 ±1.3	SD=4.1	1.0179 ±0.0009	SD=0.0025
Stipe 2	2.25, 5	18.7	60 segments	88—224 mm	1540.2 ±1.0	SD=4.6	1.0064 ±0.0007	SD=0.0032
Stacks (blade)	2	18.5	2 (4 algae)	39.43 ±0.02 mm	1574.0 ±4.0		1.0374 ±0.0026	
				39.27 ±0.02 mm	1574.0 ±4.0		1.0374 ±0.0026	
Tissue homogenate*	2	22.6	1 (4 algae)	850 ±40 ml	1589.3 ±3.7		1.0424 ±0.0024	
				**0.53 ±0.01				

Subsequently, the results were corrected for a seawater temperature of 18 ˚C to match the maximum summer conditions at the site of *E. radiata* collection in Fortescue Bay, Tasmania (Table 2.3). After correction the sound speed for submerged intact algae (1572.1 ±3.5 m/s) was higher than the sound speed averages for both stipes, which differed by 5.1 m/s (1543.3 ±1.3 m/s and 1538.2 ±1.0 m/s). These stipe sound speeds are significantly lower than those estimated for the blade stacks (1572.5 ±4.0 m/s). Sound speed calculated for the homogenate was higher than for all other methods (1579.5 ±6.6 m/s).

Table 2.3: Sound speed and compressibility values corrected for the temperature of 18 °C.

Material	Temperature corrected sound speed (m/s)	Density (g/cm^{-3})	Compressibility K (Pa^{-1})
Submerged alga	1573.3 ±3.6	1.29 ±0.01	3.135e−10 ±1.339e−11
Stipe 1	1543.3 ±1.3	1.07 ±0.01	3.924e−10 ±3.007e−12
Stipe 2	1538.2 ±1.0	1.07 ±0.01	3.982e−10 ±3.195e−12
Stacks (blade)	1572.5 ±4.0	1.26 ± 0.01	3.209e−10 ±9.313e−13
Tissue homogenate	1576.6 ±6.6	1.26 ± 0.01	3.180e−10 ±4.999e−12

2.4.4 Compressibility

Compressibility (Equation 3) varied according to tissue type, ranging from 3.180e^{-10} Pa^{-1} to 3.982e−10 Pa^{-1} (Table 2.3). Both stipes had a higher compressibility than that of intact whole macroalgae and blade tissue. Compressibility of all tissues is lower than that calculated for seawater (4.261 e−10 Pa $^{-1}$) at ambient environmental conditions at the location and time of macroalgae collection (calculated according to the Thermodynamic Equation of Seawater - 2010 (TEOS-10)) (McDougal, Barker, 2011).

2.5 Discussion

2.5.1 Density

The density of blade tissue was 9 % higher, and stipe material 6 % lower, than that of the average density of intact whole macroalgae individuals. Given that the stipe makes up only a small portion (up to≅10 %) of the total volume of a typical *E. radiata* adult sporophyte at this site, the slightly lower

values for whole alga compared to blade tissue alone reflects the contribution of the lower density of the stipe tissue to the average for the entire individual.

The marked difference in density between stipe and blade tissues reflects the morphology and anatomy of macroalgae. The blade tissue in *E. radiata* consists of thin blades (1—2mm (Figure 2.8B)). In macroalgae, this tissue achieves optimal photosynthesis because chloroplasts are tightly condensed (Demes et al., 2011) (Figure 2.8A). Compared to other cell contents, chloroplasts have a higher density (Heldt, 2005) and therefore the concentration of chloroplasts in epidermal cells in the blade leads to higher tissue density.

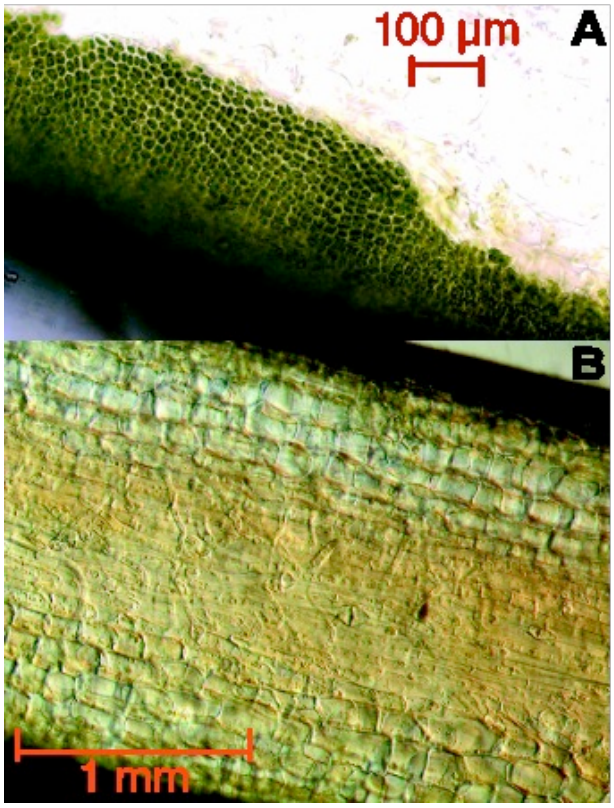

Figure 2.8: (A) Region of epidermal cells of *Ecklonia radiata* (cross section) showing densely packed chloroplast organelles; (B) longitudinal section through macroalga blade showing tissue differentiation.

The stipe tissue has marked (radial) variations in cell type and structure (Figure 2.9D), with a central medullar region of diffusely packed cells (Figure 2.9B) surrounded by a region of cortical cells (Figure 2.9A), with the external region containing more densely packed epidermal cells containing chloroplasts (Figure 2.9C). The central medulla of the stipe tissue of large brown algae contain

loosely spaced axially elongated cells which, in some species, allows movement of photosynthate inside the macroalgae (Demes et al., 2011; Lobban, Harrison, 1994). This tissue contains no photosynthetic cells due to its distance from the epidermis. It is also clear that stipe epidermal cells contain a much lower concentration of chloroplasts than blade epidermal cells, reflecting that stipes serve a primarily physical structural function rather than photosynthetic. It follows that the higher density of blade tissue results from the high concentration of densely packed cells.

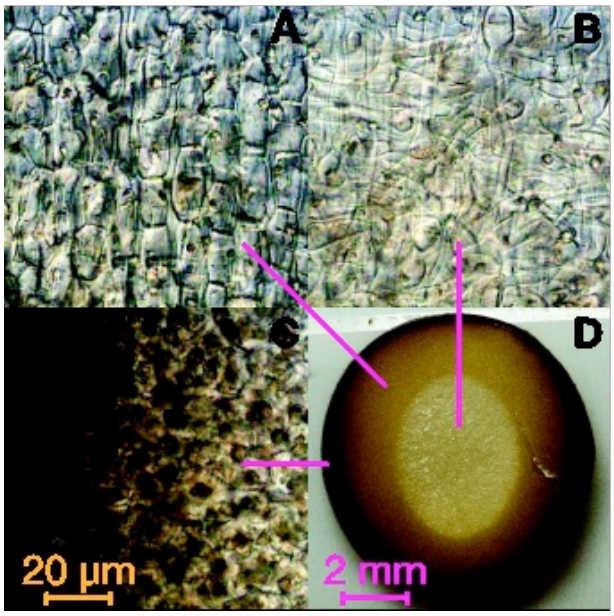

Figure 2.9: Longitudinal sections of epidermal cells of blade tissue of Ecklonia radiata showing (A) cortex; (B) loosely packed medulla region cells; (C) epidermis; and (D) cross section overview of stipe tissue.

There was also a relationship between overall mass and density for algae measured in Tasmania, with smaller individuals having lower density. Our measurements covered a wide range of sporophyte sizes, and it is unknown whether there are relationships between density and season, or nutrient availability, although these factors would likely influence growth, cell packing and concentration of cell contents such as photosynthetic pigments and alginates and other storage carbohydrates. A positive relationship between density and body size (mass) is known for other marine organisms, such as copepods (Chu, Wiebe, 2005).

2.5.2 Sound speed and compressibility

The sound speed and adiabatic compressibility (i.e., reciprocal bulk modulus) values given in this study are intrinsic acoustic properties of the tissue which can be used in an acoustic model. However, depending on the physical and structural properties the measured values can depend on the ultrasound

frequencies used which are systematically specified in this study. Furthermore, those values are related but cannot be directly compared to the "low-frequency sound speed" values which can be deduced from the bulk moduli obtained with a resonance tube (Wilson et al., 2013) as discussed at the end of the section.

The stipe medullary tissue had a lower sound speed than that of whole individuals and blade tissue, as was expected given their lower resistance to compressibility (stiffness) compared to blade tissue. The tighter cell packing and higher chloroplast concentration in blade tissue relative to the stipe results in higher stiffness. Since the increase in density (which reduces sound speed) does not compensate for the increased bulk modulus, the sound speed is higher in the blade than in the stipe. Further, for the stipes, given the clear differentiation between the medullar region and surrounding cortex of more densely packed cells (Figure 2.9C), it is important to consider the direct path of acoustic propagation. The contact transducers were centred on either end of the straightened stipe segment so that, given near-field length, focal width and beam dispersion angle of the transducers used (Table 2.1), the acoustic beam travelled for the most part through the tissue of the medulla region, contributing to the lower sound speed measured for the stipe.

Shorter segments (< 88 mm) in Stipe 2 gave higher sound speeds and were excluded due to the time they spent out of seawater during the measurement process. This result indicates that, given the sound speed of the stipe tissue is higher than that of seawater, a small reduction in water content would result in slightly higher sound speed. This is consistent with results found in terrestrial plant tissue, where, for example, reduction in moisture content in wood results in higher sound speed values (Oliveira et al., 2005). This, together with the effect of increased temperature of the stipes relative to ambient air or the storage bath as a direct result of handling the stipes, accounts for the higher sound speed observed in shorter segments. With the exclusion of shorter segments, we are confident there were no temperature fluctuations during stipe measurements of more than 0.5 ˚C. This would result in a change to estimated sound speed of ≅1.6 m/s (i.e. a change in sound speed contrast of 0.001), hence any small fluctuations will not have significantly affected sound speed estimates.

An additional consideration when estimating sound speed from travel time in cylindrical rods, such as the stipes, is a possible waveguide effect when the transverse dimension is comparable in size with the wavelength (Oliver, 1957; Tu et al., 1955). Here, the longest wavelength is approximately 0.75 mm to be compared with the diameter of inner medullar region (≅6 mm). In the presence of dispersion caused by the geometric boundary conditions, wave velocity is no longer uniquely defined. A travel time measurement will yield a sound speed with which the overall shape of the waves' amplitudes—known as the modulation or envelope of the wave—propagates through space (group velocity) is lower than the rate at which the phase of the wave propagates in space (i. e. the phase velocity) when wavelength and segment length increase. By approximating the stipes as an axially-symmetric

cylindrical rod constituted of an inner medullary layer and an outer cortical layer, acoustic waves were modelled using a Graphical User Interface for Guided Ultrasonic Waves (GUIGUW) (Marzani et al., 2009) to assess guided waves behaviour.

The predicted dispersion curves confirmed there was no significant wave velocity change in the frequency range of measurement. No dispersion effect was noticeable among measurements across the three nominal frequencies of 2.25 MHz, 6 MHz and 10 MHz and for the different lengths as seen in Figure 3, confirming the numerical prediction. This, together with the correlation between temperature and sound speed increase for the shortest segments, indicate that there was no significant waveguide effect or dispersion over the investigated frequency range.

Due to the differences in cell composition and density between cortex and medullar regions, it is expected that sound speeds would differ if measurements were taken perpendicular to the stipe axis as a significant proportion of outer cortex cells would be involved. The small diameter of the stipes sampled (<1 cm) prevented perpendicular measurements given the potential for large error due to the short length of ultrasound path. In addition, the small diameter size makes measurement of only the outer cortex material along the longitudinal direction difficult. Another consideration is directionally dependent sound speed in the material. It is well known that wood is highly anisotropic, a function of the directional characteristics of the wood fibres necessary for structural support (Schafer, 2000). Seaweed, however, does not contain these structural fibres, nor the directional vascular cells which land plants and, indeed, seagrasses have. These characteristics of macroalgae suggest that directional dependence of sound speed is an insignificant factor when considering measurement of stipe material. Although there will be differences in sound speed with perpendicular measurements due to the acoustic path passing through different tissue types, it is likely that the sound speed of each tissue type is isotropic.

The sound speed contrast of the stacked blades was very close to that of the homogenized algae blade, indicating the accuracy and interchangeability of the methods used in this study. This suggests that different methods might be applied to different species (depending on their morphology) according to convenience and still be comparable across species.

One potential issue in homogenizing algal tissue in a blender is the possible introduction of air bubbles into the medium due to mechanical action. In addition, the breakup of tissue itself could result in the release of gas bubbles in the medium, given that chemical gradients and photosynthetic processes in macroalgae have been shown to produce much higher concentrations of dissolved gases in tissues than would be expected from partial pressures alone (Johnston et al., 1992; Kubler et al., 1999). In the present experiments, the homogenate was degassed in a vacuum chamber and there was good agreement between the measured sound speeds and sound speed ratios (which are independent

of temperature) for blended tissue obtained via Urick's equation and that of the intrinsic sound speed measured from the tightly stacked intact tissue. This indicates that gas bubbles were effectively eliminated and that both methods provide an accurate means of measuring the sound speed of macroalgae and are likely to be applicable to other seaweed species. It is likely that the small differences in sound speed reflect minor errors in the volume measurements of the components of the homogenate.

When working with mixed solutions, the non-spherical form and complex internal cell structure of the biological material may affect the scattering and absorption of acoustic energy (Lofqvist et al., 2007). A mixture may only be treated as homogeneous respective to the acoustic field if the particles are numerous and small compared with the wavelength (Richards et al., 1998). For low acoustic frequencies commonly used in the field, the wavelength can easily be considered large enough to disregard these effects. However, for ultrasound with sub-millimeter wavelengths it is possible that the results of experiments similar to the one presented here could be affected, depending on the actual sizes of the particles in the homogenate. The mixture created for this was made of 47 % seawater with the remainder made up of very small cell clusters and mucous released from the macroalgae. Given the consistency of sound speed calculated from this and other methods, there is high confidence that the homogenate fulfils the requirements for accurate measurement of sound speed of the tissue through application of the mixture theory (Lofqvist et al., 2007).

The submerged whole alga method yielded a slightly lower sound speed than that of the blade tissue alone. This is due to stipe material intercepting the ultrasonic beam depending on the actual position of the alga which was randomly positioned within the water volume. Given stipe tissue makes up only a small fraction of the total mass of the macroalga ($\backsimeq$5 % to 10 % depending on the individual) there is only a small reduction in the estimated sound speed which should converge to the average sound speed of the macroalga tissue for a very large number of measurements (Hermand, Randall, 2015).

The estimates of compressibility of tissue were nearly identical for both stipe samples. Likewise, there was a good consistency in the compressibility of blade and whole macroalga materials across methods. The higher compressibility of the stipe relative to blade tissue reflects the lower density of this tissue. Compressibility of all tissue types is lower than that of seawater.

2.5.3 Sound speed dispersion

Except for the stipe for which it was not necessary, care was taken to remove gas bubbles from the aqueous systems prior to ultrasound measurements. The effectiveness of the vacuum operation was verified on the ASW samples used for the submerged alga and homogenate. In Figure 2.6, measurements at 2-MHz and 6-MHz nominal frequencies are both close to TEOS-10 prediction, suggesting that there was no significant sound speed dispersion due to bubble resonant scattering. The

presence of bubbles with resonance frequencies much smaller than 2-MHz cannot be excluded but is unlikely due to vacuuming to the point where dissolved oxygen was starting to be removed from solution.

For the submerged alga method care was taken to not introduce air bubbles when handling the macroalga. For the homogenate, sufficient time (15 min) was given to allow all bubbles to cream out of the mixture with a viscosity higher than water. The stacks were assembled underwater and then carefully vacuumed for a period of ≅6 min to remove all interstitial air between the blades, as clearly visible by bubbles forming on the edge surface of the stacks. Although the frequency-dependent effects of bubble acoustics can be problematic, these were not relevant here given (1) the morphology of *E. radiata* which has no gas void, and (2) the vacuum treatment. The ultrasound frequencies used are likely to be higher than the resonance frequency of any gas bubble or pocket formed during the preparation of the samples, thus excluding strong scattering which would depend on bubble size distribution and resulting sound speed dispersion. Although the frequency-dependent effects of bubble acoustics can be problematic, these are not relevant here given the morphology of *E. radiata* (which has no gas void) and the vacuum treatment.

2.5.4 Biology

This study shows intrinsic sound speed and compressibility values for all *E. radiata* tissue to be higher than that of seawater. Microsensor measurements in macroalgae show oxygen is produced in cortical layers and diffuses both through the diffusive boundary layer to the surrounding water and into the medullar tissue in the thallus (Spilling et al., 2010). Some macroalgal species (e.g. *Codium fragile*) can buffer extreme oxygen variations when photosynthetically active radiation levels are very high with formation of gas bubbles in the medullary tissue (Lassen et al., 1994). However, given that our samples were transported in black-out containers on ice, and measurements occurred in low artificial light conditions in laboratory, no formation of oxygen bubbles from photosynthesis would occur. In addition, any gas bubbles introduced via aeration of ASW or blending of material were removed with vacuuming. Therefore, it is assumed that effects of gas bubbles on measured sound speed can be excluded.

Sound speed and density contrasts found in this study also exceed those found at high frequency for other marine organisms including copepods, salps, jellyfish and gelatinous zooplankton (Chu, Wiebe, 2005; Hirose et al., 2009; Warren, Smith, 2007; Wiebe et al., 2010). Although these organisms showed values (slightly) greater than that of the surrounding seawater, their contrasts were much closer to unity. This reflects the ecology of these organisms and the obvious advantages of neutral buoyancy. For small animals, movement in the water column can come at high energetic cost, and the ability to remain just below neutral buoyancy is obviously beneficial (Marszalek, 1982).

In contrast, *E. radiata* is fixed to the benthos, with relatively rigid stipes providing elevation of blade tissue above the substratum. The photosynthetic blade material is elevated by the stipe but tends to either hang down from the stipe or lie relatively horizontal in current or surge, optimising its ability to intercept light. In the field it is commonly seen that detached algae (e.g. from storm activity) are negatively buoyant and remain on the benthos rather than suspended in the water column or floating to the surface. The compressibility values obtained for *E. radiata* tissue are lower than those found by Wilson *et al* 2010 (Wilson et al., 2010) for seagrass species, consistent with the higher sound speed and density found for this macroalgae.

The positioning in the water column of stipe and blade tissue may also affect sound propagation. Water column movement generally results in the presence of blade tissue from the canopy almost to the benthos, however, stipe tissue only occupies the lower section of the canopy layer. Although stipe tissue is minimal compared to blade tissue for individual macroalgae, this vertical differentiation in tissue density (and thus sound speed) may impact application of acoustic propagation modelling to measure productivity, and acoustic methods used to estimate the range and extent of submerged aquatic vegetation. This should be taken into account when using these techniques.

Another key characteristic of brown macroalgae is a high content of alginates, which can represent up to 30 % of dry weight (McKee et al., 1992). Alginates are polysaccharides whose primary biological function is structural (Percival, 1979). Because of medical and pharmaceutical uses of alginates, much is known about their material properties (Draget et al., 1997). Sound speeds and densities increase substantially with relatively small increases in concentration of alginate in laboratory tests, with sound speeds ranging from 1497 m/s to 1528 m/s for concentrations between 1 % and 2 % (Klemenz et al., 2003; Ross et al., 2006). It is expected that the high sound speed and density found here is, in part, related to alginate content. If this is verified it is expected that seasonal and regional dependencies will be observed in the acoustic material properties in relation to variations in alginate content. As high alginate content is characteristic of most large brown macroalgae, this consideration is applicable to other species.

2.5.5 Tissue intrinsic vs. individual low-frequency acoustic properties

It is interesting to compare the results we obtained by measuring the ultrasonic velocity of tissue to other acoustic studies on submerged aquatic vegetation to highlight the similarities. Results here expectedly differ from the acoustic properties measured on three seagrass species with an acoustic resonator tube (Wilson et al., 2010). However, the frequencies used by Wilson et al. (2010) are much lower than those used in our study, and since whole leaves of seagrass were placed in the tube, their gas content, tissue structure and tissue elasticity properties would all influence their measurements, making comparison with our results for *E. radiata* difficult.

Further measurements on sound speed of seagrasses (Enenstein et al., 2013) investigated sound speed independent of tissue structure using a mixture of blended tissue and artificial seawater similar to the homogenate prepared in the present research. The sound speed values, obtained at low frequency, were significantly lower than those found in the present study and may reflect fundamental morphological and anatomical differences between seagrass and phaeophytes in addition to differences in cell contents such as alginates and other storage carbohydrates. Macroalgae cells differ fundamentally from seagrass cells, most notably with the absence of large, interconnected gas-filled channels, or lacuna (Larkum et al., 2006), which facilitate fast exchange of oxygen between tissues and transport to roots and rhizomes (Armstrong, 1979). In seagrass meadows, oxygen produced through photosynthesis is also released directly into the surrounding seawater in gaseous form through the waxy cuticle of the leaf blades. In macroalgae, oxygen is produced in cortex layers and diffuses in dissolved form both in the medullar tissue in the thallus and through cell walls and the diffusive boundary layer. These factors, among others, may impact sound speed.

Also related to the present research, recent measurements on multiple kelp species using low-frequency acoustic resonance showed that Wood's equation with a two-phase frond + water model (where the frond is itself a 2-phase air + tissue model) successfully determined sound speed and compressibility of the frond structure for two species with pneumatocysts (*Macrocystis pyrifera and Egregia menziessi*) and of the tissue itself for one species with no pneumatocysts (*Laminaria solidungula*) (Wilson et al., 2013). As for *E. radiata*, the (low frequency) acoustic properties of these three species were shown to be different to seawater. For the two species with pneumatocysts, the inadequacy of an air + water + tissue model reflects the effect of tissue in restricting compressibility due to gas within the pneumatocysts. The resulting 'composite' values of sound speed and compressibility are lower and higher, respectively, than that of seawater as would be expected given the presence of gas in pneumatocysts. The intrinsic sound speed and compressibility of their tissue were not determined but removal of air from the pneumatocysts was shown to reduce the acoustic contrast with seawater. Direct determination of intrinsic sound speed with ultrasound is needed to compare these species with *E. radiata*, which does not have pneumatocysts. The species lacking pneumatocysts (*Laminaria solidungula*) in Wilson and colleagues (2013) work also showed a lower sound speed than seawater, in contrast to the values found in the present study. This may reflect species-specific differences in tissue structure and composition (e.g. alginate concentration, chloroplast density etc).

2.5.6 Extension to other SAV species

Our research shows good consistency across the different methods proposed to measure tissue sound speed and deduce compressibility. The method most suitable for the investigation of sound speed in other macroalgae species will depend, to a large degree, on the morphology of the species and the

tissue type of primary interest. Both blade stack and stipe methods by default measure sound speed for only one type of tissue, and so cannot provide average information of the macroalga as a whole. Additionally, with small species, making stacks of sufficient thickness to ensure minimal measurement error may be difficult, and stipe material may also be too short or too narrow to accommodate the diameter of contact probes.

Although the tissue homogenate could be adapted to include both stipe and blade, it is labour intensive and not applicable to species with pneumatocycts (e.g. canopy forming species such as *Macrocystis pyrifera* and *Phyllospora comosa*) as the gas filled chambers, which contribute to the acoustic response of an intact alga, would be destroyed and their gas lost in preparing a homogenate. However, this method is useful to investigate the tissue itself, and could be applied to smaller seaweed or seagrass species provided enough material is available. The submerged alga method was efficient and results consistent with the other approaches, therefore, this method is an attractive alternative for non-destructive measurement of the sound speed of macroalgae tissue. However, due to the need for constant rotation of the alga, this approach may prove difficult with smaller species due to the need for handling. This method is also inappropriate for intact seagrass due to scattering from their internal gas voids. An additional consideration is the thickness of the tissue relative to the acoustic wavelength. For smaller species measurements, higher frequencies may be impractical due to attenuation and scattering (Hermand, Randall, 2015).

It is important to control temperature when measuring sound speed in liquid media and in tissue with a high liquid content (Lofqvist et al., 2007). Temperature was measured accurately during the experiments with the submerged alga, homogenate and with the blade stacks. While care was taken to minimise temperature fluctuations during the stipe measurements, a number of our measurements had to be excluded due to temperature changes in the alga tissue as a result of unavoidable handling. Using thermal-insulated gloves or doing the measurement in a thermostatic bath would mitigate this problem. In addition, cutting of the stipe and blade material allowed loss of mucous from the macroalgae tissue, which may have led to changes in tissue composition. Maintaining the tissue at a constant and low temperature may have reduced mucous loss. However, this could also affect the tissue structure given the macroalgae came from a site with an ambient maximum temperature of 18 $^{\circ}$C.

2.5.7 Conclusions

A range of methods were developed for estimating the sound speed of *Ecklonia radiata* tissues. The acoustic material properties of density and compressibility vary according to size and tissue type, which may depend on age and season. The obtained values were likely explained by the cell type, packing and structure as well as the concentrations of alginates and other carbohydrates in the

macroalgae. These values by themselves do not describe the frequency-dependent acoustic behaviour of a whole alga or an entire macroalgae canopy. Nevertheless, they are essential input parameters to predictive numerical models (Etter, 2013). These models will advance acoustic habitat mapping and enable the development of acoustic inverse methodologies to estimate aggregate primary production over large spatial scales in temperate kelp beds or forests, and thus to inform their future management. The consistency among the results suggests that the proposed methods are robust options for future research into the acoustic properties of macroalgae that may otherwise be difficult to measure. The range of methods gives options for non-destructive sampling which is unique in enabling return of the samples to their natural environment and repeated measurements of individuals over time.

Acknowledgements

The authors would like to thank Rob Perry, Adam Stephens and Pearse Buchanan from the University of Tasmania for technical support and field assistance. Thanks to Eric Van Der Heyden and Bart Sarens from Laborelec Research Center, Belgium, and Pierre Demol from the Public Aquarium of Brussels, Belgium, for supply of equipment and laboratory assistance. The authors acknowledge the financial support (Grant agreement number N62909-13-1-N106) of the Office of Naval Research Global - Office of Naval Research (ONR), Australian Research Council (ARC), Australian National Network in Marine Science (ANNiMS), and Brussels Institute for Research and Innovation (INNOVIRIS).

Chapter 3

Acoustic investigation of the primary production of an Australian temperate macroalgal (*Ecklonia radiata*) system

3.1 Abstract

Temperate marine systems are dominated by rocky reef macroalgal habitats, and there is now evidence that some macroalgae communities are retreating in a manner consistent with climate change. Obtaining measurements of primary production across entire assemblages of algae over ecologically meaningful spatial scales is difficult, and acoustic techniques emerge as a method to consider. Acoustics has the potential to detect oxygen in gaseous form, hence it can measure primary production that is unseen by methods that use dissolved oxygen to estimate productivity. With levels of dissolved oxygen in kelp environments regularly reaching supersaturation, it is possible – even likely – that ecologically significant proportions of production have been neglected by traditional methods. To investigate the potential use of underwater acoustics in monitoring productivity of macroalgal habitats an experiment was run over two weeks during the Austral summer in February, 2012 in Canoe Bay, Tasmania. This paper details the results of Bellhop acoustic prediction model for two periods during the experiment chosen to compare contrasting diurnal productivity periods together with observed variation from the empirical experiment itself for these periods. The modelling results suggest that acoustic transmissions are able to detect ecologically significant proportions of oxygen in gaseous form in macroalgal environments (> 5% of total predicted production). However, changes of such magnitude in diurnal cycles of oxygen production were not seen in the empirical acoustic data during the experimental period, indicating that it is unlikely that there was a significant level of oxygen in gaseous form in the canopy layer. This work represents the first research into the use of acoustics to measure productivity in macroalgal systems. Further research, particularly in highly productive environments or when conditions are more favourable, will likely confirm that acoustics is a useful tool for assisting in monitoring primary productivity in macroalgal communities.

3.2 Introduction

Temperate reef macroalgal forests are amongst the most productive ecosystems on earth, providing essential structure for associated organisms including marine mammals, fish, crustaceans and molluscs (Steneck, Johnson, 2013). These habitats, with distinctive canopies primarily of brown laminarian algae (northern hemisphere), or laminarian and/or fucalean algae (southern hemisphere)

(Steneck et al., 2002), are particularly at risk from human activity. Overexploitation and the effects of coastal activities have resulted in significant habitat loss in some coastal ecosystems (Jackson, Sala, 2001), and human-induced climate change is now seen as a major threat to ecosystem health in marine systems (Richardson, Poloczanska, 2008; Wernberg et al., 2011; Wernberg et al., 2016). However, obtaining measurements of primary production across entire assemblages of algae over ecologically meaningful spatial scales is difficult, and acoustic techniques emerge as a method to consider (Hermand, 2003; Hermand et al., 1998).

Currently, there are a number of techniques that measure the productivity of marine macroalgae (seaweeds), both individually and collectively. Satellite and aerial imagery have been utilised to map changes in coverage in both seagrass (Ferwerda et al., 2007; Fletcher et al., 2009) and macroalgae (Mount, 2005; Tyberghein et al., 2012) habitats over time, and increasingly acoustic imaging is being used in marine environments to create habitat maps and characterise the benthic layer (Komatsu et al., 2002; Komatsu et al., 2003; Lucieer, 2008). Although this is now a well-established field, these techniques can only track ecosystem changes over long time periods, and they give little information on community productivity and health. In addition, there remain challenges related to background noise and detection of the presence of certain macroalgae (Urban et al., 2017; van Rein et al., 2011).

Additionally, benthic chambers are deployed to measure gas exchange/oxygen production and more recently Pulse Amplitude Modulation Fluorometry (PAM) has also become a popular tool for measurement of photosynthetic potential. Unfortunately, these techniques are limited in scale and there has been little research to compare measurements across the different techniques or quantify intraspecific spatial and temporal variability in production (however, see Edwards, Kim, 2010; Ekelund et al., 2008; Longstaff et al., 2002; Randall et al., In review).

The temperate coastline of Australia covers more than 3000 km, with southern Australia experiencing some of the largest increases in marine temperatures seen globally (Ridgway, 2007). This warming is expected to persist with a further increase of 1–3 ˚C expected in the next century (Lough, 2009). Temperate marine systems are dominated by rocky reef macroalgal habitats (Wernberg et al., 2003a), and there is now evidence that seaweed communities are retreating in a manner consistent with climate change (Johnson et al., 2011; Wernberg et al., 2011; Wernberg et al., 2016). With the synergistic effects of marine warming, overfishing and other anthropogenic changes there is now considerable concern for the future health of temperate kelp forests in Australia and in some other parts of the world (Krumhansl et al., 2016; Raybaud et al., 2013; Wernberg et al., 2011). *Ecklonia radiata* is a key habitat-forming macroalgae which dominates coastal water reef environments in southern Australia. *Ecklonia radiata* communities throughout Australia have

shown retreat consistent with recent marine warming (Wernberg et al., 2011), and/or factors indirectly related to warming, and the ability to track changes in production is important in order to monitor the future health of these shallow water environments.

Exploratory research in the Mediterranean have shown the potential of using acoustics to measure primary productivity. In seagrass meadows (*Posidonia oceanica*) daily photosynthesis dramatically increases the amount of oxygen in the water column in both dissolved and gaseous forms (Hermand et al., 1998). Variability in acoustic propagation is correlated with this diurnal productivity cycle, and can be mainly attributed to gas bubble production (Hermand, 2003; Hermand et al., 1998). Therefore, it is clear the effect of the gas bubbles on the acoustic signal can give information of photosynthetic parameters after some calibration. However, research in this area has been limited to seagrass communities. The high productivity of macroalgae (among the highest of any ecosystem; see (Cebrian, 1999) suggests that oxygen microbubbles may form in the water column due to dissolved oxygen reaching supersaturation (Ramsey, 1962). In addition, as for seagrasses, these microbubbles may accumulate on the surface of the thallus blades or in a water surface layer when supersaturation conditions are attained.

Hence, acoustics has promise as a tool that may greatly enhance ability to estimate and monitor variation in productivity in kelp forests over ecological meaningful spatial and temporal scales. Most direct estimates of production rates in macroalgal communities uses measurement of change in dissolved oxygen (DO) to estimate oxygen production. However, given the likelihood that ecologically significant proportions of the oxygen produced may be in gaseous form, there is a risk that marine ecologists are underestimating productivity in coastal environments, particularly in highly productive systems such as seaweed communities. Furthermore, the use of acoustics would allow integration of productivity measurements over large spatial and temporal scales as has been demonstrated for seagrass communities (Hermand et al., 1998).

To investigate the application of underwater acoustics in monitoring productivity of macroalgal habitats and examine the possibility that estimates of primary productivity based solely on measurements of dissolved oxygen may be biased, an experiment was run over two weeks during the Austral summer in February, 2012, in Canoe Bay, Tasmania. This paper investigates the low-frequency acoustic effects of various scenarios of bubble occurrence in the water column by means of Bellhop beam-tracing model (Porter, 2011) and Urick's mixture theory. The characteristics of the modelled impulse responses are compared to those measured during two contrasting periods of diurnal productivity of the experiment.

3.4 Methods

3.4.1 Experimental arrangement

The experiment was carried out in the sheltered and dense kelp forest of Canoe Bay (43.12583 ˚S, 147.96056 ˚E), Tasmania, over a period of sixteen days from 8th to 24th February, 2012 (Figure 3.1B). A measurement transect of 150-m length was defined on the ≅ 7.5 m-depth contour. In that area, the species *E. radiata* occupies ≅90 % of the canopy cover over dolerite reef. The relatively calm setting of the site provided stable environmental conditions for the duration of the experiment and the sheltered bay chosen for the site provided close shore proximity for cable connection to the land station. Deployment of all equipment was done by divers via small aluminium dinghy.

All acoustic stations were mounted on aluminum tower frames, with a broadband sound source (S) positioned at the western end of the transect, at a height of 145 cm from the benthos. Receiver stations 1 and 2 (R1 and R2) were positioned 75 m and 150 m east, respectively (Figure 3.1A). The source transmitted a continuous train of chirp signals linearly-frequency modulated from 200 Hz to 20 kHz with a duration of 1 s. Each receiving station featured a vertical pole made of carbon fiberglass holding two hydrophones, one (a) within the canopy (25 cm from seafloor) and one (b) above the canopy (175 cm from seafloor). The acoustic systems were built at the University of Brussels (ULB) based on designs from the earlier experiments in seagrass meadows (Hermand, 2003; Hermand et al., 1998). Station positions were determined from surface GPS readings on the stations, and distances between the stations were measured underwater with a taught transect line marked at 1 m interval and pulled tautly over the top of the canopy.

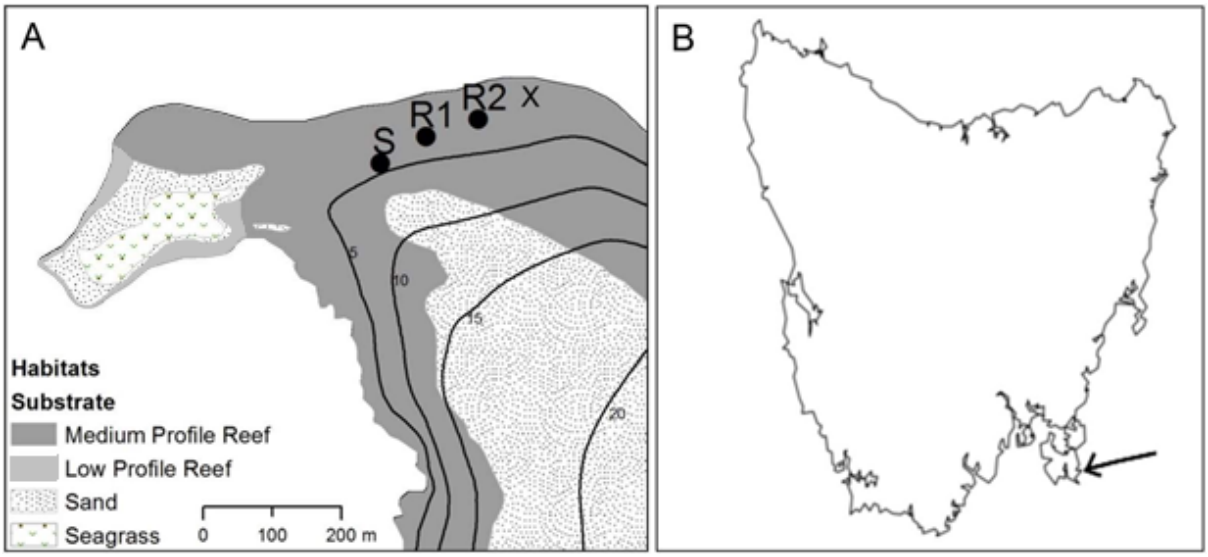

Figure 3.1: A) Location of experimental transect in Canoe Bay, Tasmania. All stations were situated on the ≅ 7.5 m contour line, with sound source (S) positioned at the western end of the transect, separated from Receiver 1 (R1) by 75 m and Receiver 2 (R2) by 150 m. Each receiving station contained a within-canopy hydrophone (25 cm from benthos) and an above-canopy hydrophone (175 cm from benthos). The "x" symbol denotes a third station that was intended but not used for acoustic measurement purposes. The area labelled "Medium Profile Reef" supports macroalgae cover. Note transect positions shown are based on GPS readings taken onsite and differ slightly from contour lines obtained via echosounder mapping. Image courtesy of Justin Hulls (IMAS), produced using SEAMAP Tasmania data (Barrett et al., 2001). B) Map of Tasmania, Australia with arrow indicating location of Canoe Bay.

In addition to the acoustic array, a large array of environmental sensors measuring pressure, temperature, salinity, and turbidity were deployed throughout the underwater acoustic section and onshore to monitor environmental factors for the duration of the experiment (Table 3.1). Dissolved oxygen and photosynthetically active radiation sensors were also positioned on the transect for monitoring of photosynthetic parameters. These sensors were autonomous data loggers (NKE) attached to the source and both receiver tower frames at different heights beneath and above the canopy. On each tower the sensors were: pressure/temperature (P/T) (SP2T), turbidity (STBD/Seapoint STM), PAR (SPAR/Licor 192SA underwater quantum sensor) and DO (SDOT/Aanderaa oxygen optode model 4330F). Pressure sensors were calibrated via a shore-based reference pressure sensor to remove the variation of atmospheric pressure and, in particular, to obtain an accurate measurement of tide height.

Additional temperature/salinity (T/S) (Hobo, USA), pressure/temperature/salinity (P/T/S) (NKE SP2T) and DO (D-Opto Logger, Zebra-Tech Ltd) sensors were attached at several depths on a weighted string moored to a surface float, positioned close to the sound source. A weather station was mounted onshore (≅ 110 m from transect, ≅1 m above sea level) to continuously record wind

speed and direction. A bottom-mounted acoustic Doppler velocity profiler was used to obtain time series of current/depth profiles and, most importantly, wave parameters to assess (non-photosynthetic) bubble production in the water layer immediately below the surface.

Table 3.1: Depth (m) and positions on the transect of the autonomous data loggers which continuously recorded pressure and temperature (P/T), DO, PAR, temperature and salinity (T/S), and pressure, temperature and salinity (P/T/S) (Fig. 3.2). These data at fixed depths as well as depth profile data (Figs. 3.3) were used to create sound speed profile inputs (Fig. 3.4) to the acoustic propagation model, to interpret the acoustic transmission measurements, and develop the oxygen model as described in Chapter 4.

Source		Receiver 1		Receiver 2		String	
Sensor	**Depth (m)**	**Sensor**	**Depth (m)**	**Sensor**	**Depth (m)**	**Sensor**	**Depth (m)**
P/T	7.2	P/T	7.2	T/S	6.8	DO	0.5, 3
		DO	6.5	PAR	6.5, 6.8	T/S	0.5, 2, 3, 5
		PAR	6.1	DO	6.8, 7.0	P/T/S	0.5, 3, 5

The substratum of the kelp forest consisted of rocky dolerite reef with a discontinuous sediment cover of less than 5 cm of course sands in some places. Dolerite (also known as diabase) is a medium-grained igneous rock largely containing plagioclase feldspar, pyroxene, and augite, with labradorite and titanaugite as additional "essential" minerals (Sloane, 1991). As the bathymetric variations along the acoustic transect were significant with respect to the transmitted wavelengths (λ > 7.5 cm) and water depth, divers measured the water depth at intervals of 1 m along a line joining the source and receiver stations, by means of calibrated digital diving depth gauges. Measurements were taken by two divers and averaged, as a key feature of the acoustic propagation modelling work was to use a detailed bathymetry profile which provides a more realistic simulation of the physical reality.

3.4.2 Environmental features

The features of the water body and seafloor acquired during the experiment served as the basis on which to build a model of the environment with a level of detail sufficient for acoustic propagation modelling and comparison with data. Our investigation required periods of high DO concentration where the occurrence of oxygen bubbles in the water column due to photosynthesis was more likely. Accordingly, the first four days of the experiment were chosen as the waters were calmer and the irradiance was higher than for the remainder of the experimental period. Within these four days, two "snapshot" periods were chosen reflecting contrasting periods of high (Hp) and low (Lp) primary productivity in the mid afternoon and late night, respectively.

Figure 3.2 shows the environmental time series from Monday 13th to Thursday 16th February. During this period, seawater temperature and salinity (Figure 3.2A, B) varied by less than 2.5 °C and 1.5 ‰ respectively among the fixed sampling points in both depth and range, resulting in an overall sound speed variability of less than 4 m s^{-1}. While wind speed was low, diurnal cycles in wind speed were evident with shore wind speeds of up to ≅ 5 m/s (Figure 3.2C). Tide showed variation in water depth of up to 0.9 m (Figure 3.2D). From photosynthetically active radiation (PAR) and dissolved oxygen (DO) sensors (Figure 3.2E, F), time periods of high (Hp) and low (Lp) productivity were chosen at which the respective tide heights were equal and wind speeds low. Difference in measured acoustic propagation characteristics between these two periods would therefore indicate, if present in sufficient quantity as compared to the bubble background, the likely presence of additional bubbles in the water column due to photosynthesis. These periods are centred at times 15 hr 30 13th February and 04 hr 45 14th February, 2012. In this way, differences in multipath arrival structure (the propagation phenomenon that results in sound waves reaching the receiver more than one path through multiple reflections at the surface and bottom) due to differences in water depth did not need to be taken into account in the comparison.

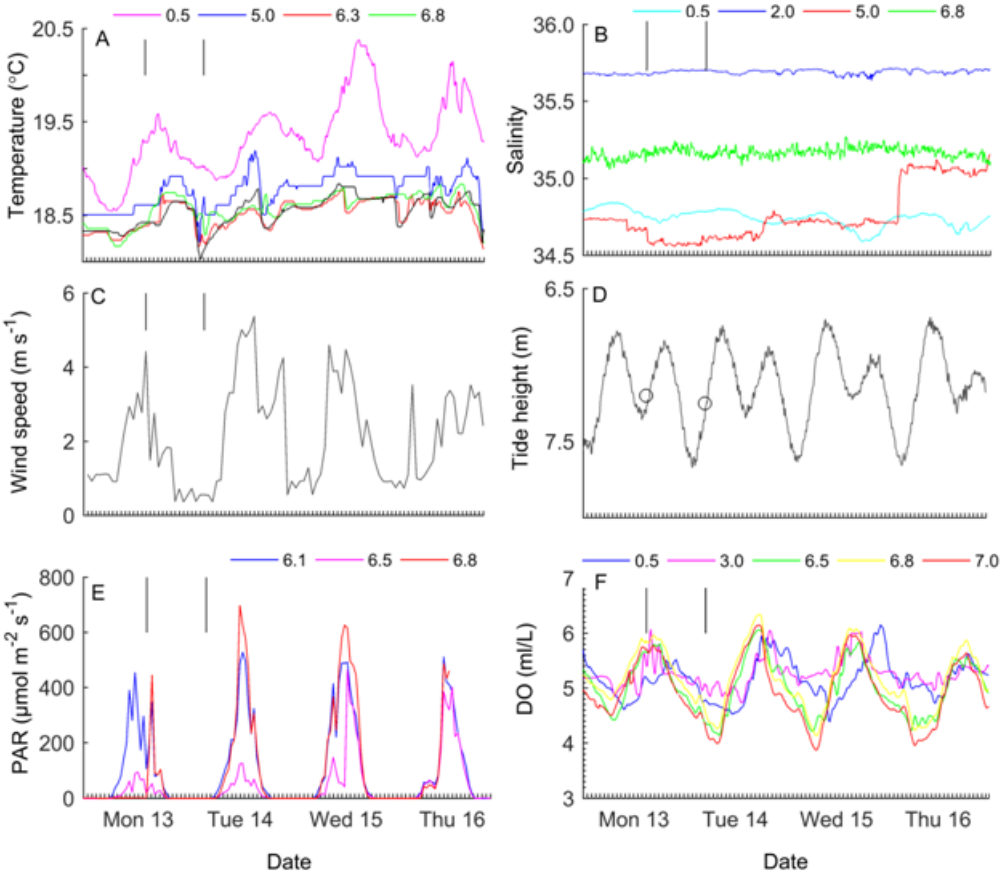

Figure 3.2: Time series of the environmental data logged during early part of FORTES 12 experiment, Canoe Bay, Tasmania, 13th to 16th February, 2012. (A) Temperature and (B) salinity showing vertical gradients. (C) Wind speed was minimal with diurnal cycles. (D) Tide variation was significant relative to average water depth along the transect. (E) Photosynthetic active radiation and (F) dissolved oxygen showed marked increases daily, with DO offset to mid afternoons. Black vertical lines (A-C, E, F) and circles (D) indicate the high and low primary production periods of interest, denoted Hp and Lp in the main text, whose centre times are 15hr30 on 13th February and 04hr45 on 14th February, 2012. The legends indicate the respective sensor depths in meter at the tide height of Hp centre time.

Temperature, salinity and DO profiles of the water column were taken at varied positions along the transect to assess small-scale variations across range and depth which may not have been captured by the fixed sensors (Sonde 6-series model 6600 V2). There was some small-scale variation in these parameters from the values recorded from the water column sensors at the time profiles were taken (Fig. 3.3). Part of these differences were likely the result of water column mixing and turbulence due to boat movement and diving operation. Nevertheless, spatial variability was negligible as compared to the temporal variability that would result from a significant increase of void fraction in the water column. Therefore, the model assumed horizontally stratification in most parts of the water column except near the bottom as discussed below.

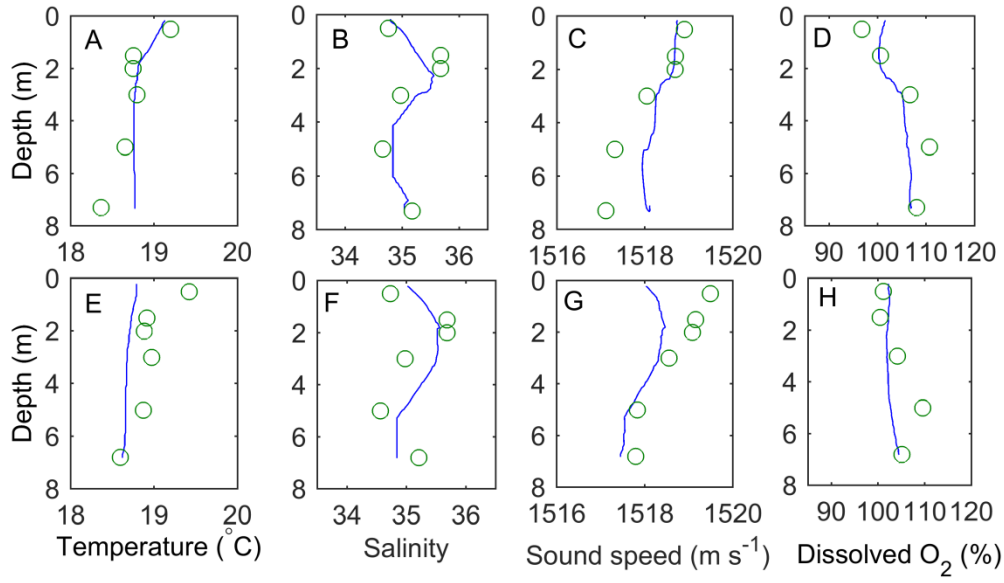

Figure 3.3: Temperature, salinity, sound speed, and dissolved oxygen comparing recorded values from water column sensors at fixed depths and a vertical profiler on 1st February 2012 at 14 hr 00 (A,C,E,G) and 19 hr 00 (B, D, F, H). Circles indicate values from fixed water column sensors with blue lines representing profiles from the Sonde instrument. Differences in depth are due to tide.

Likewise, the sound speed profile calculated from temperature and salinity measurements at fixed depths did not vary much over a 1-hour period during mid afternoon and late at night (Figure 3.4), with maximum differences in sound speed at any point in the water column <0.5 m s^{-1}. As expected due to temperature changes, sound speed was slightly higher in the mid afternoon. These observations indicate that sound speed variability due to temperature and salinity alone cannot be responsible for any important acoustic variations detected. Sound speed anomalies of tens of meters per second due to an increased void fraction from wind or from micro-bubble production during photosynthesis would have a much higher impact, simplifying the interpretation of the acoustic variations.

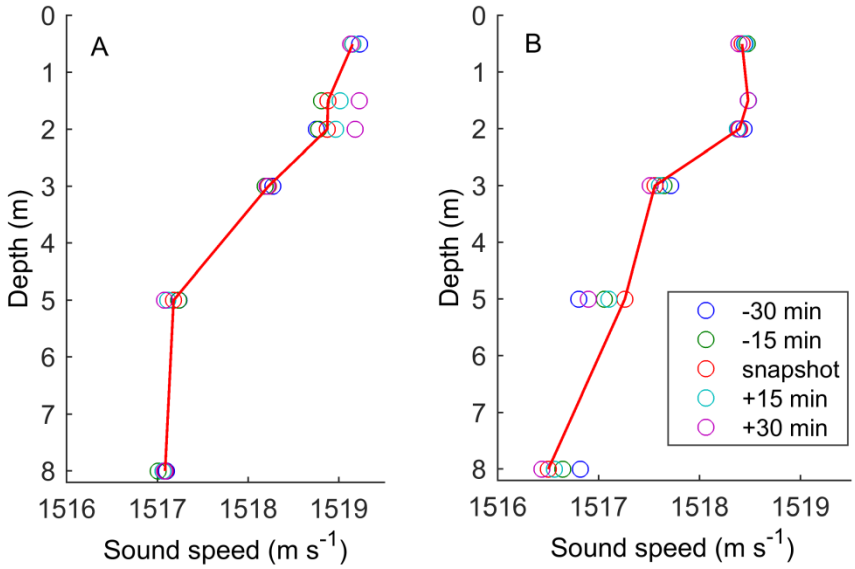

Figure 3.4: Sound speed variability in the water column. The profiles are constructed from temperature and salinity measured by the fixed sensors for (A) day period (15hr30 13th February) and (B) night period (4hr45 14th February). The profiles are shown at the respective snapshot times, and 15 and 30 minutes immediately before and after. Red lines indicate snapshot periods.

3.4.3 Acoustic propagation modelling

For modelling the acoustics of Canoe Bay environment, ray-theory solution of the wave equation was preferred because of the short distances between source and receivers and the large (tidal) bathymetric variations (~0.9 m) relative to the average water depth (7.5 m). The selected numerical model was Bellhop, a ray-tracing program (Porter, 2011) designed initially to efficiently perform two-dimensional (and now 3D) acoustic ray tracing for a given sound speed profile or sound speed field in ocean waveguides with flat or variable absorbing boundaries. The calculation of acoustic pressure is based on the theory of Gaussian beams (Oliver, 1957) which can be applied using different approximations. In comparison to standard ray tracing, the method has the advantage of being free of certain ray-tracing artefacts such as perfect shadows and infinitely high energy at caustics.

For our purpose, the numerical efficiency of the Bellhop code was instrumental in predicting the complex multipath arrival structure due to rough bathymetry and the bubble layer in the canopy from oxygen production. Bathymetric features at length scales larger or comparable to transmitted acoustic wavelengths create obstacles which scatter sound in all directions, while any bubble region causes strong refraction which, depending on sound speed change, acoustic wavelength frequency, and layer thickness, may create an effective waveguide below the sea surface or within the canopy. Hence, the number of beams had to be very large in order to obtain an arrival structure sufficiently

populated for accurate estimation of an energy decay curve (at the receiver point). Furthermore, convolution of the predicted impulse response , as synthesised from all the transmitted signal autocorrelation provided the band-limited impulse response of the acoustic channel to compare with data.

For modelling the bottom, all details of the measured bathymetric profile were incorporated in the model with particular attention to the way the bathymetric data were interpolated. Trial-and-error determined that a grid step of 10 cm was sufficient. The profile was corrected for the tide height at the time of the day and night snapshots to be modelled. The geoacoustic properties of dolerite were extrapolated from basalt, assuming an average density of 2700 kg m^{-3}, compressional and shear wave speeds of 5250 m s^{-1} and 2500 m s^{-1} respectively, and with respective attenuations of 0.1 dB/λ and 0.2 dB/λ (Jensen et al., 2000).

For modelling the water column, sound speed (in the absence of a significant void fraction) was calculated according to the Thermodynamic Equation of Seawater - 2010 (TEOS-10) (McDougal, Barker, 2011) using based on our empirical measures of temperature, salinity and depth. The sound-speed depth profile (SSP) varied temporally, reflecting that Bellhop SSP inputs were created from the fixed sensor measurements only, which were then interpolated using piecewise cubic Hermite interpolating polynomial (PCHIP) to obtain sound speed values at 1-cm depth intervals near the boundaries (from surface [0 m] to 1.5-m water depth and from 6-m depth to the variable-depth bottom). Between 1.5-m and 6.5-m depths, the step in depth was 10-cm. The resulting sound speed field determined by temperature, salinity and pressure alone was then modified to account for the low-frequency effective sound speed change due to the presence of bubbles in different layers (the so-called sound speed 'anomoly'.

The kelp layer was determined from field measurements to extend an average of 40 cm from the benthos. The volume ratio of macroalgae tissue in the canopy layer was estimated to approximately 1–2 % from laboratory measurements of average volume of kelp and biomass collected at the study site. Although laboratory measurements of density and compressibility of *E. radiata* tissue were available (Randall et al., 2014) no adjustment of the effective low-frequency sound speed in the canopy was necessary. Ignoring frequency-dependent scattering due to the macroalgae tissue (Hermand, 2016a) and given the thickness of the macroalgae layer the modelling results should be valid in the transmitted frequency range (1−20 kHz). All the model runs used a $6\ 10^{-6}$ geometric beams uniformly distributed in an angle sector of -80 ˚to 80 ˚. A quadratic approximation to the sound speed field was used, with vacuum above the surface, and an acoustic half space below the water column with the above given properties. Because of the close proximity of R2 receiver to the

seafloor could introduce modelling artefacts, all model runs were verified by interchanging source and receiver positions.

Four values of oxygen void fraction in the canopy layer were chosen for acoustic modelling for the day period. The distinct gradient in dissolved oxygen concentration (Figure 2F) in the water column shows a high concentration layer in the canopy, reaching 338.73 µmol/L for the day period (15hr30 13th February). The oxygen saturation level was calculated based on temperature and salinity using the Benson and Krausse (1984) equation:

$$\ln C_o * = A_0 + A_1 T^{-1} + A_2 T^{-2} + A_3 T^{-3} + A_4 T^{-4} A_4 + S(B_0 + B_1 T + B_2 T^2 + B_3 T^3)$$

where Co* is the solubility of oxygen per mass/volume of seawater at the temperature of equilibrium, and *T* and *S* are temperature (Kelvin) and salinity respectively, and *A* and *B* are constants. For our case study, at 15 hr 30 on13th February, with a recorded temperature of 18.4 ˚C and salinity of 35.17 ppt, the oxygen saturation point is 234.53 µmol/L. Therefore, for the period of interest, the dissolved oxygen concentration in the canopy layer had attained the level of supersaturation, although not necessarily the threshold for spontaneous formation of bubbles.

Hydrostatic pressure can cause dissolved oxygen levels to be greater than that of the saturation level without formation of oxygen bubbles if there is no or slow diffusion of oxygen from the macroalgae tissue into the surrounding sea water. However, a higher concentration of bubbles may also occur locally due to bubble formation on the macroalgae blades, as has been documented for seagrass blades (Hermand, 2003; Hermand et al., 1998), resulting in much higher void fractions in the canopy layer than in the surrounding seawater. Therefore, given that localized bubble occurrences due to photosynthesis were *a priori* possible in the environment, the void fraction values used for "bubbles-in-canopy" acoustic scenarios featured undissolved oxygen amount that are ecologically significant, and therefore useful for investigation of the effectiveness acoustic measurements in such conditions.

The void fractions were determined from estimates of the productivity of the kelp bed calculated from models estimating production of dissolved oxygen by seaweeds in the benthic layer at Canoe Bay (Chapter 4). With environmental conditions suitable for supersaturation of dissolved oxygen at the depth of the canopy during the afternoon of the chosen day period (Hp), the hypothesis is that a proportion of the production would be bubbles that remained trapped in the canopy or adhered to the surface of the seaweed blades. Hence, the total production for the thirty minutes preceding the day time 'snapshot' was calculated (0.92 ml O_2/L from model 1; Chapter 4). Different percentages of this

total production were used as the void fractions of oxygen in the canopy layer in the model. The environmental model incorporated the TS-sound speed profile measured during the same period (Hp).

A first acoustic model factored in a void fraction of 4.6 e^{-5}, corresponding to 5% of oxygen produced in gaseous form, to investigate the ability of acoustic transmission to detect a significant and ecologically feasible proportion of oxygen not sensed by a DO optode. For the second model, a void fraction of 9.2 e^{-5} (10% of oxygen in gaseous form) was tested. A third model tested a void fraction of 2.8 e^{-4} (30% of oxygen in gaseous form). A reference model was run with no void fraction in the canopy layer (or elsewhere in the water body) using the same TS-sound speed profile. For the night period (Lp) a model was run for the environmental conditions recorded at that time with a zero void fraction. All models were run for the two ranges (75 m and 150 m) separating the sound source and receivers, using both the hydrophones above (R1) and within the canopy (R2).

The decrease in low-frequency sound speed due to the presence of bubbles was calculated according to the 'effective medium' acoustic model, commonly used in underwater acoustic research (e.g. Kargl, 2002; Wilson et al., 2010). This approach is based on propagation of low frequencies in multiphase materials as proposed by Wood (1932) and developed by Urick (1947). Provided that the acoustic wavelength is larger than the characteristic size of the mixture components (i.e. bubbles) and the mixture is homogeneous, the expected sound speed of the mixture can be calculated knowing the intrinsic acoustic material properties of the components. Therefore, the effective sound speed c_{eff}, in the seawater layers, which is equal to the expected sound speed c_{exp}, is given by:

$$\frac{1}{c_{\mathrm{eff}}^2} = \frac{1}{c_{\mathrm{exp}}^2} = [\sum_i \phi_i K_i]\,[\sum_i \phi_i \rho_i] = \left[\sum_i \frac{\phi_i}{c_i^2 \rho_i}\right][\sum_i \phi_i \rho_i]\,,$$

where κ_i , c_i , ρ_i , and ϕ_i represent the compressibility, sound speed, density and volume fraction of material or component *i* in the homogeneous mixture. Table 3.2 gives the effective sound speed for the above scenarios of 5%, 10% and 30% of total oxygen production present entrapped as bubbles in the canopy. The formula is only a first order approximation when the bubbles are not suspended freely in the water column but in contact with the blade surface.

Table 3.2: Proportion of oxygen production in bubble form, corresponding void fraction in a given layer, and low-frequency effective sound speed for each model scenario.

O_2 in bubble form	30 minute O_2 production	Void fraction	Sound speed (m s^{-1})
No void fraction in canopy			1517.1
5% of productivity in canopy	0.046 ml/L	$4.6e^{-5}$	1266.8
10% productivity in canopy	0.092 ml/L	$9.2e^{-5}$	1109.9

30% productivity in canopy	0.276 ml/L	$2.8e^{-4}$	839.5
Surface layer from wind		$1.0e^{-6}$	1509.1
Water column void fraction	0.276 ml/L	$1.4e^{-5}$	1371.9
Surface supersaturation	0.276 ml/L	$1.1e^{-4}$	916.3

Additional models were run with a 10% void fraction of gaseous oxygen in the canopy at a period of low tide height (6.83 m) and high tide height (7.41 m) on the 13th February 2012. These models accounted for the tide-dependent temperature and salinity variations. These models were used to compare the respective effects of tidal height variation and void fraction variation on the multipath arrival structure and energy decay curve. The difference in environmental conditions depending on the time of day and tide (Figure 3.5) indicates that sound speed from salinity and temperature does not vary substantially, however, DO concentrations in the water column greatly fluctuate.

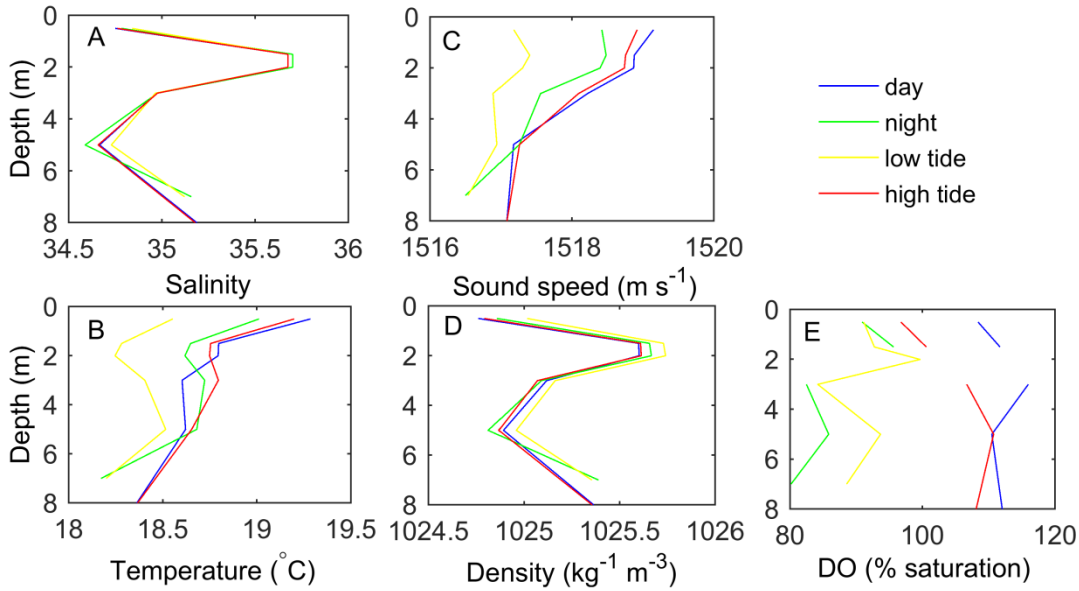

Figure 3.5: Salinity (A), temperature (B), sound speed (C), density (D), and dissolved oxygen (E) measured by fixed water column sensors in the acoustic transect for the day (15hr30), night (05hr45), high tide (14hr00), and low tide (08hr00) time periods on the 13th and 14th February 2012.

Although the surface winds in our study site were relatively low with ~0.5 m s^{-1} at night reaching 5 m s^{-1} during the day-time period, with wave heights less than 0.5 m, a bubble layer existed below the sea surface which modified acoustic propagation. Bubbles from air/sea interface can extend to ≅1 m depth with void fractions in the range of 10 e^{-7} for sea with no breaking waves (Lewis, Schwartz, 2004). Lamarre and Melville (1994) found dramatic fluctuations in sound speed in surface waters relative to wind speed, again with the majority of the effect seen in the top 1 m layer.

According to their experimental data, for a wind speed of 5 m s^{-1} (the maximum experienced during our study period), the sound speed in the surface layer decreases by ~10 m s^{-1}. Thus, to compare the predicted effects of a wind bubble layer and a canopy bubble layer, an additional model was run for a void fraction of 1.0 e^{-6} in a 1-m thick layer below the surface for the measured TS-sound speed conditions of the daytime snapshot (Hp).

Three of the previous models assumed that the oxygen in gas form would be concentrated in the canopy layer where the oxygen is produced, and the formed bubbles would be entrapped in the canopy. Indeed, the DO measurements support this scenario showing increasing concentration toward the seafloor (Figures 3.2 and 3.3). Alternatively, the presence and distribution of bubbles in the water column is subject to other factors, such as the need for a bubble nuclei and the effect of pressure at depth (Ramsey, 1962). To test this assumption, two other scenarios were investigated considering a void fraction due to supersaturated conditions in a 1-m thick surface layer and a void fraction uniformly distributed throughout the entire water column. For both models, the respective void fractions were calculated assuming that 30% of the total production was oxygen in bubble (gaseous) form (Table 3.2).

3.4.4 Acoustic measurement and processing

The continuous train of broadband-coded signals emitted by the broadband source and received on the two pairs of hydrophones at R1 and R2 after their propagation through the kelp forest were processed to extract the impulse response of the medium (Hermand 1999). The processor, called a 'matched filter', correlates the received signal plus noise with a replica of the source waveform. In the present experiment, the transmitted signals or 'chirps' consist of a linear frequency modulation from 200 Hz to 20 kHz over a duration of 1 s. The matched filtering produced a band-limited version of the medium response every second for the whole period of the experiment. The reader interested in signal processing details is referred to Hermand (2004) for an earlier, similar application of the present measurement technique in seagrass meadows. In the present experiment, sample-accurate synchronization of the source emission and received data acquisition at a sampling frequency of 96 kHz allowed measurement of absolute travel times. This synchronization allowed statistically reliable estimation of the medium response at an arbitrary repetition rate by ensemble-averaging the responses over the corresponding interval. This eliminated short-term acoustic variability and mitigated the impact of ambient noise, especially sound production by fauna in the vicinity of the receivers. For this work, the medium impulse response was estimated for the high (Hp) and low (Lp) productivity periods using 1200 realizations about the respective center times.

3.5 Results

Detailed description of the bottom features in the Bellhop range-dependent environmental model resulted in complex patterns of the ray paths connecting the source and each receiver through multiple reflections at the boundaries (Figure 3.6A). The eigenray plot is for the receiver in the canopy at 150 m from the noise signal source. The impact of the bathymetry is important because it varied by up to 0.9 m, representing more than 10% of the average water depth. A description based on a smoothed or linear fit to the original bathymetric data resulted in an organized pattern of eigenray paths and arrivals (not shown), which was not observed in the *in-situ* measurements. As the nature of the bathymetric variations does not change along the transect (Figure 3.6B), a similar level of complexity is observed at the two receiver stations R1 and R2. In the example shown, there is a clear channelling of energy in the canopy layer, which contains 30% of predicted total production in gaseous form; other similar plots show that the concentration of eigenrays trapped in the canopy layer increases with the absolute magnitude of the void fraction of gaseous oxygen.

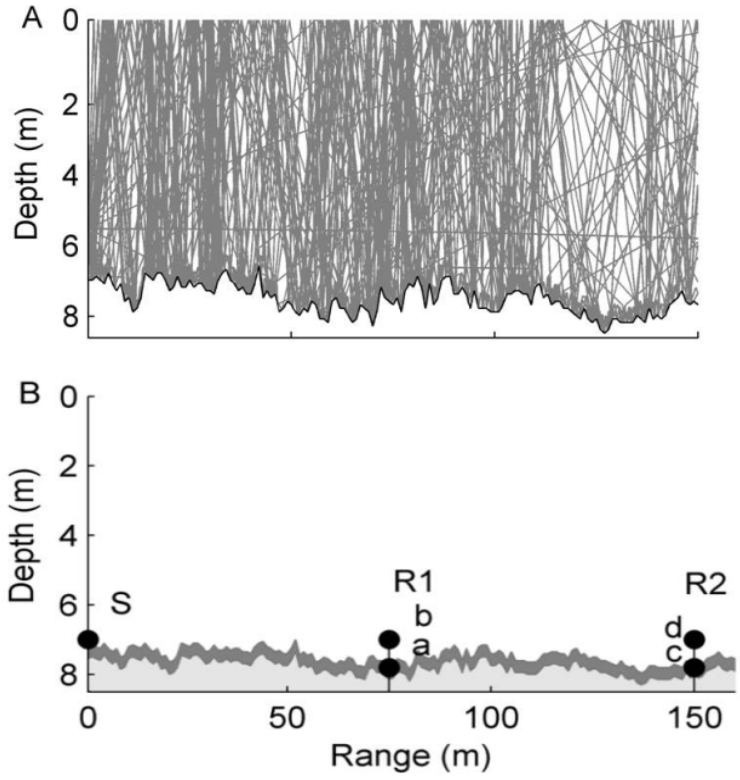

Figure 3.6: A) Eigenray plot showing the rays that connect the source and the receiver in the canopy at 150-m range (R2B) for the scenario where the void fraction of gaseous oxygen in the canopy corresponds to 30% of the predicted total production. For clarity, only a few rays are displayed. The rays travelling in the canopy layer can be recognized by the darker region just above the sea floor. The complex pattern of ray paths is due to the rugged bathymetry of the bottom. Prediction of multipath arrival structure used a fan of 1.6 million geometric beams within a beam angle sector of −80˚ to 80˚. (B) Diagaram representing the position of the sound source (S) and R1 and R2

hydrophones beneath (a,c) and above (b, d) the canopy layer (dark grey) overlying a half-space elastic bottom of dolerite (light grey). The ray-tracing code is Bellhop.

The acoustic modelling results of the scenarios described above were compared in terms of the multipath arrival structure or medium impulse response envelope (smoothed log envelope). For a given environmental model, a prediction of the band-limited impulse response as measured at sea is the convolution of the autocorrelation function of the transmitted signal with the complex-valued arrivals computed by the ray-tracing code. The multipath arrival structure as directly output by the code provides the detailed shape of energy time spreading which is an important character of the acoustic propagation environment. Filtering the broadband impulse response allows investigation separately of different frequency ranges of interest.

When comparing between the multipath arrival structures of different void fractions of oxygen in the canopy layer and the day and night time periods with no void fraction, there are clear differences in the overall energy level (in dB) and the shape of energy time spreading, including the decay rate (Figure 3.7; R2B within-canopy hydrophone). For no void fraction, similar patterns are seen for both night time and day time scenarios since the sound speeds in the water column did not vary significantly. In contrast, for void fractions of 5%, 10% and 30% of oxygen in gaseous form in the canopy layer there are clear shape differences in the predicted energy time spread. There are also marked differences in the fine structure of the early arriving rays, which appear to be very sensitive to the void fraction. Results show similar responses for both in-canopy and above-canopy hydrophones at both the R1 and R2 stations (Appendix Fig. 3A-C) but the fine structure of arrivals are quite different when examined in detail. The energy decay rates for the various scenarios are smaller at the short range (75 m) than long range (150 m) hydrophones, i.e. attenuation of sound energy is higher in the canopy and at the long range (150 m).

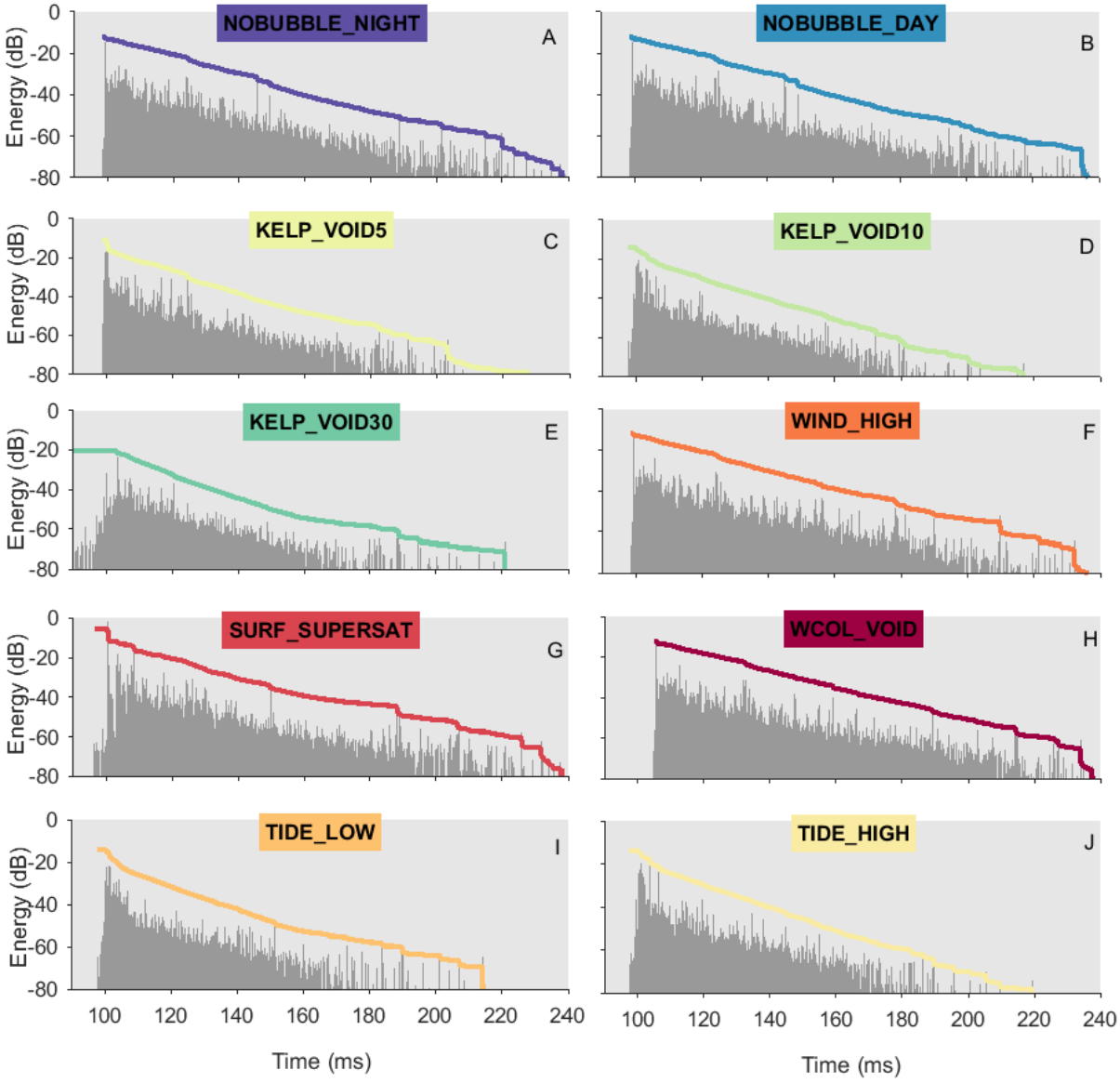

Figure 3.7: Predicted multipath arrival structure at the receiver in the canopy at the range of 150 m (R2B) for different scenarios. (A) No oxygen void fraction for the night time period at 04 hr 45 on 14th February LT. (B) No oxygen void fraction for the day time period 15 hr 30 13th February LT. (C) Oxygen void fraction of 4.6 e^{-5} (5% PTP). (D) Oxygen void fraction of 9.2 e^{-5} (5% PTP). (E) Oxygen void fraction of 2.8e^{-4} (30% PTP). (F) Inclusion of a surface bubble layer due to wind with a void fraction of 1.0 e^{-6}. (G) Supersaturation of surface layer due to photosynthesis with a void fraction of 1.1 e^{-4} (30% PTP) in the mid-afternoon period. (H) Water column with a void fraction of 1.4 e^{-5} (30% PTP) in the mid-afternoon period. (I) Low tide with a void fraction of 9.2 e^{-5} in the canopy layer (10% PTP) in the mid-afternoon period. (J) High tide with a canopy layer with a void fraction of 9.2 e^{-5} (10% PTP) for the day time period. These simulations were made with Bellhop acoustic propagation model using 1.6 million geometric beams within an angle sector of −80˚ to 80˚.

The model simulating an environment with a surface bubble layer caused by wind (Figure 3.7F) gives a similar pattern to the day time and night time (no bubble) models, even for the early arrivals. As expected, results are quite different in term of absolute travel time for the scenario of a constant

(but smaller) void fraction throughout the entire water column (Figure 3.7 H). There are no meaningful differences between the high and low tide models (Figures 3.7 I and J; run with a void fraction of 10% of oxygen in gaseous form) and the daytime for the same void fraction (Fig. 3.7 D). This indicates that tide has a smaller effect on the predicted arrival structure than the scenarios of most interest (Figures 3.7 C, D and E). The scenario of surface supersaturation (Figure 3.7G) shows an early ray arrival structure which is distinctly different from those predicted by the models with a canopy layer void fraction.

The energy decay rate can be better estimated from the so-called energy decay curve (EDC) which is obtained by reversed time integration of the squared impulse response (Schroeder, 1965). This type of integration gives the smoothest possible curve for robust comparison of the different scenarios, particularly for the tail of the response which is as important as the early arrivals. When comparing a void fraction of 30% of predicted total production remaining in gaseous form in the canopy against the day time snapshot with no void, differences as high as 10 dB are found along the respective EDCs (Figure 3.8). The differences are due to the absorption of energy from the rays with longer trajectories and many reflections, as well as the fine structure of the early arrivals. The EDC confirms that the energy decay pattern in the surface supersaturation model is clearly different to the model where the void fraction comprises microbubbles within the canopy, which shows a total energy slightly higher than the 'no void' scenario. The EDCs for models with a canopy void exhibit different behaviors for the short and long ranges as well as for above and below the canopy. At long range there is a difference in total energy of −8 dB for the hydrophone in the canopy.

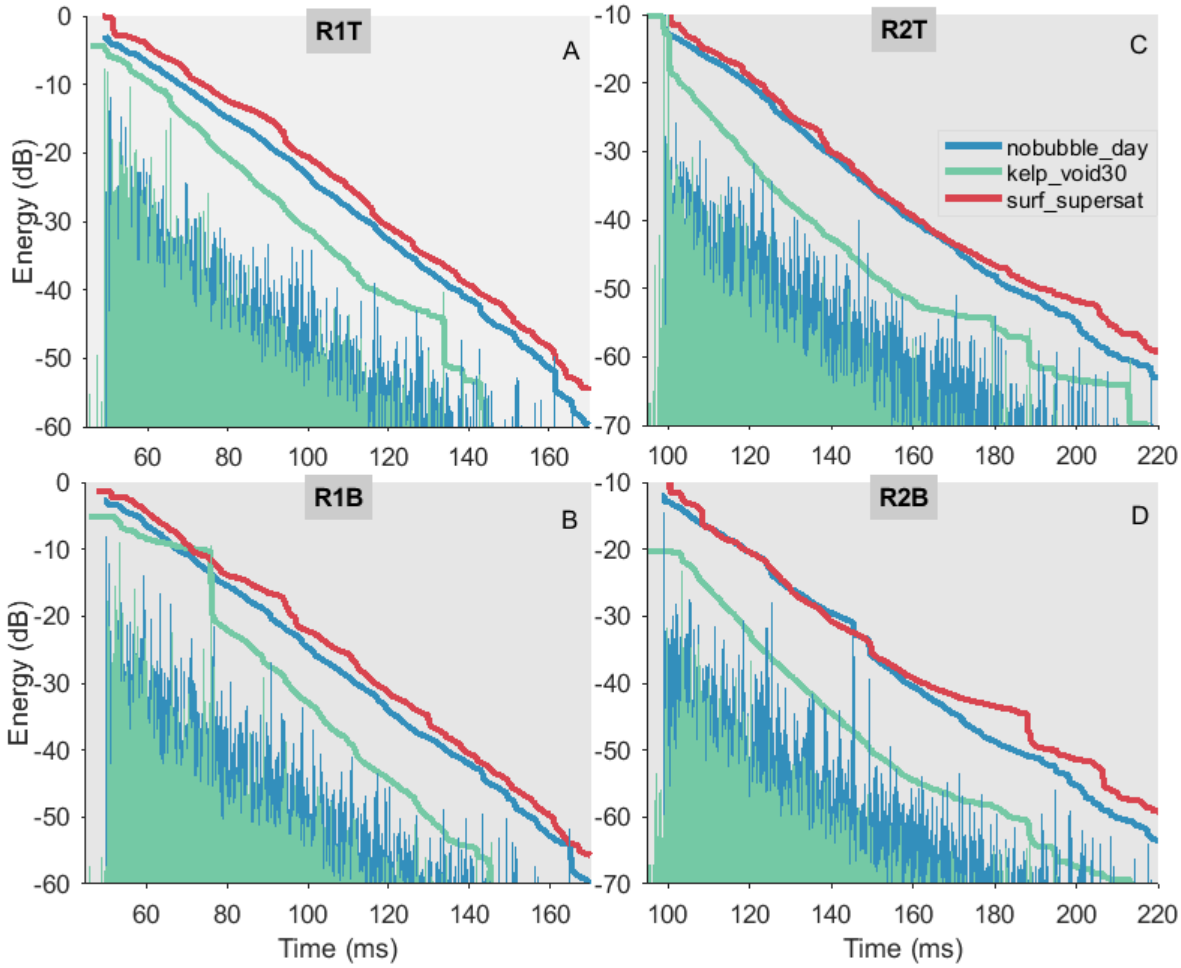

Figure 3.8: Multipath arrival structures and energy decay curves for scenarios with an oxygen void fraction (green) of $2.8e^{-4}$ (30% oxygen in gaseous form), and no void fraction (blue) for the day time period 15 hr 00 13th February received at (A) hydrophone at 75 m from sound source, above the canopy; (B) hydrophone at 75 m, within the canopy; (C) hydrophone at 150 m from source, above the canopy hydrophone; and (D) hydrophone at 150 m, within the canopy. The EDCs are obtained from the time integration of the squared impulse response. The energy level (in dB) is the maximum energy across all investigated scenarios and receivers. Note for R2 the −10 dB decrease in the axis upper limit but with the same range so that both energy levels and decay rate can be compared. These results were obtained with a Bellhop model using 1.6 million geometric beams within an angle sector of -80˚ to 80˚.

The energy decay curves highlight the differences between the ten scenarios that were modelled (Figure 3.9 for R2B, however, see Appendix 3D-F for all receivers). It is remarkable that no pair of nearly identical EDCs can be found; across any two models there are at least some meaningful differences. Even for the night-time and day-time scenarios with no void fraction of oxygen where the sound speeds are barely different, clear differences appear in the end of the tail of the respective EDCs. Of greater interest is the downward shift of the EDC as the void fraction in the canopy increases from 5% to 10% to 30% of predicted total productivity. For the water column void, the EDC is shifted to the right due to overall longer travel times associated with the lower sound speed in the water column. The high wind and supersaturation cases, which both involve void fractions in

the surface layer, behave similarly in the mid part of the curve. The higher void and thicker layer of the supersaturation case provides more efficient channelling of the energy as seen from the stronger early arrivals. The EDC shows great sensitivity, with ~40 ms and ~25 dB difference in the time of arrivals and energy decay respectively between the 30% void fraction model and the water column void fraction models.

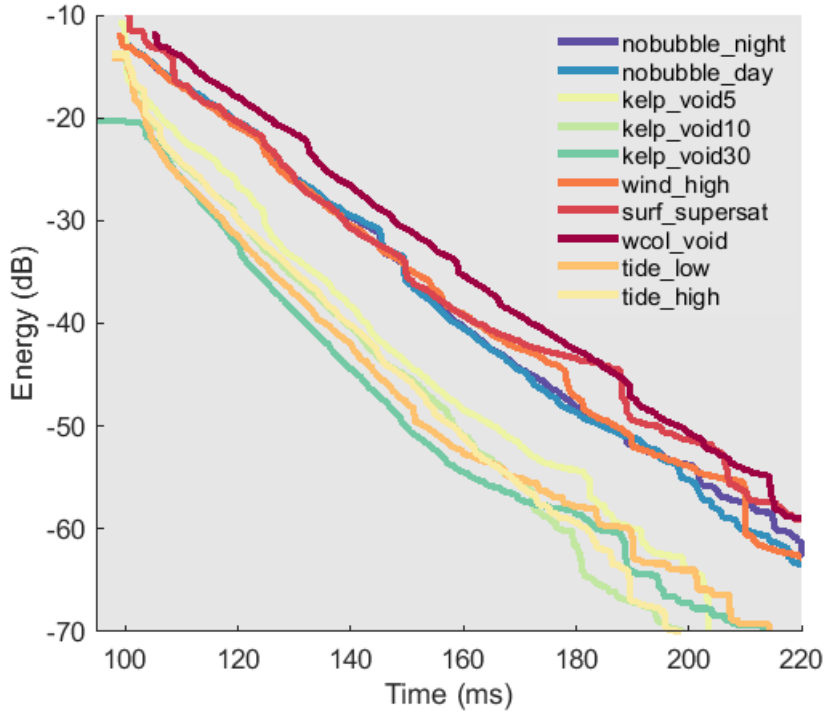

Figure 3.9: Comparison of the energy decay curves of the scenarios studied: day time (no void fraction), night time (no void fraction), oxygen void fractions of $2.8e^{-4}$ (30% oxygen in gaseous form), $9.2e^{-5}$ (10%), $4.6e^{-5}$ (5%), surface supersaturation, high tide, low tide, water column void, and surface wind bubble layer at Receiver 2 in canopy hydrophone at 15 hr 00 13th February and 04 hr 45 14t^{h} February 2012 LT. The EDC curves were obtained from the time integration of the respective squared impulse responses predicted by the Bellhop model using 1.6 million geometric beams within an angle sector of −80˚ to 80˚.

Canoe Bay acoustic data

Due to large ensemble averaging, the acoustic data provide very accurate estimates of the band-limited impulse response of the medium for comparison with the modelling results for the different scenarios. In this work, we focussed on the impulse response measured during the high productivity (Hp) period during day time and a low productivity (Lp) period at night time. Firstly, the data shows a marked increase in the ambient noise level between the day and night periods (Figure 3.10). In contrast to the noise-free model, the tail of the impulse response cannot be extracted in its entirety because it is hidden once it crosses the noise floor (where the response cannot be discerned from

background noise). Nonetheless, the data have a high peak signal-to-noise ratio making most part of the impulse response available for comparison with the model. As in the model, the peak energy levels decrease when the receiver is in the canopy or further away, and the relative values between the four receivers are consistent with the model. The general shapes of the impulse response envelope are similar with faster decay rates at the longer range. The decay at the long range is not close to exponential as it is at the short range. Comparison of the day and night differences does not indicate major difference between the overall shapes. Careful examination indicates that differences occur in the fine structure of arrivals, including in the late arrivals. Typically, these differences do not exceed a couple of decibels locally and thus they are not of sufficient magnitude to affect the energy decay curve as modeled in Fig. 3.9.

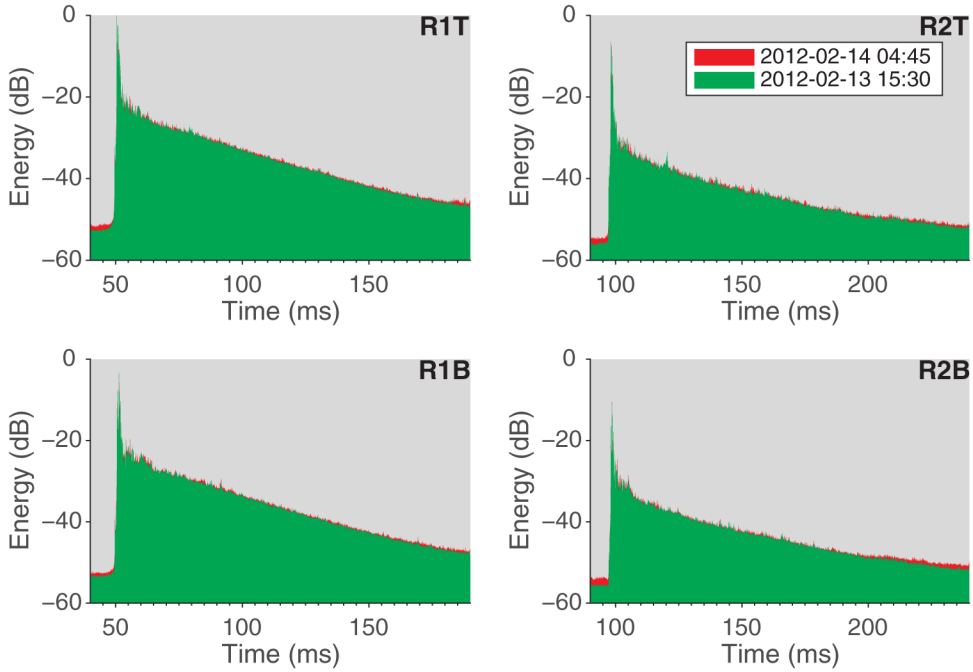

Figure 3.10: Mean envelope of the channel impulse response from acoustic data processing results filtered in the frequency range 10 kHz to 20 kHz received at (top left) Receiver 1 (75 m), within canopy hydrophone; (bottom left) Receiver 1, above canopy hydrophone; (top right) Receiver 2, within canopy hydrophone; and (bottom right) Receiver 2 above canopy hydrophone, for the day-time period 15 hr 30 13th February (green) and night-time period 04 hr 45 14th February (red). Each curve is the results of ensemble averaging of 1200 impulse response measurements centered about the prescribed times. The absence of clear differences in the day- and night-time curves suggests that there is not significant bubble formation in the canopy layer.

3.6 Discussion

The void fractions of oxygen were based on productivity estimates calculated from dissolved oxygen measurements during the experiment. The amounts of non-dissolved oxygen were chosen to represent quantities that the authors considered to be an ecologically important percentage of the productivity. If more than 5% of all oxygen produced were in gaseous form there would be

significant implications for ecological research where the primary means of estimating productivity involves measurement of dissolved oxygen. For acoustic monitoring to be an effective tool for measuring productivity in macroalgal communities it is essential that the acoustic signal could show a response for these levels.

Although the void fractions chosen were high, it reflects the high productivity of these systems. Macroalgae growing on temperate reefs have rates of primary productivity that are among the highest of any ecosystem (Cebrian, 1999), and such high productivity suggests that conditions favourable for gas bubble formation in the canopy would regularly occur. In South Australia, for example, Fairhead and Cheshire (2004b) report net daily productivity of *E. radiata* as measured by oxygen exchange chambers at a depth of 10 m (South Australia) as 382 µmol O_2 g^{-1} dwt which, when scaled for average macroalgae weight and biomass at Canoe Bay and using a ratio of wet weight:dry weight of 7.1 (Shepherd, 2013) would result in a total daily productivity estimate of ~200 mmol m^{-2} seafloor day^{-1}. This compares with peak hourly productivity values reported for seagrass (*Halodule wrightii*) of 200–350 µmol O_2 g^{-1} dwt hr^{-1} (Dunton, 1996). During peak photosynthesis, dissolved oxygen in the water column throughout temperate Australia regularly reaches super-saturation (J. Randall, unpub. data) at which time bubble formation is possible.

The void fraction values used in the modelling were large (reducing the sound speed from ~300–800 m s^{-1} depending on the proportion of total production used) however, these void fractions are possible in the kelp forest of Canoe bay. Results from benthic chamber oxygen evolution data show total daily production rates for *E. radiata* in Canoe Bay during the experiment of 204 (SE ± 13) mmol O_2 d^{-1} m^{-2} after correction for kelp biomass (Chapter 4). This compares to production estimated for the entire macroalgae assemblage from dissolved oxygen modelling of 464 (SE ± 28) mmol O_2 d^{-1} m^{-2}. Peak production occurs in the afternoon when the water column is already at super-saturation level. Much of this oxygen will be lost due to water mixing and equilibrium with the water/surface interface, however, discounting these factors and assuming a baseline of close to 100 % dissolved oxygen saturation (easily the norm during the peak irradiance periods of this study) it is clear that productivity is high and there is the potential for a substantial void fraction of oxygen bubbles in the area. These oxygen levels are higher than the >10 L day^{-1} m^2 (~44 mmol O_2 d^{-1} m^2) reported in meadows of Mediterranean endemic seagrass species *Posidonia oceanica* where acoustics has been shown to successfully detect diurnal cycles in oxygen bubble occurrence (Hermand et al., 1998), hence large enough to observe an acoustic effect if conditions are favourable for bubble formation and retention (i.e. low mixing and continuous production from photosynthesis).

Recent underwater video footage in the Mediterranean in a bed of *Cymodocea nodosa* (Hermand, 2016b) shows both bubbles of visible size on the surface of the leaf blades and streams of bubbles rising to the surface. This was definetely not observed at any time during the experiment either by

the divers on the long underwater video footage recorded at Canoe bay. Furthermore, a submersible digital holographic microscope (Hermand et al., 2014) was deployed on a sunny day in February 2013, almost exactly one year after the experiment, to investigate the bubble population at the top of the canopy (Hermand, unpubl. data). From the reconstructed holographic frames recorded during day time, all bubbles passing through the sampling volume were identified one by one, sized and enumerated. However, in spite of measured DO and supersaturation conditions in the mid afternoon, no marked variation in the bubble population was observed from analysis of this data which could be related to the diel cycle of photosynthesis (Hermand, unpubl. data).

Additionally, the morphology and physiology of seaweeds are conducive to situations where high oxygen concentrations are likely to be present in the canopy layer. Chemical gradients and photosynthetic processes in macroalgae have been shown to produce much higher concentration of dissolved gases in tissues than would be expected from partial pressures alone (Johnston et al., 1992; Kubler et al., 1999). The strong oxygen gradient drives diffusion of oxygen into the surrounding seawater. The presence of a boundary layer at the blade surface creates conditions where oxygen concentrations may be much greater than that of the surrounding seawater, providing water movement is low (Littler, 1979a). In macroalgae, water flow is decreased by the presence of a wrinkled blade surface and, in some species, marginal spines (Lobban, Harrison, 1994). This suggests that the canopy layer may contain a high level of oxygen in gas form relative to that of the water column, particularly where bubbles adhere to the macroalgae blade surface.

Clear effects were seen with the addition of all of the void fractions in the models (although the effect was less apparent for a 5% void fraction), with significant decrease in amplitude and increase in duration of the predicted impulse response with increasing void fraction. The void fractions caused substantial reductions in the low-frequency effective sound speed in the canopy layer, resulting in a slower medium with greater absorption of sound, particularly for rays with many bounces (i.e., more reflections). However, this was not seen in the acoustic data, indicating that the void fraction in the canopy layer was lower than 5% of the production in the kelp bed for the 30 minutes preceding the experiment. This is in contrast to seagrass experiments where distinct diurnal patterns are seen in the acoustic signal (Hermand, 2003). Various factors would contribute to this, including the morphological structure of the macroalgae and the differences in productivity and mixing conditions between seagrass and macroalgae communities. The video footage taken during the experiment did indeed show movements of the canopy and suspended particles. Although ADCP measurements showed both vertical and horizontal water movements during the experiment to be low, seagrass meadows are characterised by particularly low water movement, and, in high density populations, it is the seagrass itself that restricts water movement (Koch, Gust, 1999). This prevents

mixing between the water above and within the canopy (Heiss et al., 2000) and may, in part, be responsible for allowing a high concentration of oxygen bubbles to build up in the seagrass layer.

Macroalgae cells differ fundamentally from seagrass cells, most notably with the absence of large, interconnected gas-filled channels, or lacuna (Larkum et al., 2006), which facilitate fast exchange of oxygen between tissues and transport to roots and rhizomes (Armstrong, 1979). In seagrass meadows, oxygen produced through photosynthesis is also released directly into the surrounding seawater in gaseous form through the waxy cuticle of the leaf blades. In macroalgae, oxygen is produced in cortex layers and diffuses in dissolved form both in the medullar tissue in the thallus and through cell walls and the diffusive boundary layer to the surrounding water (Spilling et al., 2010).

An additional consideration when interpreting these results is the assumption that the void fraction of oxygen would remain concentrated in the canopy layer. Ramsey (1962) provides a summary of the theory of bubble presence in the water column due to photosynthesis and supersaturation. In contrast to the present study, however, the work concentrates on the likelihood of bubbles in the surface layer. It is important to note that work undertaken in that study showed clear gradients in DO with a high increase in the surface layers, a strong thermocline, and majority of production from phytoplankton distributed in the surface and mid waters. The present study in a shallow water environment with minimal thermocline, minimal background photosynthesis from phytoplankton, and a DO gradient with maximum levels in the canopy layer. In our situation, if the production in gas bubble form was dispersed throughout the entire water column the modelling results (at 30% of the predicted total production but also at smaller percentages) show that measurement of absolute travel times is able to detect the occurrence and quantify the void fraction. This was not observed in the very accurate measurements made in Canoe bay.

Likewise, the modelling results show that the onset of supersaturation conditions in a surface layer accumulating parts of the predicted total production would be easily distinguishable from the structural change in the early arrivals. In our case study, however, from DO readings it is possible that oxygen in bubble form is concentrated in the canopy layer, but at void fractions not sufficiently high to be measured by the acoustic features investigated here. More sophisticated data processing may extract attributes of the received signal that can resolve the low void fractions. The wind speed used to calculate the wind-induced bubble void in the surface layer showed little effect on shape of the energy decay curve. This wind speed was conservative (although the maximum recorded during the study period). The effect on sound propagation would obviously be greater with more wind speed, however, this effect could not be examined in the available data.

The ability of acoustics to measure change addition of void fraction of gaseous oxygen in gas form in the canopy layer are not limited to the effective sound speed. *Ecklonia radiata* has a higher sound speed than that of the seawater (Randall et al., 2014). Because macroalgae tissue represents only a small volume fraction of the canopy layer (1-2 %) application of the mixture theory only increases the effective sound speed by ≅ 0.5-1 m s^{-1}. However, the impedance contrast with respect to surrounding water is sufficiently high to create significant scattering as frequency increases to several kilohertz's (Hermand 2016). Although the detailed scattering effects could not be modelled by the Bellhop code, they are present in the acoustic data. The occurrence of many bubbles on the blades would modify the macroalgae scattering function and therefore the character of the acoustic propagation measurement.

There are also several limitations of the 2D Bellhop model used that need to be considered. The 3D version can account for horizontal refraction and reflections from the shore. Here, a horizontally stratified medium and a "mirror-like" sea surface were assumed. Scattering due to other factors including small-scale seafloor and benthos roughness, fish and invertebrate populations, sea surface roughness, bubble clouds below the sea surface, composition of macroalgae assemblage etc. can have large effects on sound propagation (Lin, Lynch, 2017), which cannot be predicted by a ray - theory model. Hence, it cannot be expected that an environmental model would completely match the acoustic data even if the model and actual void fractions were the same. However, no clear differences can be seen in the energy time spread of the acoustic pulse between the day and night periods in the acoustic data, indicating that there was at least no dramatic variation of gas bubble amount in the Canoe bay environment during our experiment.

As seen from the modelling results, there is no strong difference in the acoustic response from low to high tide due the small height variation in this experiment, but small differences are seen in the arrival structure, as it is also observed in acoustic data. This shows that the Bellhop model is robust enough to detect the effects of void fractions in the canopy layer and to resolve small-scale changes in the environment. In contrast, dramatic differences are apparent when a detailed range-dependent bathymetry is not included in the environmental model. Less energy is lost and there is a discrete pattern of ray paths and arrivals instead of the complex arrival structure. This highlights the importance of detailed bathymetry for accuracy in acoustic propagation modelling.

Despite very high levels of production, the results suggest that a significant proportion of oxygen (> 5%) produced in the environment is not in gaseous form. The low wind speeds and currents, high PAR, and productivity estimates from dissolved oxygen measurement during the experiment indicate that the study period was representative of conditions *a prior* favourable for the use of acoustics. There was no strong evidence, neither optical nor acoustical, however, it is probable that mixing/stirring conditions in the environment result in difficulties when using relatively non-

complicated analysis of environmental acoustic data. During the experimental period large plastic bags were placed in the kelp bed around several *E. radiata* individuals to attempt to visualize bubble formation but no bubbles were seen at the end of the day. Presence of excess amounts of microbubbles in the water column was excluded by the submersible microscope measurement (Hermand unpubl. data). Obviously, this does not preclude the presence of microbubbles on the leaf blades but it does provide an indication that significant void fractions simply were not present at the time of the experiment as it was in other photographic and video material collected in another very shallow kelp bed showing large bubbles attached to the blades (Hermand unpubl. data).

The acoustic response does show marked differences in ambient noise depending on the time, with substantially higher noise in the night time period (also seen in seagrass; Hermand, 2003). This result was obviously not apparent in the model results and reflects the diurnal biological cycles in the rocky reef habitat with many fish and invertebrates becoming active over the night time period and sheltering during the day to avoid predators (Lin, Lynch, 2017). The day/night difference in ambient noise is evident in the raw acoustic data and the ensemble-average impulse response envelope in the form of a background noise floor, which can partially mask the response tail, at any of the four receivers.

Given that the presence of even small amounts of gas bubbles will have a profound affect on underwater sound (Wood, 1932), and as seen from our modelling results accounting for effective sound speed change, it is clear that during the experimental period the presence of a significant amount of oxygen bubbles in the canopy would be easily detected from empirical acoustic data. More advanced investigation of the acoustic data is not in the scope of the present work but it may be able to resolve small diurnal differences in oxygen bubble concentration in the environment of Canoe Bay, Tasmania. During the experimental period other small-scale environmental changes (e.g., in soundscape character) were apparent, which constitutes a very interesting set of data for other research.

Using acoustic sensing methods to detect primary production is a new field of research, and even the detection of kelp using these methods can be difficult (Suggett et al., 2003). Efforts to measure gas bubbles have proven challenging due to issues with background noise (Urban et al., 2017), and while these techniques are continually advancing there remain limitations. Despite the present work finding no evidence of significant bubble presence in the environment, the approach holds promise for further advancement.

The modelling shows that even with relatively small proportions of the oxygen produced by the kelp bed in gaseous form the acoustic response is noticeably altered, therefore it is probable that there was not a substantial bubble presence in the canopy. This does not preclude the successful use of

acoustics to measure productivity in other macroalgae systems. It is possible that further work, particularly in very highly productive environments and shallow water systems, and with more sophisticated acoustic data analysis, may prove acoustics to be a useful tool for assisting in monitoring primary productivity in seaweed communities.

Acknowledgments

The authors would like to thank Rob Perry, Pearse Buchanan and many student volunteers from the University of Tasmania for technical support and field assistance. The authors would like to acknowledge the US Office of Naval Research and Office of Naval Research Global (Grant # N62909-13-1-N106), Australian Research Council (ARC), Australian National Network in Marine Science (ANNiMS), and Brussels Institute for Research and Innovation (INNOVIRIS).

Chapter 4

An *in situ* study of production from diel oxygen modelling, oxygen exchange, and electron transport rate in the kelp *Ecklonia radiata*

4.1 Abstract

This study provides a unique comparison of the estimates of production or potential production in a kelp bed in Tasmania using three different measurement methods: diel oxygen gross primary production (GPP) models based on measurements of dissolved oxygen (DO) through the water column, benthic chambers measuring DO, and electron transport rate in photosystem II (PSII) measured using PAM fluorometry. All three methods were run concurrently *in situ* during a 10 day period where midday irradiance measured at the top of the canopy peaked at ~450 μmol photons m^{-2} s^{-1}, with the common kelp *Ecklonia radiata* as the focus species. Two approaches to modelling diel oxygen flux showed a good fit with environmental DO, and estimated gross oxygen production of the entire kelp bed assemblage ranged between ~0-20 and ~0-6 µmol O_2 m^2 s^{-1} with total daily gross production of 464 (SE ± 28) and 347 (SE ± 7) mmol O_2 m^{-2} of benthos depending on the model used. The oxygen production rate of *E. radiata* measured in the benthic chambers reached a maximum rate of 1.2 μmol O_2 s^{-1} for each m^2 of algal surface. After scaling for biomass and density of the kelp, total daily production of *E. radiata* was estimated to be 204 (SE ± 13) mmol O_2 $m^2$of benthos, about half of the estimated total daily production of the kelp bed from the modelling. Photosynthetic capacity (rETRmax) derived from rapid light curves measured by PAM fluorometry showed a rapid increase with ambient photon flux density before tending towards an asymptote at 200 µmol photons m^{-2} s^{-1}. The peak value for rETRmax was 49 μmol e− m^{-2} s^{-1} at PAR of 208 µmol m^2 s^{-1}. Oxygen evolution from benthic chambers and electron transport rates derived from PAM fluorometry showed good correlation, however, the results indicate that the latter method may overestimate potential oxygen production. This study suggests that water column DO, benthic oxygen exchange chambers, and PAM fluorescence can all provide good indications of productivity in shallow water marine environments. However, care must be taken in interpretation of results as each method differs in the type of productivity estimates it provides. While PAM fluorometry can provide an easy and instantaneous measurement of photosynthetic potential, larger scale measurements are needed to get a true estimate of individual/community productivity. Benthic chambers can provide precise estimates of individual alga photosynthesis which can be scaled up to the population level, however, for community-wide primary production of reefs, water column DO models are most likely to provide representative estimates.

4.2 Introduction

Macroalgal beds provide the ecological foundation for most shallow reef ecosystems in temperate marine environments. These communities are among the most productive ecosystems on earth, providing essential structure for associated organisms including marine mammals, fish, crustaceans and molluscs (Mann, 1973b). With distinctive canopies primarily of laminarian algae (northern hemisphere), or fucoid and laminarian algae (southern hemisphere) (Steneck et al., 2002; Steneck, Johnson, 2013), these habitats support rich biodiversity, support valuable fisheries, and provide a range of other ecosystem services to humans.

Overexploitation and the effects of coastal activities have resulted in significant habitat loss in coastal ecosystems (Jackson, Sala, 2001), and human-induced climate change is now seen as a major threat to ecosystem health in many marine systems (Richardson, Poloczanska, 2008; Wernberg et al., 2011). Climate change is predicted to increase the importance of ecosystem engineers in maintaining healthy ecosystems because of their capacity to mitigate environmental stressors (Bruno et al., 2003). As a result, macroalgae are likely to play an increasingly important role in buffering the effects of climate change on temperate reef communities through, for example, affecting local acidity of seawater (Britton et al., 2016) and dissipating wave energy (Duarte et al., 2013).

Successful management of marine systems requires robust understanding of ecosystem processes and functioning, particularly productivity, and therefore suitable tools are required for accurate measurement in space and time. This is particularly critical when considering ecosystem engineering species that play a fundamental role in determining community structure and ecological processes. Knowledge of the productivity of these systems is largely from studies conducted over small spatial scales utilising a variety of methods that generally measure different characteristics or proxies of production. This is both at the level of individual algae and of entire assemblages of algae (IMOS, 2017). As a result of the diversity of measurement methods, estimates of gross primary productivity (GPP) and macroalgal biomass for temperate reefs are numerous and variable (Schreiber, 2004a). This can lead to challenges for ecologists attempting to amalgamate research findings to facilitate long-term, broad-scale perspectives, or to compare research between different studies that are spatially or temporally separated. However, to date there has been little research to quantify and compare differences in productivity estimates across the different techniques applied simultaneously to the same system.

Perhaps the oldest and most extensively utilised method of measuring primary productivity in aquatic ecosystems uses diel changes in "free water" dissolved oxygen (DO) to calculate rates of production and respiration (Cole et al., 1998; Gelda, Effler, 2002; Lauster et al., 2006). Although first applied in coral reef systems (Sargent, Austin, 1949) the diel oxygen method (DOM) became widely accepted

after work by the Odum brothers in the 1950s broadened application from coral reef metabolism into river and lake systems (Odum, 1956; 1957; Odum, Odum, 1955). The technique has now been extensively used in a range of aquatic ecosystems (e.g.,Cole et al., 1998; Gattuso et al., 1993; Hanson et al., 2003; Kemp, Boynton, 1980; Smith, Key, 1975; Staehr et al., 2010; Van de Bogert et al., 2007). At their simplest, DOM models estimate gross primary productivity (GPP) from DO measurements through time, factoring ecosystem respiration (estimated from night time changes in DO), exchange of O_2 from the atmosphere (typically modelled as a function of the concentration gradient between water and atmosphere with a wind-derived coefficient and dependent on temperature), and vertical and horizontal advection (Staehr et al., 2010). Technology development has made it easy to continuously measure DO concentrations and relevant physical and chemical parameters accurately, allowing for detailed description of temporal variability and calculation of metabolism. However, despite the obvious advantages, questions remain about the extent to which free-water measurements actually represent whole-system metabolism (Coloso et al., 2008; Lauster et al., 2006; Van de Bogert et al., 2007). In particular, assumptions associated with advection, quantification of the air-water exchange and respiration estimates require consideration (Staehr et al., 2010). Also, depending on the scale and precision at which advective and diffusive processes are captured, these models can be numerically complex.

Another widely used method of measuring photosynthetic rate in macroalgae involves enclosing entire individuals in chambers to measure changes in dissolved oxygen (O_2) or, more rarely, carbon dioxide (CO_2). *In situ* measurements to estimate the initial slope (α) of the irradiance-dependent O_2 evolution curve, the rate of maximum photosynthesis (i.e. oxygen production), irradiance where α intercepts the maximum rate of oxygen production under light saturation (P_{max}), and dark respiration rates were made possible with the design of data-logging oxygen exchange devices (Chalker et al., 1985; Cheshire et al., 1995; Cheshire et al., 1996b; Hatcher, 1977). Since respiration can also be estimated, the method can determine both gross and net primary productivity over periods of 24 hours. Using this kind of apparatus, primary productivity and photosynthesis has been measured for macroalgae (Cheshire et al., 1997; Hatcher, 1977; Longstaff et al., 2002), seagrass (Ralph, Burchett, 1995), invertebrate symbioses (Cheshire et al., 1997; Hoegh-Guldberg, Jones, 1999), and turf algae (Klumpp, McKinnon, 1989; Westphalen, Cheshire, 1997). This method allows specific measurement of the primary productivity of a species/individual of interest. However, the need to enclose the algae inside a chamber substantially limits scale, and results are sensitive to the level of stirring/water movement in the chamber and boundary layer issues.

Simplicity and convenience have led to the increasing use of Pulse Amplitude Modulation (PAM) fluorometry as a non-invasive method to monitor the functional state of photosynthetic organisms in real-time. PAM fluorometry measures chlorophyll (Chl) *a* fluorescence associated with photosystem

II (PSII) (Rosenqvist, van Kooten, 2003) as a measure of photosynthetic potential, and is increasingly used to assess the physiology of macroalgae *in situ* under varying environmental conditions (Edwards, Kim, 2010; Franklin, Badger, 2001; Kim, Garbary, 2006; Longstaff et al., 2002). Fluorescence measurements can provide estimates for a number of different photosynthetic characteristics which indicate various aspects of an organism's photophysiology (Ralph, Gademann, 2005). Electron transport rate (ETR) or, when an absorbance factor is not used, relative electron transport rate (rETR), is measured at increasing light intensities to produce rapid light curves (RLCs). Curves fitted to raw rETR data facilitate derivation of the saturating light intensity (*Ek*), relative maximum electron transport rate or photosynthetic capacity (rETRmax), and light harvesting efficiency of photosynthesis (α).

Collectively the parameters derived from PAM fluorometry have been interpreted as a measure of potential photosynthetic performance. Electron transport rate (ETR) has been found to relate to photosynthetic activity as measured by CO_2 uptake or oxygen evolution (Beer et al., 1998), and so PAM fluorometry is often interpreted as a comparable method of measuring photosynthetic performance, or at least potential photosynthetic performance, with the benefit of providing virtually instantaneous (90 second) measurements. However, there are indications that rates of photosynthesis from PAM fluorometry only correlate well with those obtained using O_2 exchange apparatuses at low irradiances, with increasing discrepancies at high irradiances (Beer et al., 2000; Beer et al., 1998; Colombo-Pallotta et al., 2006; Enríquez, Rodríguez-Román, 2006; Häder et al., 1997; Longstaff et al., 2002; Nielsen, Nielsen, 2008). Moreover, at a basic theoretical level, there are a raft of reasons why activity in PSII need not equate to production of O_2.

Undoubtedly, there are fundamental dissimilarities in the nature of the measurements made by each of these methods. PAM fluorometry gives an instantaneous measure of ETR in PSII from a single (and very small) location on the surface of the thallus; it says nothing about the downstream molecular machinery between that point and the fixation of carbon or production of photosynthate, or the state of PSII elsewhere on that thallus. Oxygen exchange measured in closed chambers *in situ* provides an integrated measure of oxygen evolved under a complex natural light environment for a sample (comprising a thallus portion, whole plant, or even a part of an algal assemblage). Open system models estimate GPP over an entire community, with the estimated productivity in an area often attributed to the largest and most populous species despite the presence, usually, of diverse sub-canopy and understorey species. Can these methods be used to assess *in situ* photosynthesis in comparable situations? What are the limitations and how can they be overcome?

This study compares these most widely used methods for measuring productivity in macroalgae, and to our knowledge is the first of its kind. We used benthic chambers in a shallow water temperate reef environment in Tasmania to measure oxygen exchange in *Ecklonia radiata*, the single-most important

habitat-forming marine macroalga species in temperate Australia. Concurrent diurnal PAM fluorometry measurements were taken to estimate the saturating light intensity (*Ek*), maximum electron transport rate or photosynthetic capacity (rETRmax), and light harvesting efficiency of photosynthesis (α). In addition, diel changes in "free water" dissolved oxygen at various heights in the water column were recorded to facilitate estimating rates of production and respiration for the entire system by fitting two kinds of diel gross primary production (GPP) models.

4.3 Methods

The experiment ran over a sixteen day period 8-24th February, 2012. A transect was placed along the ~ 7 m contour line in Canoe Bay (43.12583 ˚S 147.96056 ˚E), Tasmania, which supports a sheltered and dense *E. radiata* forest, averaging ~90 % kelp canopy cover over dolerite reef (see Figure 3.1 for site location and transect layout). The relatively calm setting of the site provided stable environmental conditions for the duration of the experiment. The average density of adult *E. radiata* sporophytes at the site was 7.9 (SE±0.5) m^2, of average individual size 499 (SE±26) g. Over the experimental period vertical profiles of dissolved oxygen, temperature, turbidity and salinity were measured using a hand-held sensor (YSI Sonde 6-series model 6600 V2) at varying times of the day (*n=12*). Deployment of all other equipment was by divers, with sampling occurring within 10 m of the experimental transect. The tidal range was <0.90 m during the experimental period.

4.3.1 Modelling ambient dissolved oxygen

Dissolved oxygen was measured at 10 minute intervals from mid day 12th - 23rd February 2012 by a series of sensors deployed in the water column (~7.2 m depth). Two sensors (D-Opto Logger, Zebra-Tech Ltd) were placed on a weighted and elasticised "string" moored from a large float to ensure that sensors remained at a constant depth in the water column. The sensors were positioned at 0.5 m and 3.0 m from the surface. A further three sensors were fixed at positions 0.30, 0.50, and 0.80 m above the benthos (NexSens SDL500 data logger with Ponsel conductivity/salinity sensor; Aanderaa oxygen optode 4175). A sensor (Licor 192SA Underwater Quantum Sensor) to measure photosynthetically active radiation (PAR) and associated data logger were situated at a depth of 1.2 m above the benthos, at the top of the kelp canopy. Temperature and salinity in the water column were recorded at 10 minute intervals at depths of 0.5 m and 3.0 m from the surface ("string") and 0.70 m above the benthos. A weather station was mounted onshore (~ 110 m from transect, ~1 m above sea level) to continuously record wind speed and direction.

Two models were developed that bookend either end of a spectrum of possible approaches. The first involved fitting a Fourier series to the DO data ignoring any DO/PAR relationship. The Fourier elements were then fitted back to the periodic DO data using least squares in a linear model approach to estimate forcing (O_2 production) from the kelp layer. At the other extreme the second model also

utilises the periodic DO data, however a DO/PAR relationship is assumed. The parameters of this relationship were estimated by fitting to the DO data using least squares and from this the forcing (O_2 production) from the kelp layer was estimated.

For both models, it was assumed that the system was horizontally isotropic, with uniform coverage of macroalgae. It was also assumed that there was no vertical stratification in the water column (supported by empirical data from the SONDE profiles) and no significant effect of waves and tide. Thus, any horizontal fluxes were discounted and the system was treated as one dimensional in the vertical. A coordinate system was constructed so that $z = 0$ is the benthos, $z = h$ is the top of the macroalgae canopy and $z = H$ is the ocean surface. Assuming that vertical advection can be ignored, then the concentration of dissolved oxygen $\Psi_{(z,t)}$ satisfies a diffusion equation in the form

$$\frac{\partial \psi(z,t)}{\partial t} = F(z,t) + K\nabla^2\psi(z,t)$$

where $F_{(z,t)}$ represents the generation and consumption of O_2 within the water column and K is a diffusion constant. Assuming that oxygen is generated and consumed uniformly within the macroalgal bed, there may also be a small constant consumption throughout the water column, so that F takes the form

$$F(z,t) = f(t)u(h - z)$$

where u is the Heavyside step function and f represents the rate of uniform generation throughout the kelp forest.

We disregard any respiration in the sediment and so at the lower boundary we have a no flux condition

$$\left.\frac{\partial \psi}{\partial z}\right|_{z=0} = 0$$

At the surface we have the condition

$$\frac{\partial \psi}{\partial z}|_{z=H} + k\left(\psi(H - l, t) - \psi^{(sat)}(t)\right) = 0$$

where $k = k_b/K$ (see Baird et al., 2014) and the transfer rate k_b is

$$k_b = \frac{0.0283}{360000}u^3\left(\frac{S_c}{660}\right)^{-1/2}$$

where u is the wind speed, Sc the Schmidt number (from Wanninkhof, 1992), and k_b and u are both in units of ms^{-1} (Baird et al., 2014). A periodic condition was adopted for the initial condition

$$\psi(z,0) = \psi(z,1).$$

To make the time series indefinitely periodic, the ends of the 10-days time series were joined. To do this, an initial segment of data was replaced with a weighted average of itself and a corresponding segment at the end of the data that smoothly transitioned between the two, and then the end segment was dropped. Thus the dissolved oxygen data for the first 12 hours is an amalgam of the true first 12 hours and the last 12 hours, and the last 12 hours has been discarded. The oxygen concentrations for the exact probe heights were calculated by linearly interpolating the finite difference solution.

Finite differences were used to solve the system for a given forcing (Smith, 1985). A simple implicit scheme was adopted

$$\frac{\psi_{i,j}-\psi_{i,j-1}}{\Delta t} = F_{i,j} + \frac{K}{(\Delta z)^2}(\psi_{i-1,j} - 2\psi_{i,j} + \psi_{i+1,j}).$$

The system was solved on a grid offset in the vertical to span both the upper and lower boundaries so that at the surface the boundary condition takes the form

$$-rK_j\psi_{i-1,j} + (2rK_j + 1)\psi_{i,j} - rK_j\psi_{i+1,j} - \psi_{i,j-1} = \Delta t F_{i,j}$$

where $r = \frac{\Delta t}{(\Delta z)^2}$.

The oxygen concentrations for the exact probe heights were calculated by linearly interpolating the finite difference solution.

In model 1, the forcing is expressed as a sum of Fourier components

$$f(t) = a_0 + \sum_{k=1}^{N} a_k \sin(2k\pi t) + b_k \cos(2k\pi t)$$

The finite difference solver was used to determine the expected DO concentrations at the probe heights for each Fourier (sine or cosine) component of the forcing, and the unknown coefficients (the

a_i and b_i) were determined by fitting the expected DO concentrations to the observed concentrations by least squares.

In model 2, the forcing is assumed to be a rigid function of the observed photosynthetic active radiation (PAR),

$$f = a + b(1 - \exp(-cPAR))$$

which defines the relationship between O_2 production and PAR (after Platt et al., 1980). Again, the undetermined coefficients *a*, *b* and *c* are determined by fitting the expected DO concentrations determined by finite differences to the observed concentrations by least squares. However, in this case the problem is non-linear and the unknown coefficients must be determined by numerical minimization.

For both models, the vertical profiles of dissolved oxygen measured during the experiment were compared to the expected concentrations predicted by the model to further evaluate further evaluate the validity of the forced solutions. After compensating for respiration determined during the night time periods, oxygen generated in the macroalgae bed and canopy was expressed per m^2 of benthos (canopy height 0.40 m) and plotted against the average incident photon flux density (PAR; μmol photons m^{-2} s^{-1} as measured at the top of the canopy layer) for each model. Daily productivity rates were calculated from the daily sum of these values for each of the models.

4.3.2 Benthic chambers

Benthic oxygen evolution chambers were deployed on five days during the experimental period (13th, 15th, 19th, 21st and 23rd February 2012). Each chamber was situated in close proximity to the transect at a depth of 7-8 m (depending on tide), and contained a single, randomly chosen complete adult *E. radiata* sporophyte of average size and condition. Thalli were sourced from within 10 m of the transect from 7-8 m depth. Each individual was placed in the chamber with intact holdfast, but holdfast fauna were first removed. Chambers were cylindrical (0.145 m diameter x 0.6 m high) clear Perspex with a volume of 40 l, constructed at the University of Tasmania based on the design of Chalker et al. (1985). Each chamber cycle consisted of a 24 hour period with flushing of the internal seawater every two hours, and chambers contained a battery operated stirring mechanism to ensure mixing in the chamber to minimise establishment of a boundary layer on the algae and avoid stratification of oxygen in the water.

At the completion of the experiment, the wet weight of each individual were recorded and surface area of the thallus estimated. Estimates of thallus area were based on the thallus area to weight ratio calculated for *Ecklonia radiata* in the Canoe Bay site. To estimate this ratio 20 individuals, chosen to

encompass the full size spectrum present in the study area, were returned to the laboratory where mass was recorded and thallus surface area measured by tracing the kelp outline onto grid paper. The relationship ($R^2 = 0.94$) between mass (m, grams) and surface area (s, m^2) is given as:

$$s = 0.0019m + 0.0308$$

Background photosynthesis by phytoplankton in local waters during this period is typically very low due to depleted nutrient concentrations (at nearby Maria Island [42°34'38.41"S, 148° 3'45.65"E] during February 2012 and 2013, production in chambers containing seawater only was <2 μmol O_2/hr per benthic chamber), and so was not considered further. Respiration was measured during the night and assumed to be constant over 24 hour cycles so that gross oxygen production could be calculated for daylight hours by compensating for respiration. Average photosynthetic rates for each flushed cycle were expressed per unit of estimated algal surface area (considering both sides of the thallus) and plotted against the average incident photon flux density (PAR; μmol photons m^{-2} s^{-1}) for each cycle to produce a photosynthesis/irradiance (P vs. I) curve. In order to calculate daily production estimates comparable to those calculated by the open water oxygen models, the daily sum of productivity for each m^2 of tissue in each chamber was used. After scaling for the density of adult sporophytes on the benthos and average sporophyte size at the study site (as measured from 28 randomly selected individuals) a total surface area of tissue (7.824 SE± 0.403 m^2) was calculated for each m^{-2} of benthos. This was used to calculate daily production rates for each m^2 of benthos.

4.3.3 Pulse Amplitude Modulation (PAM) Fluorometry

PAM measurements occurred on five days during the experimental period (13th, 15th, 19th, 21st and 23rd February, 2012). On each day sampling was undertaken between 5-6 am, 7-8 am, 10-11 am, 1-2 pm, 1600-1700 hr and 7-8 pm. For each time period measurements were taken from a set of ten healthy mature sporophytes selected randomly within 10 m of the transect (7-8 m depth). The sampled area on each thallus was on a lateral (secondary lamina) located at one-third the length of the lamina from the top of the stipe, and one-third from the end of the branch/lateral (Figure 4.1).

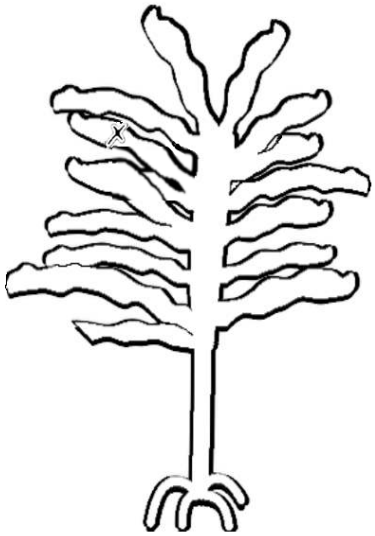

Figure 4.1: Diagram of Ecklonia radiata showing location on thallus for sampling position.

Activity of Photosystem II (PSII) was estimated *in situ* by chlorophyll *a* fluorescence using a blue LED Diving PAM (Walz, Germany). A "dark leaf clip" was connected to the algal thalli to ensure consistent spacing of the PAM fiber optic cable from the surface of the tissue and enable fluorescence measurements without ambient light interference. Rapid light curves (RLCs) were produced for ambient light-acclimated tissue using an inbuilt software routine, where actinic light intensity was increased in eight steps (reaching a maximum of 463 μmol photons m^{-2} s^{-1} at 650 nm) of 10 seconds in duration. Before light-acclimated RLCs were commenced, tissue was quasi-dark adapted for 5-10 s to allow re-oxidation of the primary electron acceptor (e.g. Schreiber, 2004b; Stirbet, 2011) . All RLCs were conducted on fresh tissue *in situ*, with the area first gently wiped to remove visible epiphytic growth.

As large variation in tissue light absorption could be expected in the macroalgae (see Discussion for further details), we did not attempt to approximate actual ETR by using an absorption factor to represent the fraction of incident light absorbed by thalli (as recommended by Saroussi, Beer, 2007b). Curves were fitted to raw rETR data to derive the saturating light intensity (*Ek*), maximum electron transport rate or photosynthetic capacity (rETRmax), and initial slope of the RLC (α) as a measure of the light harvesting efficiency of PSII. The empirical double exponential decay model of Platt et al. (1980) was selected as it effectively describes both the initial linear response and allows for photoinhibition at high light intensity:

$$rETR = P_s\left(1 - exp\left(\frac{-\alpha E_d}{P_s}\right)\right) \times exp\left(\frac{-\beta E_d}{P_s}\right)$$

where α is the light harvesting efficiency as measured by the initial slope of the RLC before light saturation, E_d is the downwelling actinic irradiance of the PAM's internal halogen light, β is the negative slope of the RLC at high irradiance, and P_s is a scaling factor defined as the maximum potential rETR in the absence of any photoinhibition (if $\beta = 0$, this is equal to rETRmax). The nonlinear least-squares function in the 'R' software environment (v 3.0.0) was used to fit the model to each set of RLC data, and the parameters rETRmax and *Ek* were estimated according to equations given in Ralph and Gademann (2005). The following parameters were used in the curve-fitting routine to ensure convergence: iterations = 100; stepsize = 1/1024; tolerance = 0.00001; initial seed value for rETR = maximum rETR derived from raw data, α = slope of linear regression fitted to first three points of raw data (typically in the range 0.7 – 1.0).

4.4 Results

4.4.1 Estimating production using the ambient DO model

Both models provided estimates of DO that matched well with those recorded in the environment, particularly for the depths matching the lowest three sensors in or just above the kelp canopy (Figure 4.2A,B: P3-5). For the sensors closest to the surface (P1, P2) the match was less accurate, with the models tending to slightly underestimate oxygen in the water column. Small-scale perturbations in ambient DO were not reflected in either model (e.g. P2, Day 3 peak). There was a tendency for the models to slightly overestimate DO during night time periods for the three sensors closest to the seafloor.

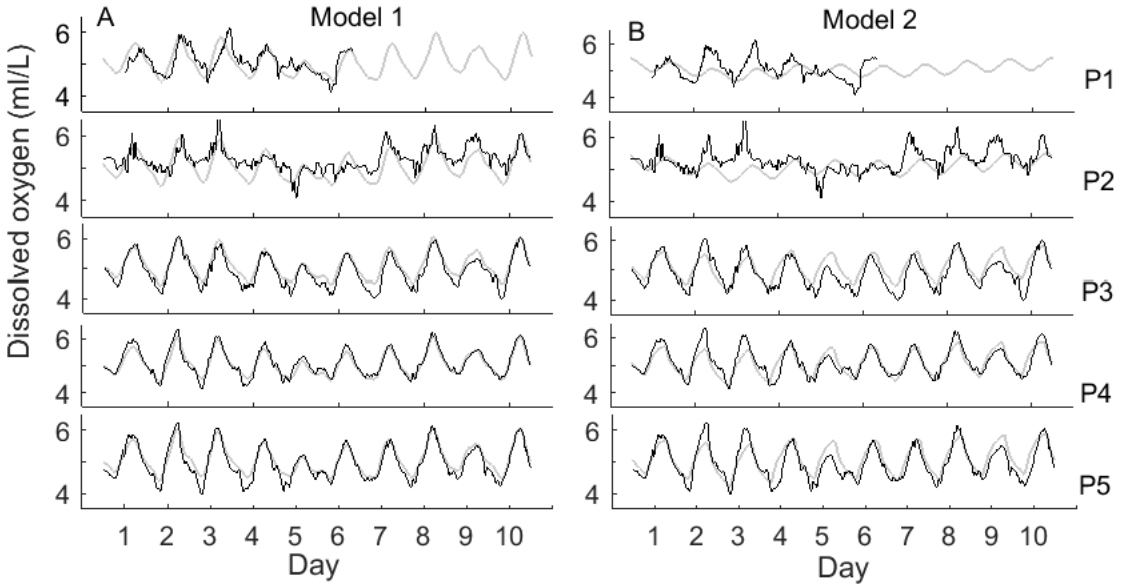

Figure 4.2: The dissolved oxygen recorded at each probe (black line) and the dissolved oxygen predicted by the diel oxygen method (gray line) for model 1 (A) and model 2 (B) over the period 12-

23rd February 2012. P1-5 indicate the dissolved oxygen sensors at depths corresponding to 0.5 and 3.0 m from the surface, and 0.3, 0.5, and 0.8 m from the seafloor respectively.

The accuracy of the match between the vertical DO profiles and the DO by both models at the five sensor depths was variable. For some profiles for both models there was a good fit to the DO seen in the water column (profiles 2, 5, 7, 9 and 10; Figure 4.3; shown here for model 1), however, others showed more variation. No predicted value was >0.75 ml/L from that of the measured profile, with most falling within a range <0.5 ml/L from that of the measured value.

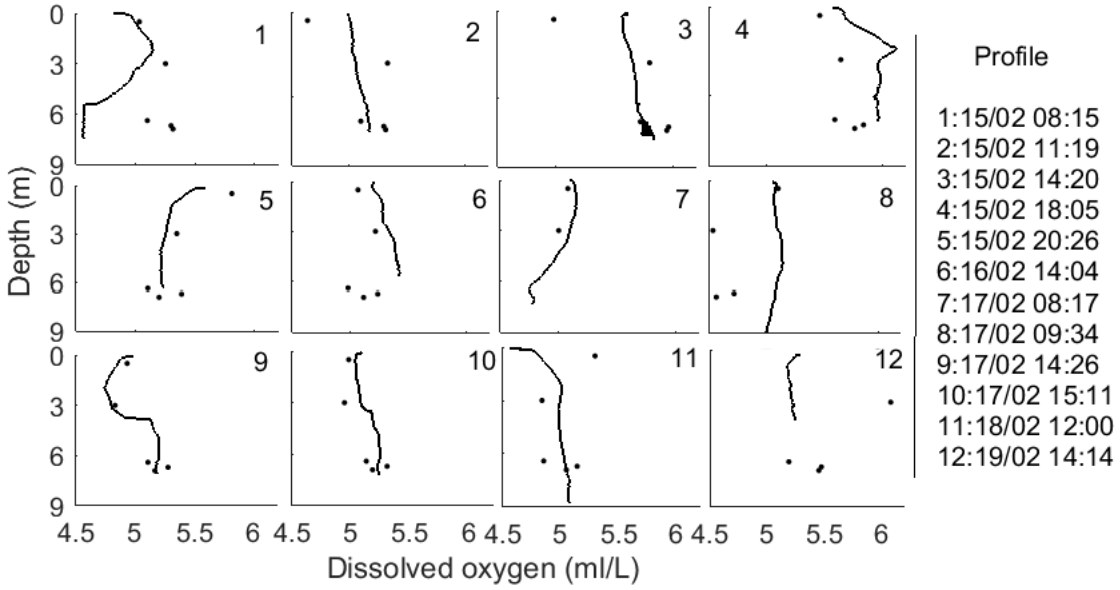

Figure 4.3: Dissolved oxygen measured as vertical profiles using a SONDE unit (solid lines) over the period 12-23rd February 2012, predictions of DO from model 1 (shown as dots) at depths corresponding to the position of DO sensors in the water column.

The rate of oxygen production per unit area of seafloor as a function of ambient PAR estimated from the ambient oxygen models ranged between ~0-20 µmol O_2 m^2 s^{-1} (model 1) and ~ 0-8 µmol O_2 m^2 s^{-1} (model 2; Figure 4.4). For model 1, maximum oxygen production increased with increasing PAR but there was large variation in oxygen production at low PAR levels. This variation was not evident at high light levels with, for the most part, only high oxygen production predicted by the model for PAR over 200 µmol m^2 s^{-1}. For model 2 oxygen production increased rapidly before reaching a plateau at PAR ~20 µmol m^2 s^{-1}. Total (gross) daily oxygen production was estimated to be 464 (SE ± 28) and 347 (SE ± 7) mmol O_2 m^2 for model 1 and model 2 respectively (Table 4.1).

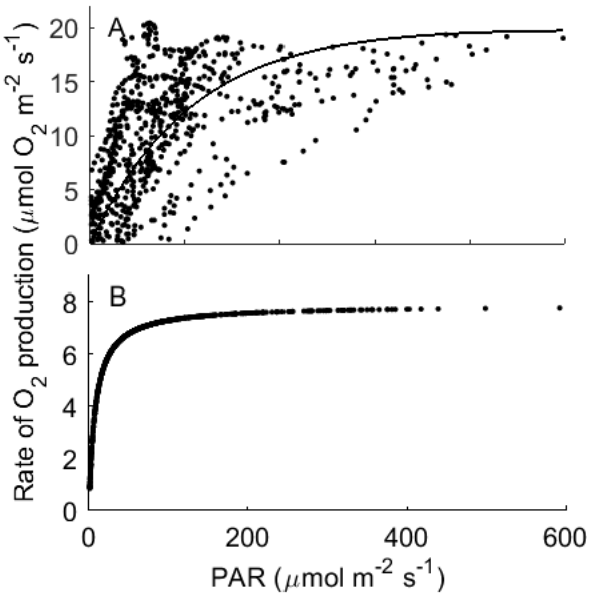

Figure 4.4: Photosynthesis vs. irradiance (PAR) curve obtained from the diel oxygen method from the 12-23rd February 2012 for model 1 (A) where the model was not constrained by a DO *vs*. PAR relationship, and model 2 (B) where the model was constrained by a DO *vs*. PAR relationship (see Methods). For model 1 the curve is fitted according to Platt et al. (1980) where P_s = 20.422, α = 0.187, and β = 0. Dissolved oxygen is calculated from 10 minute 'blocks' throughout the day time period and PAR is an average of the 10 minute period.

Table 4.1: Total gross daily production estimated by the benthic chambers and diel oxygen models for 12-23rd February 2012. Units of production are mmol O_2 d^{-1} m^2 seafloor. Chamber values have been scaled to mean biomass density of kelp on the reef.

Source	14th	15th	16th	17th	18th	19th	20th	21st	22nd	23rd	Gross 24 h production
Chamber 1		170				193		218		209	197 (SE ± 11)
Chamber 2		202				217		272		149	210 (SE ± 25)
Chambers		186				205		245		179	204 (SE ± 13)
Model 1	562	492	420	308	418	479	551	398	542		464 (SE ± 28)
Model 2	346	388	378	332	347	339	362	357	353		347 (SE ± 7)

4.4.2 Benthic chambers

Ambient photon flux density at 6 m depth on days during which benthic oxygen chambers and PAM fluorometry measurements were undertaken peaked at ≅450 μmol photons m^{-2} s^{-1} during midday of the 15th February (Day 3 of the diel models), with a comparable, but shorter, peak on the 13th February (Day 1) (Figure 4.5A). Ambient PAR showed substantial variation between days, reflecting variable

cloud cover, with a peak on the 21st February <150 μmol photons m^{-2} s^{-1}. Oxygen net photosynthetic rate for each m^2 surface area of tissue increased with increasing irradiance, reaching a maximum rate of 1.1 μmol O_2 m^2 s^{-1} on 15th February at an ambient photon flux density of 457 μmol photons m^{-2} s^{-1} (Figure 4.5B). After scaling for the density of kelp sporophytes and average sporophyte size at the study site oxygen net photosynthetic rate reached a maximum of 9.6 μmol O_2 m^2 s^{-1}. The rate of oxygen production with PAR increased gradually until ≅200 μmol photons m^{-2} s^{-1}, then tended towards an asymptote. The relationship between oxygen production and ambient light intensity was consistent regardless of the day of measurement. Daily O_2 production averaged 25 (SE ±2) mmol O_2 m^2 of algal tissue and 204 (SE ± 13) mmol O_2 m^2 of benthos.

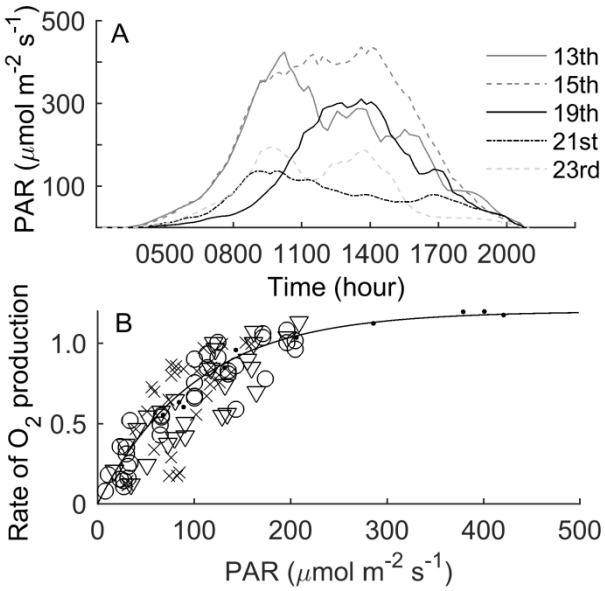

Figure 4.5: A) Diurnal irradiance (PAR) in Fortescue Bay for the days of PAM fluorometry and oxygen evolution chamber measurements (13th, 15th, 19th, 21st and 23rd February 2012). Irradiance was measured at a depth of ~6 m. B) Photosynthesis *vs*. irradiance (PAR) obtained from oxygen evolution chambers. Curve is fitted according to Platt et al. (1980) where $P_s = 1.2$, $\alpha = 0.012$, and $\beta = 0$. Rate of O_2 production is for each m^2 of algal tissue (both sides of thallus) in units of μmol O_2 m^2 s^{-1}. Day is: dot = 15th; circle = 19th; cross = 21st; triangle = 23rd.

4.4.3 PAM fluorometry

Photosynthetic capacity (rETRmax) and saturating light intensity (*Ek*) derived from RLCs measured by PAM fluorometry showed a rapid increase with ambient photon flux density before tending towards an asymptote at 200 µmol photons m^{-2} s^{-1} (Figure 4.6A,C). The peak value for rETRmax was

49 μmol e– m^2 s^{-1}, at PAR of 208 µmol m^2 s^{-1}, with a peak in *Ek* of 98 μmol photons m^{-2} s^{-1} at the same PAR. Light harvesting efficiency of photosynthesis (α) declined until PAR of 200 µmol m^2 s^{-1} after which values again levelled out (Figure 4.6B). Values ranged between 0.9-1.2 μmol m^{-2} s^{-1}. There were no differences in the relationship between any of the photosynthetic parameters and ambient light intensity for each of the days.

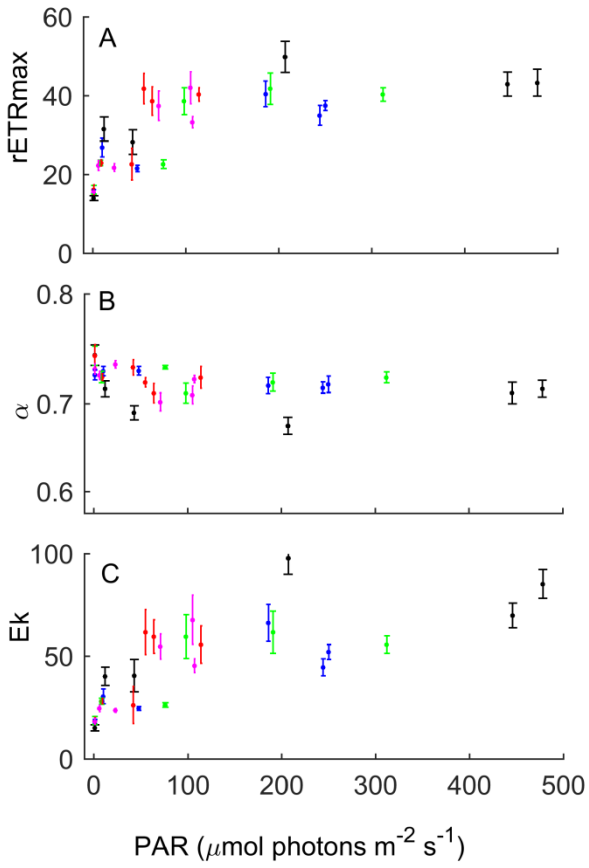

Figure 4.6: Photosynthetic characteristics of *Ecklonia radiata* in Fortescue Bay during February, 2012 as a function of ambient PAR at the time of measurement. Plots show (A) maximum relative electron transport rate (rETRmax); (B) light harvesting efficiency of photosynthesis (α), and (C) saturating light intensity (*Ek*), all derived from Rapid Light Curves measured by PAM fluorometry. Days are indicated as: blue = 13th; black = 15th; green = 19th; red = 21st; pink = 23rd. Units for the PAM fluorometer are: ETRmax, μmol e– m^2 s^{-1}, Ek μmol photons m^{-2} s^{-1} and α, μmol m^2 s^{-1}.

4.5 Discussion

Measurement of photosynthesis in marine communities *in situ* presents many challenges and uncertainties. This study details an attempt to quantify productivity in *Ecklonia radiata*, a prolific habitat-forming macroalgae species in southern hemisphere temperate marine communities. Diel oxygen modelling, benthic oxygen exchange chambers, and PAM fluorometry methods are all established methods for estimating macroalgal productivity or potential productivity in marine environments, however, all are subject to limitations. Conducting all three methods simultaneously in the field permits assessment of their utility and practicality to measure photosynthesis, or proxies thereof, of seaweed or seaweed beds *in situ*.

4.5.1 Modelling ambient dissolved oxygen

The diel oxygen models assume perfect horizontal mixing and a vertical diffusion constant in the water column, uniform macroalgal coverage and no significant effects of waves or tide. Despite these simplifying assumptions, both models provided an excellent fit to the observed water column DO data. This fits suggest that the assumptions are, largely, valid for the study environment. The models tended to slightly underestimate DO in the upper water column for night time periods, with a corresponding overestimation of DO close to the benthos. This may indicate a slight inaccuracy in the estimate of vertical diffusion of DO at night when respiration is the key driver of change in water column DO. The models also showed, for the most part, good correlation with the vertical DO profile data, although there was some variation at several time periods. While the DO sensor positions were fixed for the duration of the experiment, vertical profiles were undertaken at varying locations in the experimental site. This could indicate small scale spatial variation in DO concentrations in the environment, or again, reflect inaccuracies in estimating vertical diffusion at some times in the diurnal cycle. Further information on local water column dynamics would help to better establish recurrent diurnal patterns and improve the accuracy of the models. However, vertical profile data during the experimental period was limited. Nonetheless, as a whole, both models provide excellent fit with the observed environmental DO.

The first model produced estimates of DO that show large variability at low irradiances, and it is probable this is a reflection of high variability in the observed ambient DO at low irradiances. This is likely due to the fact that rates of change in DO are different at the beginning and end of the day when PAR is equally low. As irradiance increases in the morning DO rises in the water column from low levels reached overnight. This can result in high rates of DO change corresponding to relatively low PAR. DO builds up in the water column over the day time period and in the afternoon, when irradiance again becomes low, DO levels show only minimal increase (or actually decrease) from the peak reached in the middle of the day. Model 2 must produce estimates of production tightly coupled

to PAR because this model is constrained by a known form of relationship between production and PAR, the parameters of which were estimated from fitting to the empirical data. The maximum production rate was less than half of that of the first model, although total daily production was only 25% lower. The sharp increase in production at relatively low PAR indicates that the model is estimating productivity close to maximum levels for a large portion of the day, in contrast to the first model where maximum productivity occurs only during short periods. Hence, although peak productivity rates are much lower, total daily production is reasonably close to that of model 1.

Overall, both models indicate estimates of DO production much greater (model 1 >100% and model 2 ~75% greater) than values produced by incubating kelp in benthic chambers *in situ* and correcting for average biomass density of kelp on the reef. This result is in contrast to previous research in stream and coral reef systems where these different methods have been found to be comparable (Bott et al., 1978; Leclercq et al., 1999). However, the nature of the study systems in the previous studies allowed sections of the entire photosynthetic community to be enclosed in the benthic chambers, whereas in the present work DO estimates from the oxygen exchange method are solely the product of individual *E. radiata*. The rocky reef environment contains a diverse understory with a myriad of red, green, and other brown seaweed species of a range of sizes. These species are generally adapted to a low light environment beneath the *E. radiata* canopy and contribute greatly to overall system productivity (Larkum et al., 2006; Lobban, Harrison, 2000). Given that the benthic chambers record oxygen productivity solely by *E. radiata*, it is to be expected that estimates of productivity from the diel oxygen model will be substantially larger as the DO probes integrate the total oxygen output from the entire community.

Fairhead and Cheshire (2004b) report net daily productivity of *Ecklonia radiata* as measured by oxygen exchange chambers at a depth of 10 m (South Australia) as 382 umol O_2 g^{-1} dwt which, when scaled for average algae weight and biomass at Canoe Bay and using a ratio of wet weight:dry weight of 7.1 (Shepherd, 2013) would result in a total daily productivity estimate of ~200 mmol m^{-2} seafloor day^{-1}. This rate is virtually identical to that which we measured (daily production of 204 mmol O_2 m^{-2} of benthos) with the benthic chamber method, indicating that productivity in this Tasmanian kelp forest is on par with other regions. Given that the kelp beds are dominated by large kelps or fucoids it is generally assumed that scaling up estimates of productivity from small scale measurements (e.g. oxygen exchange chambers) of individual kelps will give reliable estimates of whole assemblage production. However, the results of our diel models suggest that this will grossly underestimate community productivity; at Fortescue Bay we estimated production of the whole assemblage to be about double that based on measurement of *E. radiata* alone. The diel oxygen method potentially addresses a need for better measurements at large scales of whole assemblage production integrated over all species and over longer time periods.

To the author's knowledge no research has utilised measurements of ambient DO to estimate community productivity in *Ecklonia radiata* kelp forests so the accuracy of either model is difficult to ascertain. The method has been widely used in kelp beds dominated by *Macrocystis pyrifera* with values of 1 mol m^2 s^{-1} reported by Jackson (1977) and similar results given by Towle and Pearse (1973). Although this value is ~2 times that estimated in this work for *E. radiata*, it is important to consider that *M. pyrifera* is a much larger and faster growing species that spans the entire water column, so total biomass m^2 seafloor will be much greater.

It is clear that for estimates of community production large scale holistic methods are needed, and diel oxygen models can provide this approach. The two models presented here illustrate opposite ends of a spectrum - model 1 allows modelling of O_2 production as a very flexible function of time but assumes no relation between O_2 production and PAR, whereas model 2 assumes O_2 production to be a very simple function of PAR, and it is envisaged that ultimately the best method will be a compromise between the two. In addition, it is important to note that the models presented are, deliberately, simplified designs. There are obvious limitations and future developments could benefit by explicit numerical consideration of additional factors such as wave action, tides, and currents.

4.5.2 Benthic chambers

The benthic chambers yielded results in line with other studies of macroalga production. For example, daily production of *Ulva lactuca* has been measured at 24 ± 5 mmol O_2 m^2 (Longstaff et al., 2002) and Cheshire et al. (1996b) measured production in sub-samples of fucalean-dominated macroalgal community with estimates ranging from 73-167 µmol O_2 g^1 wet weight day^{-1} in summer (which converts to ~36-84 mmol using the mass:surface area relationship discussed earlier). Many other studies report estimates in terms of carbon fixation. If estimates of productivity (in terms of carbon) are to be based on O_2 measurements they must be corrected for the ratio of CO_2 fixed:O_2 released, called the photosynthetic quotient (PQ) (Hurd et al., 2014a). Few measurements of PQ have been made for seaweeds, however, the few studies that have been done give values that range from 0.42-1.50 (Hatcher, 1977; Rosenberg et al., 1995). Generally, in practice, a 1:1 ratio is assumed; using this ratio and taking a production value of 1 µmol O_2 m^2 s^{-1} at PAR >200 μmol photons m^{-2} s^{-1} using the chamber method converts to ~115 mg C m^2 h^{-1}. Estimates of carbon production vary widely depending on species and even within species according to season, for example production of *Ascophyllum nodosum* is estimated to range between 187 mg C m^2 h^{-1} in December to 846 mg C m^2 h^{-1} in August in the northern hemisphere (Golléty et al., 2008). However, it is important to note that these values are expressed in terms of seafloor area rather than tissue biomass; scaling our values according to sea floor tissue biomass would result in values ~900 mg C m^2 h^{-1}.

As mentioned earlier, production per unit area of sea floor attributed to kelp (*Ecklonia radiata*) alone using this method is about half of the estimated gross production from modelling ambient DO. While other species undoubtedly account for a significant amount of the discrepancy, it is also possible that methods using benthic chambers underestimate DO production in nature. Longstaff et al. (2002) reported concerns with self-shading when using the oxygen exchange technique, and no doubt this is a factor to consider (as it is in nature) when interpreting the results of this method. While it is likely that considerable dynamic self-shading occurs, this shading effect is much more likely in relatively low volume chambers where the water is relatively still and individuals may not be fully extended. Hence, the projected surface area of the algae exposed to light was likely overestimated. Another issue is the magnitude of water motion over the surface of the thallus, which affects boundary layer properties and thus gas diffusion and nutrient uptake rates (Patterson et al., 1991). Although the benthic chambers used in this method were adequate for the size of the *E. radiata* individuals used in the experiment, the algae were sheltered from the water movement they typically encounter (i.e. surge) in their natural environment. Algae in the natural habitat are semi-erect and move constantly in all directions, therefore, the chambers may artificially reduce gas diffusion and nutrient uptake, thus reducing photosynthetic rate.

Oxygen production in the benthic chambers rose gradually with PAR before tending towards an asymptote above 200 μmol photons m^{-2} s^{-1}, again, similar to that found in other studies (Cheshire et al., 1996b; Longstaff et al., 2002). Although the DO model 1 also showed production at these levels to taper off, the estimates at lower light intensities were highly variable (Figure 4.3). It can be seen (Figure 4.4A) that on the 21st and 23rd February (days 8 and 10 of the experiment) there were substantially lower maximum PAR levels, but this is not reflected in the ambient dissolved oxygen (Figure 4.1). Understorey species, particularly red algae, are known for high photosynthetic efficiency at low light levels (Brouwer, 1996; Eggert, Wiencke, 2000; Weykam, Wiencke, 1996) and it is possible that these species are contributing to high oxygen during days of low light when a lower productivity in the *E. radiata* canopy would be expected. However, the high variation in productivity at low light levels estimated from the first model suggests that there may also be other factors influencing these measurements.

4.5.3 PAM fluorometry

The PAM fluorescence method showed estimates of photosynthetic capacity in line with previous research for *E. radiata* (Flukes, 2015; Flukes et al., 2015b; Randall et al., In review). Estimates of rETRmax derived from rapid light curves determined using the PAM instrument showed a similar pattern to the oxygen evolution as measured in the respirometry, with both rETRs and O_2 evolution rates increasing until ~200 µmol photons m^{-2} s^{-1}, then tending to an asymptote. However, at irradiances <200 µmol photons m^{2} s^{-1}, the rate of increase was greater for rETRs, indicating that

increasing numbers of electrons were passing through PSII for every molecule of O_2 evolved. The similar asymptotic trend for rETRs and oxygen evolution at irradiances >200 µmol photons m^{-2} s^{-1} indicates that both methods show an inhibitory response at high light levels. Similar photoinhibition has been reported in many other macroalgae (e.g. Henley, 1993; Longstaff et al., 2002).

Previous studies have found that at saturating light intensities ETR values tend to overestimate O_2 evolution rates (Enríquez, Rodríguez-Román, 2006; Franklin, Badger, 2001). Although the relationship between ETR and O_2 evolution can be expected to be tightly coupled as both fluorescence and O_2 evolution are tied to PSII, the relationship is not always linear (e.g. Longstaff et al., 2002). Fluorescence measurements yield estimates of photosynthetic potential but these do not factor alternative electron sinks which may consume O_2 (e.g. Mehler reaction and chlororespiration) (Consalvey et al., 2005). It is important to consider that PAM fluorometry measurements are an indication of maximum potential photosynthesis, and actual photosynthesis may be substantially lower. It is important to also consider that research in PAM methodology is ongoing, and fast repetition rate (FRR) fluorometry is showing good convergence with electron to carbon conversion (i.e. Suggett et al., 2003).

Another key factor contributing to this overestimation may be error in the estimation of light available to photosynthesis in the tissue. Generally, an absorption factor is used to calculate ETR, based on the ability of the tissue to absorb light. Several methods can be used to estimate this absorbance, although both are complicated and are associated with methodological errors (see Enríquez, Borowitzka, 2010). In addition, aquatic macrophytes show great variation in tissue light absorption within individuals and communities (Enríquez et al., 1994), and changes also occur diurnally due to chloroplast movement (Hanelt, Nultsch, 1991; Sharon, Beer, 2008).

Individual species can show significant differences in photosynthetic rates between different tissues on an individual (Gerard, 1986; Sakanishi et al., 1991). Research suggests that photosynthetic capacity and efficiency appears to reflect only the health of photosystems at the immediate location on an individual and are strongly influenced by tissue age, condition, and light history (including self-shading) (Enríquez, Borowitzka, 2010; Oláh et al., 2010). We have noticed in our own work that it is possible to obtain normal rapid light curves and *F*v/*F*m values from small areas of healthy tissue when >90% of the individual alga appears necrotic and senescing. These effects cannot be ignored, and it is important that individual measurements should not be used to predict organism-scale physiology, and applying one absorption factor to a multitude of situations is likely to result in over/under-estimation of ETR. Relative ETR was used in this study as it was considered that the errors inherent in applying absorption factors would negate any advantage. Regardless, the use of rETR still assumes consistency in light absorption across measurements (just without the multiplication factor), so the risk of over/under-estimation of ETR remains. In addition, because a

multiplication factor is not used, light absorption is assumed to be at a factor of one, therefore the likelihood of overestimation of ETR is actually greater as all light is considered absorbed.

4.5.4 Conclusions

The diel oxygen modelling method, benthic oxygen exchange chambers, and PAM fluorometry were used concurrently to provide *in situ* estimates of primary productivity or proxies in a shallow water marine environment. The ambient oxygen models use a regression of Fourier components fitted to the model of DO in the water column to estimate DO production in the macroalgae layer on the sea floor, and they provide a good fit to measurements of daily fluctuations in DO throughout the water column. Importantly, this approach provided estimates of DO production rates substantially higher than those estimating from incubation of intact *Ecklonia radiata* sporophytes in benthic respirometry chambers, as might be expected given that the approach with the chambers ignores contributions from all other species of macroalgae. The high variability in predicted DO values at low light levels in the first environmental DO model may be improved with further development. The second model constrains productivity to PAR with a commonly used function, however, the dramatic increase in productivity with low PAR may not be representative of the environment. It is envisaged that ultimately the best method for modelling the kelp bed system will be a (more complicated) hybrid of both approaches that will both define the relationship between O_2 production and PAR and fit Fourier components. This would provide an improved fit to the empirical measurements and more accurate estimates of total production in the kelp layer. The high correlation between O_2 flux and electron transport rates in this study also highlights the effectiveness of both oxygen exchange and PAM fluorescence methods in measuring photosynthetic rates of marine plants, but these measurements are valid only for individuals or parts of individual algae.

For estimating production of entire assemblages of benthic algae (or other photosynthetic organisms), particularly when questions address larger spatial and temporal scales than can be addressed by other techniques, the approach to model ambient oxygen levels holds great potential. Equipment and labour requirements are modest (fixed and profiling DO, temperature, and light sensors, and instruments to measure wind speed) and, once sensors are deployed, data can be collected over extended periods. This method provides an estimate of total assemblage productivity, and not surprisingly, is likely to provide greater estimates of productivity than methods focussed on single canopy-forming species only. However, the approach isn't suitable to estimate production rates of single species.

Benthic oxygen exchange chambers again allow capturing whole plant processes, although, for those communities where biomasses are small (e.g. coral reefs) sometimes community assemblage measurements are possible (e.g. Klumpp, McKinnon, 1989). Typically, such as in macroalgal communities, they are only suitable for measuring photosynthetic performance for single species.

This technique can be particularly useful for estimating the contribution of particular algal species to overall community productivity, although care should be taken when considering self-shading in nature and in the chamber and disparities between water movement in the chamber and in unmanipulated conditions.

Both oxygen flux methods are superior in providing assemblage or whole algae estimates of productivity compared to PAM fluorescence, which only measures activity in PSII and thus need not equate to realised photosynthesis at all. Moreover, even as a proxy for potential photosynthesis, results relate only to the small area of tissue under analysis which need not reflect the physiology or metabolism elsewhere on the alga. We have shown considerable intra-individual variation in parameters measured from application of PAM fluorescence (Randall et al., In review), and obtained high readings indicating healthy tissue (i.e. an appropriate *F*v/*F*m ratio) and highly active PSII on individuals that are clearly at an advanced stage of senescence.

The main advantage of PAM fluorometry is ease of use and ability to provide instantaneous measurements. It can also provide other photosynthetic information relating to photochemical and non-photochemical quenching (Osmond et al., 1993; Schreiber, 2004b). In this study, dynamic changes in electron transport rates determined from RLCs showed good correlation with DO from the oxygen exchange method, however, consideration must be given to assumptions of light absorbance in addition to alternative electron sinks in PSII.

Overall, this research shows that each method of measurement has distinct advantages and disadvantages. When planning future research or comparing other studies, it will be important to consider that each method provides different kinds of estimates of production or proxies of actual or potential production, and that there needs to be considerable clarity in the question being tackled before selecting a suitable technique for research.

Acknowledgements

The authors would like to thank Rob Perry, Pearse Buchanan and many student volunteers from the University of Tasmania for technical support and field assistance. The authors acknowledge the financial support of the Australian Research Council (ARC) and Australian National Network in Marine Science (ANNiMS).

Chapter 5

Space-time variability in *in situ* PAM fluorometry measures in three key habitat-forming macroalgae

5.1 Abstract

Macroalgae play a dominant role in ecological processes on shallow temperate reefs. A widely used non-invasive method to monitor the functional state of photosynthetic organisms in real-time is Pulse Amplitude Modulation (PAM) fluorometry. This technique has become a powerful tool for assessing one aspect of the photophysiology of macroalgae *in situ* under varying environmental conditions. However, estimates of photosynthetic performance derived from PAM fluorometry may vary greatly depending on the sampling methodology utilised. This study assesses the use of PAM fluorometry as a tool for evaluating the photophysiology of three key habitat-forming macroalgae (*Ecklonia radiata, Phyllospora comosa* and *Macrocystis pyrifera*) across different times of day, depths, latitudinal regions, seasons, and locations on the thallus. The outcomes of PAM fluorometry measurements were strongly dependent on choices of these sampling parameters, and were influenced by complex interactions between seasonal and regional variations in environmental conditions. For any one study, and to compare between studies, it is thus important that sampling measurements are standardised for the time of day, plant part, and depth. Seasonal and regional variations in environmental conditions also need to be considered. The similar patterns we observed for both light- and dark-adapted rapid light curves show that, although absolute values of PAM fluorometry metrics vary depending on whether algal tissue is light- or dark-adapted prior to sampling, both approaches are valid provided there is consistency across measurements. We show that sampling design strongly influences outputs of PAM fluorometry, which has important implications for planning studies and interpreting temporal and spatial patterns in macroalgal photophysiology using fluorescence techniques.

5.2 Introduction

Macroalgal forests provide the ecological foundations of most temperate shallow marine reef ecosystems (Steneck, Johnson, 2013). Comprised of distinctive canopies, primarily of laminarian algae (northern hemisphere) or laminarian and fucalean algae (southern hemisphere), kelp forests are among the most productive ecosystems on earth (Mann, 1973a). Macroalgal communities provide essential structure for associated organisms including marine mammals, fish, crustaceans and molluscs. *Ecklonia radiata* (C. Agardh), *Phyllospora comosa* (C. Agardh), and *Macrocystis pyrifera* (C. Agardh), are the dominant canopy-forming macroalgae on shallow temperate reefs in Australia

beyond the wave-washed *Durvillaea potatorum* zone (Steneck, Johnson, 2013), and play important functional roles as ecosystem engineers (Jones et al., 1996) and in regulating ecological processes and community structure. Because of their important ecological role, it is likely that macroalgae will become increasingly important in shielding temperate reef communities against some of the effects of climate change (Russell, Connell, 2005; Russell et al., 2009; Wernberg et al., 2011). It follows that it is useful to understand parameters of potential primary production in marine macroalgae as one measure of their ecological functioning. However, interpreting these kinds of measurements requires a clear understanding of how photosynthetic parameters may vary spatially and temporally (Urban et al., 2017).

A widely used non-invasive method to monitor the functional state of photosynthetic organisms *in situ* is Pulse Amplitude Modulation (PAM) fluorometry, which measures chlorophyll *a* (chl *a*) fluorescence associated with Photosystem II (hereafter PSII) (Rosenqvist, van Kooten, 2003) as a measure of photosynthetic potential. PAM fluorometry is increasingly used to assess the photophysiology of macroalgae and seagrasses *in situ* under varying environmental conditions (e.g. (Edwards, Kim, 2010; Enríquez, Borowitzka, 2010; Kim, Garbary, 2006). Traditional methods of assessing kelp productivity such as using chambers to measure oxygen evolution and/or CO_2 uptake (e.g. Golléty et al., 2008; Suggett et al., 2003), or measurements of lateral extension (e.g. Hanelt, Nultsch, 1991) to estimate biomass increase, directly measure net rates of productivity/photosynthesis. In contrast, fluorescence measurements assess several properties of one part of the photosynthetic apparatus (Schreiber, 2004b) and thus provide a deeper understanding of the processes and mechanisms regulating the physiological success of macroalgae. However, these measurements are not a proxy for photosynthesis per se.

Fluorescence measurements can provide estimates for a number of different photosynthetic characteristics which indicate various aspects of an organism's photophysiology (Ralph, Gademann, 2005). Electron transport rate (ETR) or, when an absorbance factor is not used, relative electron transport rate (rETR), is measured at increasing light intensities to produce rapid light curves (RLCs). Curves fitted to raw rETR data allow derivation of the minimum saturating light intensity (*Ek*), maximum electron transport rate or photosynthetic capacity (rETRmax), and light harvesting efficiency of photosynthesis α (for light-adapted tissue, see Falkowski, Raven, 1997). Collectively these parameters can be interpreted as a measure of potential photosynthetic performance. Electron transport rate (ETR) has been found to relate closely to photosynthetic activity as measured by CO_2 uptake or oxygen evolution as with traditional P-I curves (Beer et al., 1998). The rise of the curve in the light limiting region (α) is proportional to efficiency of light capture (effective quantum yield; Schreiber, 2004b). The minimum saturating irradiance (*Ek*) (determined by finding the interception of α with the maximum photosynthetic rate), is related to quenching, where photochemical quenching

dominates below *Ek*, and non-photochemical quenching dominates the fluorescence quenching above *Ek* (Henley, 1993). Hence, PAM fluorometry is often interpreted as a comparable method of measuring photosynthetic capacity with the benefit of providing virtually instantaneous (90 second) measurements.

PAM fluorometry measurements are instantaneous and strongly influenced by the plant's immediate history of ambient light (Schreiber, 2004b; Schreiber et al., 1997; White, Critchley, 1999). Consequently, the parameters measured using a PAM fluorometer may vary depending on the time of day at which measurements are made and/or the sun's position in the sky. This is due to short term changes in photoprotective mechanisms (such as xanthophyll pigments) and longer term cycles (including changes in pigment concentrations) as a response to the irradiance received. Changes in the spectral quality, quantity and wavelength of irradiance with depth may cause individuals in shallow water to exhibit different patterns in photosynthetic responses (diurnal or seasonal) than those in deeper water (Edwards, Kim, 2010; Ekelund et al., 2008). This applies both to species where individuals occur over a range of depths, and to species where the thallus or fronds of an individual may span several vertical metres through the water column. In the latter scenario, individual algae are exposed to a range of irradiances at different points across their structure, and measurements of photosynthetic performance may yield different values depending on the position on the thalli at which they are taken (Nielsen et al., 2006; Silva et al., 1998). Given that diurnal variation in irradiance is relatively low close to the benthos compared to shallow waters, it follows that seasonal and/or diurnal variation in photosynthetic performance may also vary with depth. Additionally, self/neighbour-shading can also create within-thallus differences in the ambient light climate. The effect of these factors on photosynthetic performance may vary in both pattern and/or magnitude with latitude, as a result of selection or differential up-regulation of genes (i.e. phenotypic plasticity). Physiological performance of macroalgae has been shown to vary latitudinally due to acclimation and adaptation by means of compensatory mechanisms at various biochemical levels (Davison, Davison, 1987; Flukes et al., 2015b; Raven, Geider, 2003; Wernberg et al., 2010). Hence, the effects of depth and/or position on the thallus where PAM fluorometry measurements are taken may vary between geographic regions. Additionally, latitudinal variation in the magnitude of diurnal light cycles may influence the effect of seasonal variations in irradiance on photophysiological measurements, leading to regionally-dependent effects of season on photosynthetic measurements taken at different times of the day.

It follows that appropriate interpretation of studies using PAM fluorometry to measure (potential) photosynthetic performance must consider patterns of diurnal, seasonal and latitudinal variability in ambient light and how these affect photophysiological parameters, as well as possible effects associated with depth, within- and between-alga variation in PSII performance, and latitudinal effects

unrelated to the light climate (such as temperature). Here we consider these sources of variability in PAM-derived parameters, and assess the use of PAM fluorometry as a tool for evaluating the photophysiology of three dominant canopy-forming macroalgae (*E. radiata, P. comosa* and *M. pyrifera)*. In considering the effect of sampling design with regards to interpretation of PAM-derived measures, we provide recommendations for the application of PAM fluorometry in future ecological research.

5.3 Methods

Pulse Amplitude Modulation (PAM) Fluorometry

Photosynthetic activity was estimated by chlorophyll *a* fluorescence using a blue LED Diving PAM (Walz, Germany) *in situ*. A "dark leaf clip" was connected to the algal thalli to ensure consistent spacing of the PAM fibre optic cable from the surface of the tissue and enable fluorescence measurements without ambient light interference. Rapid light curves (RLCs) were produced for ambient light-acclimated tissue using an inbuilt software routine, where actinic light intensity was increased in eight steps (reaching a maximum of 463 μmol photons m^{-2} s^{-1} at 650 nm) of 10 seconds in duration. To minimise potential variability in photosynthetic activity due to diurnal cycles of non-photochemical quenching (Belshe et al., 2007) all PAM fluorometry for each comparable subset of data was conducted at the same time each day (separate trials were conducted to examine the effect of time-of-day on resultant measures). Before light-acclimated RLCs were commenced, tissue was quasi-dark adapted for 5-10 s to allow re-oxidation of the primary electron acceptor (e.g. Schreiber 2004, Stirbet & Govindjee 2011). With *Macrocystis pyrifera* some measurements were conducted after 15–20 minutes of dark-adaptation of tissue as determined by pilot study to be sufficient to allow oxidation of the electron transport chain and relaxation of photoprotective mechanisms (Flukes et al., 2015b). In theory, light- and dark-adapted RLCs can give different results and, indeed, this may be true in some cases (e.g. see Rascher et al., 2000). Generally it is considered that dark-acclimation 'standardises' the pre-manipulation light history and reflects the inherent physiological state of photosystems (Ralph, Gademann, 2005). However, extensive measurements were run for all species which this work is based on and found no difference in the patterns derived from light- and dark-adapted curves (Flukes, 2015). Therefore, all RLCs in this study were carried out on light-adapted tissue (excluding the light- and dark-adapted comparison or *Macrocystis pyrifera*; see below).

All RLCs were conducted on fresh tissue free of visible epiphytic growth *in situ*, with the area first wiped gently to remove any epiphytes not visible to the naked eye. As we were primarily interested in relative patterns in the photophysiology of seaweeds rather than quantifying actual photosynthetic rates, we did not attempt to approximate actual ETR by using an absorption factor to represent the fraction of incident light absorbed by thalli (as recommended by Saroussi, Beer, 2007b) and instead

interpreted rETR as a proxy for electron transport rate. Mathematical curves were fitted to raw rETR data to derive the minimum saturating light intensity (*Ek*), maximum electron transport rate or photosynthetic capacity (rETRmax), and initial slope of the RLC (α) as a measure of the light harvesting efficiency of Photosystem II. The empirical double exponential decay model of Platt and Harrison (1980) was selected as it effectively describes both the initial linear response and the region of photoinhibition:

$$rETR = P_s\left(1 - exp\left(\frac{-\alpha E_d}{P_s}\right)\right) \times exp\left(\frac{-\beta E_d}{P_s}\right)$$

where α is the light harvesting efficiency as measured by the initial slope of the RLC before light saturation, *Ed* is the downwelling actinic irradiance of the PAM's internal halogen light, β is the negative slope of the RLC at high irradiance, and *Ps* is a scaling factor defined as the maximum potential rETR in the absence of any photoinhibition (if $\beta = 0$, this is equal to rETRmax). The nonlinear least-squares function in the 'R' software environment (v 3.0.0) was used to fit the model to each set of RLC data, and the parameters rETRmax and *Ek* were estimated according to equations given in Ralph and Gademann (2005). The following parameters were used in the curve-fitting routine to ensure convergence: iterations = 100; stepsize = 1/1024; tolerance = 0.00001; initial seed value for rETR = maximum rETR derived from raw data, α = slope of linear regression fitted to first three points of raw data (typically in the range 0.7 – 1.0).

Study sites

Measurements were undertaken at seven study sites across Australia (Figure 5.1). Western Australia included three sites situated at Jurien Bay, Marmion and Hamelin Bay. There was a single site in Port Stephens, NSW, and three sites in Tasmania consisting of St Helens, Fortescue Bay and Southport. The monthly averages of environmental data for each site at the times of sampling are given in Table 5.1.

Table 5.1: Monthly averages for SST and irradiance for the study sites during the months of sampling. Irradiance (MJ m^{-2}) monthly averages (BOM, 2011). SST (C°) monthly night time averages (IMOS, 2017). Exposure status is observational.

	Summer		Winter		
Location	**SST**	**Irradiance**	**SST**	**Irradiance**	**Exposure**
Jurien Bay	26.95	25.8	20.35	18.1	exposed
Marmion	25.65	26.5	19.59	16.8	exposed
Hamelin Bay	23.09	25.7	18.78	15.8	exposed
Port Stephens	23.96	19.2	18.66	16.6	sheltered
St Helens	18.23	17.4	13.22	13.4	moderately exposed
Fortescue Bay	17.76	16.8	13.46	11.9	sheltered
Southport	16.69	17	13.65	10.8	moderately exposed

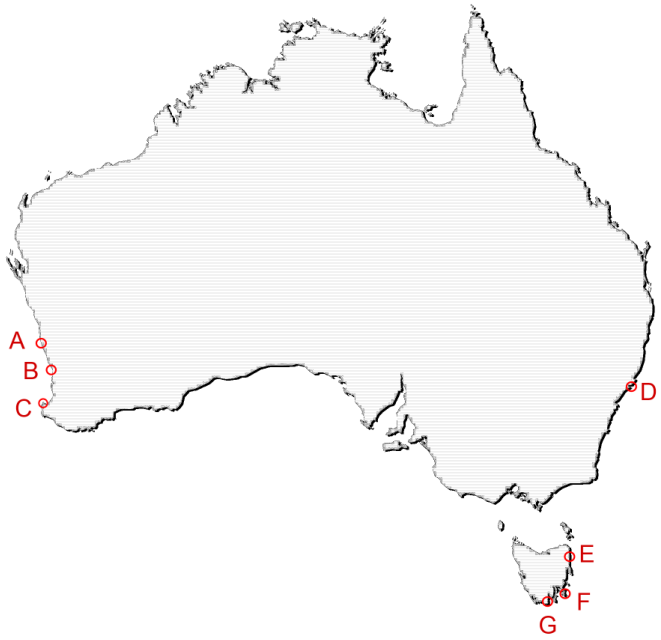

Figure 5.1: Diagram showing study sites for PAM fluorometry measurements of *Ecklonia radiata*, *Phyllospora comosa*, and *Mcrocystis Pyrifera*. WA sites included Jurien Bay (A), Marmion (B), and Hamelin Bay (C). NSW site consisted of Port Stephens (D). TAS sites included St Helens (E), Fortescue Bay (F), and Southport (G).

Ecklonia radiata

Ecklonia radiata (Laminariales) is the key habitat-forming kelp in southern Australia, with a larger depth (4-75+ m) and latitudinal (27.5-43.5 °S) range than any other canopy-forming macroalga (Steinberg, Kendrick, 1999). *Ecklonia radiata* has a single stipe bearing a flattened blade with distinct lateral fronds, and grows to 0.7-1.3 m in height (Wernberg et al., 2003b). Variation in RLC parameters of *Ecklonia radiata* were compared diurnally, across depths, sites and latitude, and between thalli sampling positions within individuals. Measurements were taken in February 2011 and repeated in September of the same year to coincide with the Austral summer and winter periods, with the exception of sites in Western Australia (WA) where measurements were only made in the summer (February 2012). PAM fluorometry measurements at all sites and times were taken from a set of 10 individual algae selected randomly from those that appeared healthy and mature (stage 3 Kirkman, 1981).

Diurnal variation in PAM fluorometry measurements was assessed among *E. radiata* individuals (n = 10) growing on shallow (9-10 m) reefs in Fortescue Bay, Tasmania (43. 12471° S, 147. 97558° E), near Port Stephens, NSW (32.63059 °S, 152.30962 °E), and at Marmion, WA (31.47327° S,

115.40736° E). Diurnal variation among algae (n = 10) in deep water (28-30 m) was also conducted at the Tasmanian and NSW sites. RLC measurements were taken between 0800-0900 hr, 1200-1300 hr and 1600-1700 hr. The sampled area on each thallus was on a lateral (secondary lamina) located at one-third the length of the lamina from the top of the stipe, and one-third along the branch lateral from the centre of the thallus midrib.

Within-thallus variation in PAM measurements was assessed between 1200-1300 hr in each of 10 individuals growing in shallow (9-10 m) water at Jurien Bay (30.18214° S, 114.59348° E), Marmion (31.47327° S, 115.40736° E) and Hamelin Bay (34.16089° S, 115.01159° E) in WA, and at St Helens (41.15258° S, 148.20395° E), Fortescue Bay (43. 12471° S, 147. 97558° E), and Southport (43.31449° S, 146.57360° E) in Tasmania. RLC measurements were taken from six positions on each alga (Figure 5.2A): on the midrib of the central primary lamina close to the stipe and at the apex, and on lower and upper lateral secondary laminae at points proximal and distal to the midrib (~10 cm from the centre line of the primary lamina and ~10 cm from the end of the blade of the selected secondary lamina).

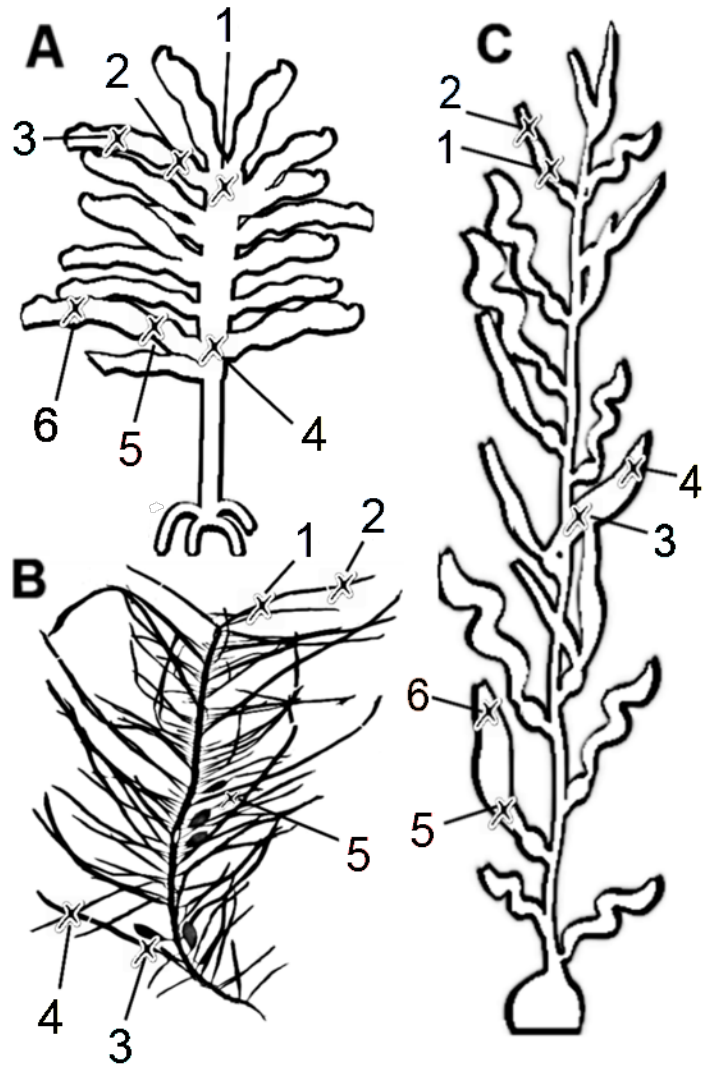

Figure 5.2: Diagram showing thalli locations for within-thallus variation sampling. *Ecklonia radiata* (A) numbering indicates position: 1 = midrib of the central primary lamina at the apex; 2 = upper lateral secondary lamina proximal to the midrib; 3 = upper lateral secondary lamina distal to the midrib; 4 = midrib of the central primary lamina at the bottom; 5 = lower lateral secondary lamina proximal to the midrib; 6 = lower lateral secondary laminae distal to the midrib. *Phyllospora comosa* (B) numbering indicates position: 1 = upper lateral blade proximal to stipe; 2 = upper lateral blade distal to stipe; 3 = lower lateral blade proximal to stipe; 4 = lower lateral blade distal to stipe; 5 = mid way along a blade terminating in a gas-filled float. *Macrocystis pyrifera* (C) numbering indicates position: 1 = upper lateral blade proximal to stipe (0.5 m depth); 2 = upper lateral blade distal to stipe (0.5 m depth); 3 = mid lateral blade proximal to stipe (5 m depth); 4 = mid lateral blade distal to stipe (5 m depth); 5 = lower lateral blade proximal to stipe (10-11 m depth); 6 = lower lateral blade distal to stipe (10-11 m depth). Note diagram is not to scale and is for illustrative purposes only.

Phyllospora comosa

Phyllospora comosa (Fucales) is a large brown fucoid alga restricted to southeastern Australia from Robe (South Australia) to Port Macquarie (NSW) where it dominates the shallow high wave-energy zone from 0-5 m (Campbell et al., 2014). This species grows to ~0.5-3 m in length, and has a short stipe bearing multiple primary branches. All PAM fluorometry measurements of *P. comosa* were taken from algae growing between 5-6 m depth. Diurnal and within-alga variation in PSII performance, together with variation among sites, latitudes, and seasons were examined. Measurements were taken in February 2011 and repeated in September of the same year.

Diurnal PAM fluorometry sampling was conducted *in situ* on n = 10 individuals at Fortescue Bay, Tasmania (43. 12471° S, 147. 97558° E) and near Port Stephens, NSW (32.78937°S, 152.08804 °E). Measurements were taken between 0800-0900 hr, 1200-1300 hr and 1600-1700 hr, with the samples on each individual standardised as one-third up the blade from the top of the stipe, and one-third along the branch lateral from the centre of the midrib.

To investigate whether variation in PSII performance was dependent on the part of the alga sampled, *in situ* measurements were taken from five positions (n = 10 individuals): on lower and upper lateral blades at points ~10 cm from the distal and proximal ends of the blade and from mid way along a blade which terminated in a gas-filled float (Figure 5.2B). Measurements were taken between 12-2 pm at St Helens, Fortescue Bay and Southport in Tasmania.

Macrocystis pyrifera

Macrocystis pyrifera (Laminariales), the largest of the brown algae, historically grows from 5-45 m in depth from the benthos to the surface and forms dense beds in nutrient-rich waters along the inshore subtidal reefs of southeast South Australia, Victoria and Tasmania, although it is now largely restricted to southern Tasmania. Each individual comprises several fronds arising from a holdfast and branching three or four times from near the base, with blades developing at irregular intervals along the frond, and with a single pneumatocyst at the base of each blade. Diurnal and within-alga variation in PSII performance of *Macrocystis pyrifera*, as well as variation across sites and depths, was measured in algae in Tasmania.

In situ diurnal measurements were taken from eight randomly selected individuals in Fortescue Bay (43.74806° S, 147.57386° E) between 0800-0900 hr, 1200-1300 hr and 1600-1700 hr. On each sampling occasion, individual RLC measurements were made on blades at three depths (0.5 m, 5 m and between 10-11 m). Within-alga and depth variation in RLC characteristics were investigated at three sites (Fortescue Bay, Blackmans Bay (43.05916° S, 147.19486° E) and Southport (43.31449° S, 146.57360° E). Measurements from n = 10 individuals were made from blades growing at 0.5 m, 5 m

and 10-11 m, except at Blackmans Bay where it was only possible to measure blades at 0.5 m and 5 m depth due to the shallower nature of the site. All measurements of *M. pyrifera* were conducted on blades at positions 15 cm from the base and 10 cm from the blade termination (Figure 5.2C).

Additionally, light-adapted and dark-adapted RLCs were conducted consecutively at different depths (on adjacent laminae) to investigate the effects of prior light history on patterns of variation of photosynthetic performance. Both dark- and light-acclimated measurements were taken in February 2011 and repeated in September of the same year at the Fortescue Bay site. Samples were taken at depths of 10-11 m, 5 m, and 0.5 m between 12-2 pm.

Statistical analyses

For all response variables (rETRmax, *Ek*, α), Analysis of Variance (ANOVA) was conducted for each species to determine the significance of differences in the means. For all ANOVA, data were checked for conformity to the assumptions of homoscedasticity and normality of residuals. Where heteroscedastic, the transformations to stabilise variances were determined by the relationship between standard deviations and means of groups (Draper, Smith, 1981). The statistical package 'R' (v 3.0.0) was used for all analyses.

5.4 Results

5.4.1 Variability in photosynthetic characteristics within and between regions

Light harvesting efficiency of photosynthesis (α) and rETRmax of *Ecklonia radiata* varied significantly across different sites within a region depending on the season (site*season interaction, α: $F_{4, 119} = 1.93$, $p = 0.0412$; rETRmax: $F_{4, 119} = 3.17$, $p = 0.0201$), although the pattern of differences among sites varied by region. In WA the highest values of both α and rETRmax occurred at the central latitude compared to northern and southern sites, but in Tasmania in summer rETRmax was highest in thalli at the most northern site (St Helens) (Figure 5.3A,B). Saturating light intensity (*Ek*) of thalli was highest in the central sites within each region, but this was not statistically significant (Figure 5.3C). Thalli at all sites in WA in both seasons had significantly higher values for saturating light intensity than those at Tasmanian sites ($F_{1, 119} = 0.46$, $p = <0.0001$).

There were significant differences among regions for rETRmax ($F_{2, 59} = 17.38$, $p = <0.0001$), *Ek* ($F_{2, 59} = 8.59$, $p = 0.0007$), and α ($F_{2, 59} = 4.62$, $p = 0.0148$) when comparing midday measurements made at central sites in the three regions. rETRmax and *Ek* were consistently lowest in Tasmania in both seasons. There was a significant effect of season on light harvesting efficiency of photosynthesis (α) ($F_{1, 59} = 10.78$, $p = 0.0019$) which was lowest in Tasmania over summer, but this was not reflected in winter when NSW *E. radiata* showed lowest values of α.

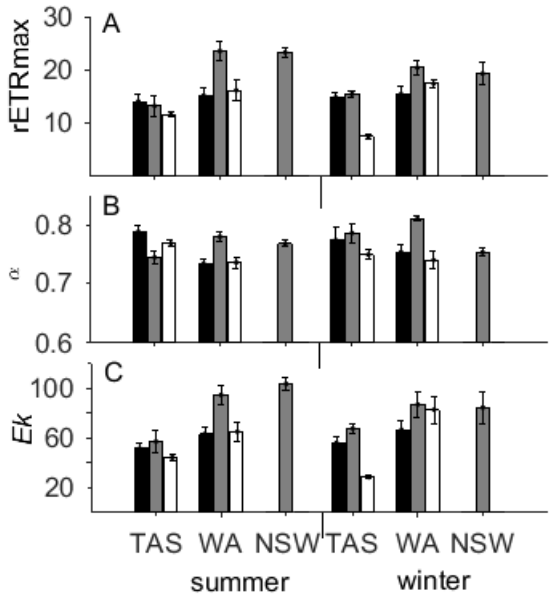

Figure 5.3: Characteristics of PSII for *Ecklonia radiata* sampled between 1200-1300 hr in Tasmania (TAS), Western Australia (WA), and New South Wales (NSW). Colours indicate different sampling sites within regions: northern (black bars), central (grey bars) and southern (white bars). Sites sampled were St Helens, Fortescue Bay and Southport (TAS), Jurien Bay, Marmion and Hamelin Bay (WA), and Broughton Island (NSW). Plots show estimates of (A) maximum relative electron transport rate (rETRmax), (B) light harvesting efficiency of photosynthesis (α), and (C) saturating light intensity (*Ek*), all as derived from RLCs measured by PAM fluorometry.

5.4.2 Diurnal variability in photosynthetic characteristics

Ecklonia radiata

RLCs revealed significant differences in daily patterns depending on the season and region for rETRmax (season*region, $F_{4, 156} = 4.71$, $p = 0.0013$) and *Ek* ($F_{4, 156} = 3.17$, $p = 0.0155$) of shallow *E. radiata* (Figure 5.4A,C). In both summer and winter, individuals in Tasmania and WA showed higher photosynthetic capacity (rETRmax) and saturating light intensity (*Ek*) in the middle of the day while these parameters increased throughout the day in NSW thalli. Thalli in Tasmania had lower rETRmax than both NSW and WA thalli during summer, while Tasmanian and WA seaweeds shared similar values of all rETRmax, α and *Ek* in winter. Light harvesting efficiency of photosynthesis (α) was generally lowest during midday sampling, although this was dependent on both region and season (period*region*season, $F_{2, 156} = 9.97$, $p = <0.0001$), with WA algae demonstrating lowest values of α during the evening measurements over summer (Figure 5.4B).

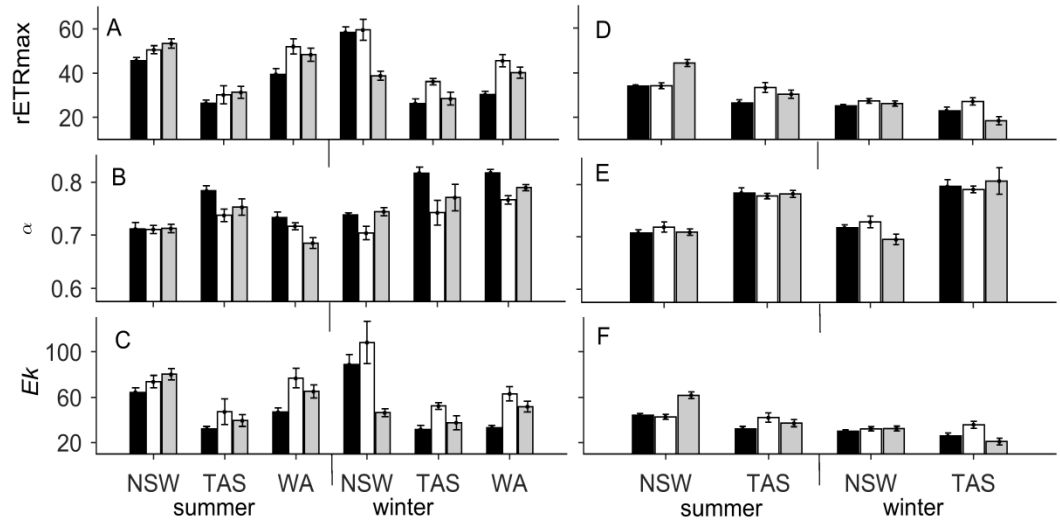

Figure 5.4: Characteristics of PSII for *Ecklonia radiata* sampled between 0800-0900 hr (black bars), 1200-1300 hr (white bars) and 1600-1700 hr (grey bars). Plots show estimates for shallow *Ecklonia radiata* (8-9 m) in NSW, Tasmania and WA (A,B,C), and deep *E. radiata* (28-30 m) in NSW and Tasmania (D,E,F). Plots show estimates for (A,D) maximum relative electron transport rate (rETRmax), (B,E) light harvesting efficiency of photosynthesis (α), and (C,F) saturating light intensity (*Ek*), all derived from RLCs measured by PAM fluorometry.

Shallow and deep *E. radiata* in both Tasmania and NSW revealed significant diurnal differences in photophysiology (Figure 5.4D-F). Thalli measured at midday were generally characterised by higher photosynthetic capacity (rETRmax) and saturating light intensity (*Ek*), with the exception of NSW thalli at both depths in summer in which the highest values of both parameters occurred in the afternoon/evening. In NSW photosynthetic capacity (rETRmax) and *Ek* were greater in shallow seaweeds in both summer and winter, however in Tasmania this effect was only observed in winter. There was a significant interaction between time of day, depth, region and season for rETRmax ($F_{2, 210} = 4.28$, $p = 0.0151$) with highest values generally occurring at midday in shallow water individuals, with the exception of NSW and Tasmanian thalli in summer which had maximum values of rETRmax in the afternoon). This effect was similar but not as pronounced in deep water (28-30 m) individuals. There was also an interaction between time of day, depth and region for *Ek* ($F_{2, 156} = 6.20$, $p = 0.0024$) which was generally greatest at midday sampling, with the exception of NSW thalli in summer which showed higher values of *Ek* in the afternoon. There was no consistent diurnal pattern across seasons for NSW seaweeds at 30 m.

Light harvesting efficiency of photosynthesis (α) was generally low at midday for shallow seaweeds in winter in all regions, and Tasmanian seaweeds at all depths tended to have lower α at midday throughout the year. Again, this effect was more pronounced in thalli growing in shallow water than at 30 m. These patterns are reflected in the significant interactions between time of day and depth ($F_{2,}$

$_{156}$ = 5.21, p = 0.0062), time of day and region ($F_{2, 156}$ = 3.37, p = 0.0363) and depth and region ($F_{1, 156}$ = 9.28, p = 0.0026).

Phyllospora comosa

Phyllospora comosa also showed differences in diurnal patterns of rETRmax and *Ek* depending on region ($F_{2, 100}$ = 6.20, p = 0.0029); Figure 5.5) and season ($F_{2, 100}$ = 6.11, p = 0.0032). Individuals showed higher photosynthetic capacity (rETRmax) and saturating light intensity (*Ek*) during midday sampling with the exception of NSW thalli in the summer where maximum values of *Ek* were not attained until later in the afternoon (1600-1700 hr). Light harvesting efficiency of photosynthesis (α) varied significantly with the time of day ($F_{2, 100}$ = 5.36, p = 0.0061), region ($F_{1, 100}$ = 88.92, p =< 0.0001) and season ($F_{1, 100}$ = 32.41, p = <0.0001), with minimal values of α occurring in the midday sampling, higher values in Tasmanian individuals than in NSW thalli, and higher values occurring in winter in both regions.

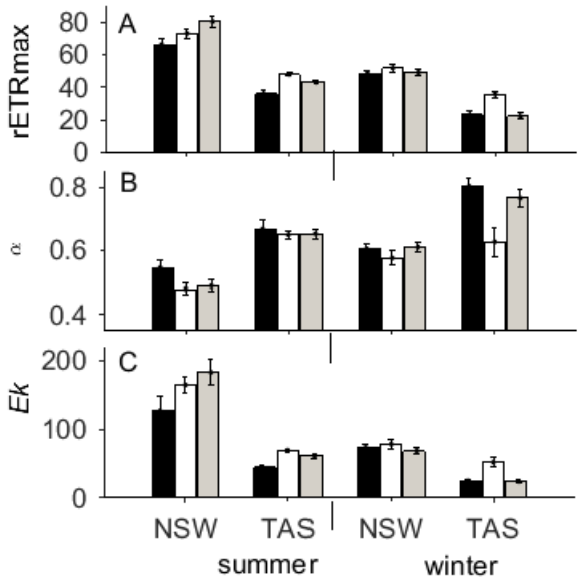

Figure 5.5: Characteristics of PSII for *Phyllospora comosa* (5-6 m) sampled between 0800-0900 hr (black bars), 1200-1300 hr (white bars) and 1600-1700 hr (grey bars) in NSW and Tasmania. Plots show estimates of (A) maximum relative electron transport rate (rETRmax), (B) light harvesting efficiency of photosynthesis (α), and (C) saturating light intensity (*Ek*), as derived from RLCs measured by PAM fluorometry.

Macrocystis pyrifera

Diurnal RLCs conducted on *Macrocystis pyrifera* at 10-11 m (deep), 5 m (mid-water) and 0.5 m (shallow) demonstrated diurnal variation in photosynthetic capacity (rETRmax), but the nature of diurnal patterns depended on both depth and season (period*depth*season, $F_{4, 100} = 3.33$, $p = 0.0131$). The pattern of diurnal variation in saturating light intensity (*Ek*) depend on the season (period*season, $F_{2, 100} = 5.71$, $p = 0.0045$). Over summer, thalli sampled in deep and mid-water showed distinctly higher values of rETRmax and *Ek* during the middle part of the day, while shallow thalli displayed maximum values later in the day (Figure 5.6). Over winter, both deep and shallow thalli showed peaks at midday, whilst mid-water measurements were at maximum levels during the morning. Patterns in α were the inverse of rETRmax and *Ek*, but seasonal and diurnal patterns were not statistically significant.

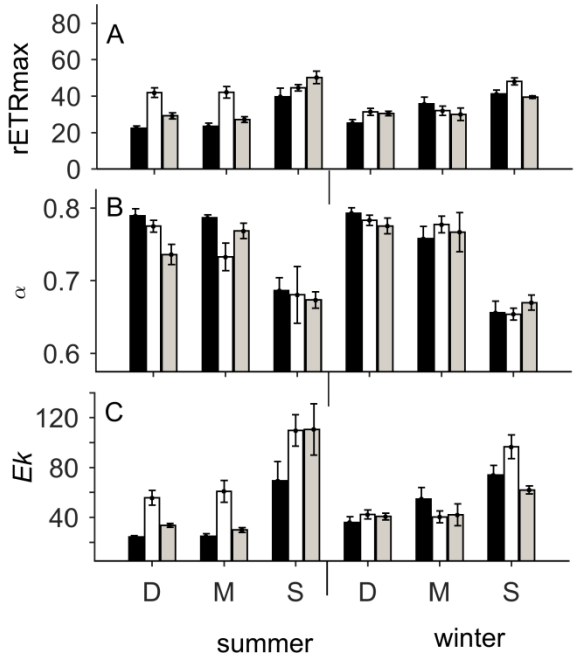

Figure 5.6: Characteristics of PSII for *Macrocystis pyrifera* in Fortescue Bay, Tasmania. Measurements were taken from deep (D), mid (M) and shallow (S) depths with sampling at 0800-0900 hr (black bars), 1200-1300 hr (white bars) and 1600-1700 hr (grey bars). Plots show estimates of (A) maximum relative electron transport rate (rETRmax), (B) light harvesting efficiency of photosynthesis (α), and (C) saturating light intensity (*Ek*), all derived from RLCs measured by PAM fluorometry.

5.4.3 Intra-thallus variation

Ecklonia radiata

Estimates of photosynthetic capacity (rETRmax), saturating light intensity (*Ek*) and light harvesting efficiency of photosynthesis (α) in *E. radiata* differed significantly depending on the part of the thallus from which measurements were taken, but the pattern of these differences depended on region (Tasmania and WA), site (within region) and season (position*region*site*season, rETRmax: $F_{20, 599} = 3.37$, $p = <0.0001$; *Ek*: $F_{20, 599} = 2.05$, $p = 0.0047$; α: $F_{20, 599} = 2.35$, $p = 0.0008$). Maximum values of rETRmax and *Ek* generally occurred in measurements taken from the upper distal lateral blade (Figure 5.7). Measurements at the upper midrib, upper proximal lateral blade and lower distal lateral blade also showed higher values of rETRmax and *Ek* than at the lower proximal lateral blade, however, the absolute values of estimates for lower distal lateral blade varied greatly between sites.

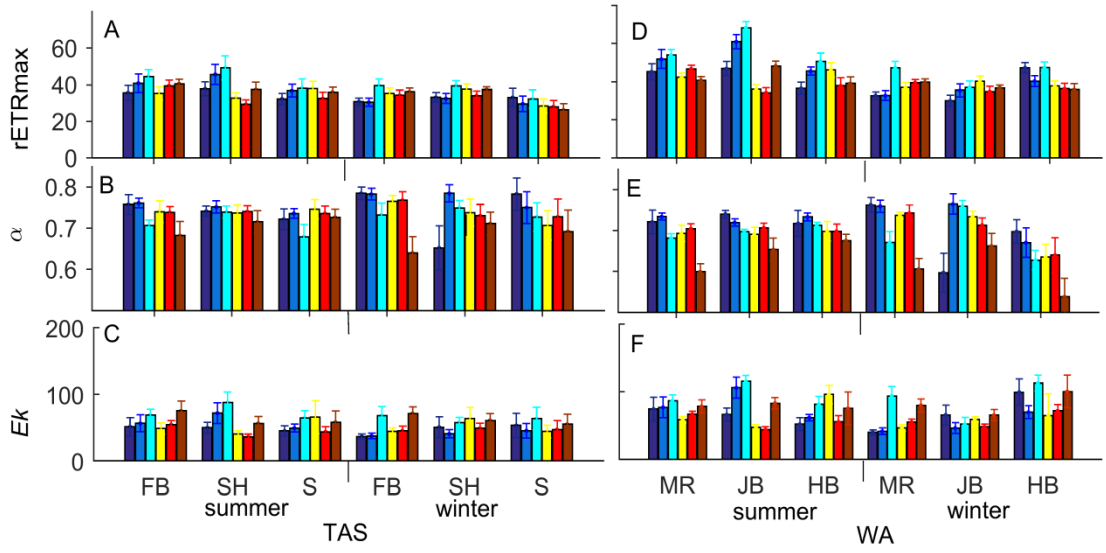

Figure 5.7: Characteristics of PSII for *Ecklonia radiata* in Fortescue Bay, St Helens and Southport, Tasmania (A, B, C respectively) and Marmion, Jurien Bay and Hamelin Bay, WA (D, E, F respectively). Alga parts are indicated by (from left to right, coloured bars): navy blue = midrib blade, upper; mid-blue = proximal lateral blade, upper; light blue = distal lateral blade, upper; yellow = midrib blade, lower; light red = proximal lateral blade, lower; dark red = distal lateral blade, lower (see Figure 1). Plots show estimates of (A, D) maximum relative electron transport rate (rETRmax), (B, E) light harvesting efficiency of photosynthesis (α), and (C, F) saturating light intensity (*Ek*), as derived from RLCs measured by PAM fluorometry.

Phyllospora comosa

Photosynthetic capacity (rETRmax), saturating light intensity (*Ek*) and the light harvesting efficiency of photosynthesis (α) of *P. comosa* also varied with the position on the thallus that was sampled, with the nature of differences depending on site and season (position*site*season, rETRmax: $F_{8, 292} = 4.38$, $p = <0.0001$; *Ek*: $F_{8, 292} = 2.90$, $p = 0.0239$; α: $F_{8, 292} = 3.62$, $p = 0.0006$). In general, maximum values for rETRmax and *Ek* were found on the upper blades of the thallus at positions either proximal or distal to the stipe, although at some sites tissue on distal positions on the lower blades also showed

high values of these parameters (Figure 5.8). Values of α were also lowest for upper thalli positions and lower distal blades.

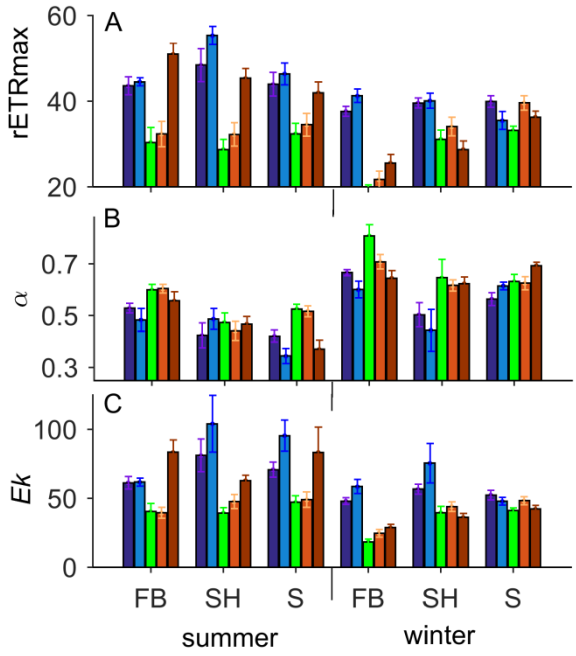

Figure 5.8: Characteristics of PSII for *Phyllospora comosa* (5-6 m) sampled between 12-2 pm in Fortescue Bay, St Helens and Southport, Tasmania. Thallus positions are indicated by (from left to right, coloured bars): navy blue = proximal blade, upper; mid-blue = distal blade, upper; light green = proximal blade, lower; orange =distal blade, lower; dark red = pneumatocyst-bearing blade (see Figure 1). Plots show estimates of (A) maximum relative electron transport rate (rETRmax), (B) light harvesting efficiency of photosynthesis (α), and (C) saturating light intensity (*Ek*), all derived from RLCs measured by PAM fluorometry.

Macrocystis pyrifera

Not surprisingly given the large size of individuals and thus with different blades of an individual growing at different depths, characteristics of PSII also varied with sampling location on the thallus in *Macrocystis pyrifera* (rETRmax: $F_{8, 257} = 10.35$, $p = <0.0001$; *Ek*: $F_{8, 257} = 12.13$, $p = <0.0001$; α: $F_{8, 257} = 11.94$, $p = <0.0001$; Figure 5.9). rETRmax and *Ek* were greatest for measurements taken from proximal and distal blade tissue growing close to the water surface (upper), with measurements of mid- and deep-water blades yielding lower values. This pattern was reversed for α. However, the nature of differences in estimates among different parts of the alga depended on both site and season (Figure 5.9), with maximum values of rETRmax and *Ek* occurring either on proximal or distal tissue of the shallowest blades.

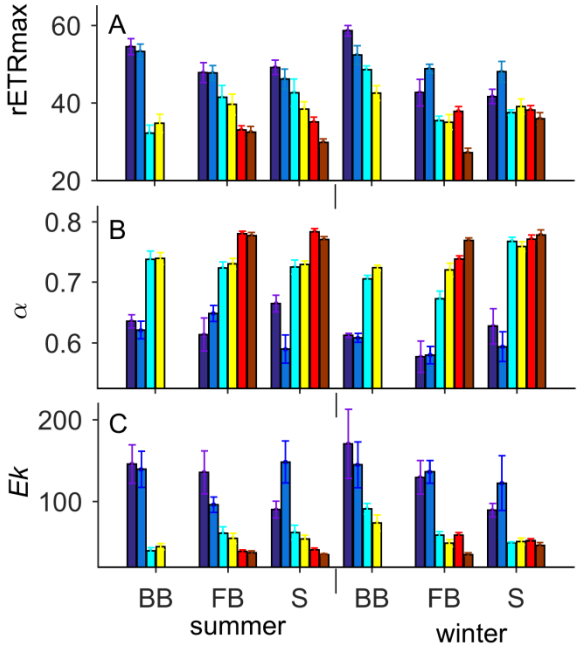

Figure 5.9: Characteristics of PSII for *Macrocystis pyrifera* sampled between 12-2pm in Blackmans Bay (BB), Fortescue Bay (FB), and Southport (S), Tasmania. Thallus positions are indicated by (from left to right, coloured bars): dark blue = upper proximal blade (1 m); light blue = upper distal blade; aqua = mid water proximal blade (5 m); yellow = mid water distal blade; red = bottom proximal blade (11 m); and brown = bottom distal blade (see Figure 1). Plots show estimates of (A) maximum relative electron transport rate (rETRmax), (B) light harvesting efficiency of photosynthesis (α), and (C) saturating light intensity (*Ek*), as derived from RLCs measured by PAM fluorometry.

5.4.4 Effects of dark-adapting tissue

Estimates of parameters from PAM measurements differed significantly among light- and dark-adapted *M. pyrifera* tissue (rETRmax: $F_{1,96} = 25.97$, $p < 0.0001$; *Ek*: $F_{1,96} = 19.66$, $p < 0.0001$; α: $F_{1,96} = 2.92$, $p = 0.0490$). However, depth and seasonal patterns were consistent for RLCs across light- and dark-adapted tissue (Figure 5.10). rETRmax and *Ek* were greatest for dark-adapted individuals, while α was lowest in dark-adapted individuals in shallow water. Patterns in the α varied with depth in both light- and dark-adapted tissue.

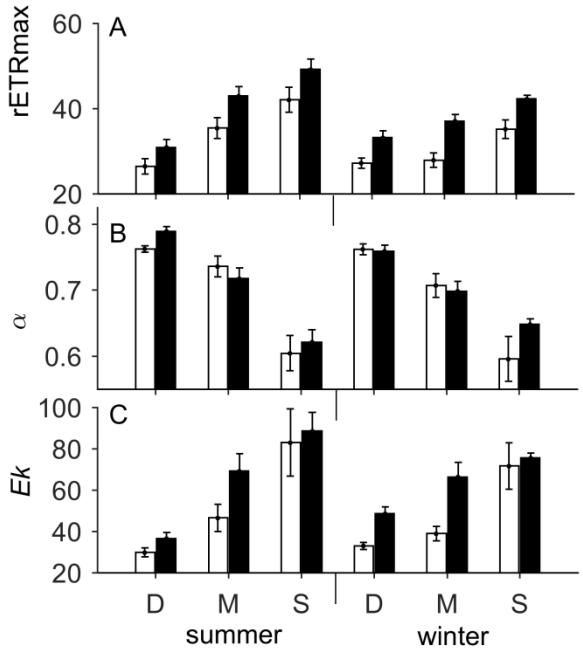

Figure 5.10: Characteristics of PSII for non-dark adapted (='light-adapted', white bars) and dark-adapted (black bars) tissue of *Macrocystis pyrifera* sampled between 12-2pm in Fortescue Bay, Tasmania. Samples were taken at 11 m (D), 5 m (M), and 0.5 m (S). Plots show estimates of (A) maximum relative electron transport rate (rETRmax), (B) light harvesting efficiency of photosynthesis (α), and (C) saturating light intensity (*Ek*), all derived from RLCs measured by PAM fluorometry.

5.5 Discussion

We aimed to evaluate the use of PAM fluorometry as a tool for assessing photophysiology in three key habitat-forming species (*Ecklonia radiata, Phyllospora comosa* and *Macrocystis pyrifera*). Because of widespread use of PAM measurements to infer potential photosynthesis, to interpret these kinds of measures and compare values across different studies, it is necessary to understand factors that can underpin variability in estimates. Here we investigated the effects of a range of variables reflecting choices in sampling design on PAM measurements, namely: time of day, depth, thallus position, region, sites within regions, and season. The results showed complex interactions between the variables, with strong seasonal and regional variation in particular having considerable impacts on PAM fluorometry outputs.

5.5.1 Diurnal patterns in photosynthetic potential

The strong diurnal patterns showing peak photosynthetic capacity (rETR) and saturating light intensity (*Ek*) during the midday period for shallow *E. radiata* and *P. comosa* are likely a result of the higher photosynthetic irradiance at this time. Energy can only be funnelled through PSII when the primary electron acceptor is open to accept electrons. When the amount of captured light increases, the possibility of being closed (not able to accept electrons) increases, and this results in a greater amount of fluorescence being emitted (Ralph, Gademann, 2005; White, Critchley, 1999). Hence, fluorescence yield is dependent on the previous short-term light history.

The exception to the general pattern was in NSW in summer, and may be indicative of a photoinhibitory response to high irradiance levels. Under high irradiance, not all the light energy absorbed by pigments can be effectively utilised in photosynthesis. Photoprotective mechanisms are used by some seaweed species and may allow dissipation of excess light through the xanthophyll cycle in what is known as 'dynamic photoinhibition' (Demmig-Adams, Adams, 1996; Hanelt et al., 1997; Krause, 1988). Species without photoprotective capacity may experience photo-oxidative damage to PSII reaction centres and other cellular components (Krause, 1988). The absence of any increase in light harvesting efficiency of photosynthesis (α) for these NSW individuals after midday also suggests some degree of photodamage such that photoprotective mechanisms were inadequate to dissipate the excess energy at midday (Ralph, Gademann, 2005). Although irradiance can be higher (both instantaneous values and integrated daily flux) in Tasmania during summer the response of NSW seaweeds indicating photodamage may be related to a lack of (or very low) self-shading in the canopy. In NSW, individual algae were much smaller, with minimal branching and much lower canopy cover than in Tasmanian *E. radiata* beds, and therefore may be more susceptible to high irradiance.

An additional consideration is the relationship between photosynthetic reactions and temperature. As with most enzyme-controlled reactions, the rate of electron transport through PSII (ETR) generally increases with temperature due to the temperature-specific activity of Calvin cycle enzymes (Lobban, Harrison, 2000; Raven, Geider, 2003). With summer seawater temperature in NSW during February 2011 reaching nearly 23˚C it is possible that temperature-related stress was a factor in the reduced photosynthetic capacity seen in these algae. The combined effects of high irradiance and temperature in NSW may be why stress was evident in NSW thalli in summer yet not in Tasmanian thalli where water temperatures at the study sites typically do not exceed 18˚C, but irradiance significantly exceeds that in NSW.

The general patterns in photosynthetic characteristics seen for shallow *E. radiata* were replicated in individuals measured in deep water in NSW and Tasmania, although there was noticeably less diurnal

and between-thalli variation within a given sampling occasion. This may be a result of smaller diurnal fluctuations in irradiance at depth. Moreover, while dense *E. radiata* canopies in shallow water may reduce incident irradiance by more than 90%, the density of adult *E. radiata* sporophytes is typically much lower in deeper water and often as low as ~1 m^{-2} at 30 m (J. Randall pers. observation). Hence, incident irradiance experienced by individuals in shallow water may differ markedly depending on the degree of shading by adjacent conspecifics. In contrast, the absence of a closed canopy in deep water reduces (and perhaps even eliminates) this kind of variation.

Comparing measurements made at 7 sites spanning more than 13° latitude and 37° longitude showed that the highest photosynthetic capacity and saturating light intensity in *Ecklonia radiata* occurred in shallow water individuals growing in NSW in the middle of the day, despite that higher irradiances occurred at more southern sites (BOM, 2011). In Tasmania the greatly reduced rETRmax and *Ek* at the southern-most site (Southport) in winter indicates that despite significantly increasing pigment concentration in Tasmanian seaweeds in winter (Flukes, 2015), they are unable to compensate adequately for the chronically low light intensities at this latitude in this season. *Ecklonia radiata* in Tasmania demonstrated significantly lower photosynthetic capacity (measured as rETRmax and *Ek*) than thalli from both NSW and WA at any time of year, arguably reflective of the strong temperature-dependence of the rate of electron transport through PSII (rETR) (Lobban, Harrison, 2000; Raven, Geider, 2003). However, the relatively high light harvesting efficiency of photosynthesis (α) in Tasmanian seaweeds in winter suggests acclimation or adaptation to enable efficient utilisation of the extremely limited available light.

For both deep (11 m) and mid-water (5 m) *M. pyrifera* blades, rETR and *Ek* values also showed strong diurnal patterns with peak photosynthetic capacity during the midday period, however in thalli from shallow water (1 m depth), these parameters continued to increase throughout the day with maximums reached in the afternoon. This is in contrast to previous research on this species off San Diego, USA, which showed highest photosynthetic performance at midday for all depths regardless of the time of year (Edwards, Kim, 2010). These differing results are likely to be related to latitudinal differences in patterns of irradiance. In Tasmania, PAR values in surface waters during midday in summer reach in excess of 1000 μmol photons m^{-2} s^{-1} (E. Flukes unpub. data) and thus photoinhibition is highly likely in these conditions. The continual decrease in α over the course of a summer day for blades in shallow water in Tasmania also suggests photoinhibition and potentially some degree of photodamage.

Values of rETR and *Ek* for *M. pyrifera* were similar in winter and summer and this likely reflects the seasonal acclimation of *M. pyrifera* to reduction in PAR by way of photoadaptation, although further investigation of this was beyond the scope of this work. *M. pyrifera* in Tasmania shows a 3-4 fold increase in the ration of fucoxanthin : chl *a* over winter (Flukes et al., 2015b) which indicates an

enhanced photon absorption capacity per unit thallus biomass (Fairhead, Cheshire, 2004a; Rosenberg, Ramus, 1982). Thus, despite much lower light levels in winter than in summer in Tasmania, photosynthetic capacity at each depth remains at similar levels.

5.5.2 Patterns in photosynthetic potential over longer periods

While there were clear seasonal fluctuations in the photosynthetic capacity of deep water (28-30 m) *E. radiata* in NSW and Tasmania and in individuals growing in shallow water (8 m) in WA, this was not the case for *E. radiata* in shallow water (8 m) in Tasmania. These individuals maintained similar values of photosynthetic capacity in summer and winter despite dramatic seasonal differences in irradiance (the magnitude of seasonal differences in daily PAR in Tasmania was approximately double that of NSW; Flukes, 2015). Photosynthetic characteristics in seaweeds (measured by PAM fluorometry) have been found to show strong seasonal fluctuations (e.g. Fairhead, Cheshire, 2004a; Flores-Moya et al., 1995; Kim et al., 2004; Lüder et al., 2002; Robeldo, Freile-Pelegrin, 2005; Saroussi, Beer, 2007a; Smith et al., 1983). However, many laminarians (Davison, Davidson, 1987; Fairhead, Cheshire, 2004a; Sakanishi et al., 1989) can adjust their light harvesting efficiency and specific activity of Calvin cycle enzymes to compensate for seasonal changes in temperature and irradiance (Cheshire et al., 1996a; Fairhead, Cheshire, 2004a), and these mechanisms are possibly invoked in Tasmania sporophytes growing in shallow water.

Tasmanian seaweeds are known to show a strong pattern of pigment concentration increasing from February (summer) through to maximum levels in August-September (late winter), coinciding with low irradiance (Flukes et al., 2015b). NSW seaweeds do not compensate for reduced irradiance in the same manner, suggesting either that they are unable to respond to lowered irradiance by increasing pigment synthesis, or that it is energetically unnecessary to do so at lower latitudes (Flukes et al., 2015b) such as the sites sampled in NSW and WA. For deep *E. radiata* in Tasmania, there was a clear reduction in photosynthetic capacity from summer to winter. This suggests that while deep water individuals in NSW may compensate for a very low light environment by increasing pigment concentration, the very low irradiances reaching 30 m in Tasmania in winter are insufficient to meet the energetic costs involved with the synthesis of large quantities of pigments (Hurd et al., 2014b). This indicates these thalli have an inherently restricted photosynthetic capacity.

In contrast to both shallow *E. radiata* and *M. pyrifera*, values for photosynthetic capacity and saturating light intensity for *P. comosa* in Tasmania, and particularly in NSW, were lower in winter. This supports previous work which indicates that, like *M. pyrifera* and *E. radiata*, *P. comosa* is (at least partially) capable of compensating for seasonal fluctuations in environmental conditions, largely by increasing pigment concentration in winter relative to levels in summer (Fairhead, Cheshire, 2004a; Flukes et al., 2015b). The low light harvesting efficiency (α) of both NSW and Tasmanian

seaweeds during summer also demonstrates a reduction in photosynthetic efficiency, which we interpret to indicate high light stress (Cordi et al., 1997; Gévaert et al., 2002; Ralph, Burchett, 1995).

5.5.3 Intra-thallus variation

In all species we examined, the magnitude of estimates of PAM fluorometric parameters depended on the position on the alga from which the measurements were taken. For both *E. radiata* and *P. comosa*, variation in photosynthetic capacity among different parts of the thallus correlates more with the position in the water column and extent of shading than with the age of the tissue. This is in contrast with results for other laminarians and fucoids where photosynthetic capacity, light harvesting efficiency of photosynthesis, and photosynthetic rates are related to tissue age (Dunton, Jodwalis, 1988; Gao, Umezaki, 1988). For most sites in both summer and winter the highest values of all parameters measured for *E. radiata* were for the upper distal lateral blade, with upper midrib blade, upper proximal lateral blade and lower distal lateral blade also demonstrating high values. For *P. comosa* these parameters were greatest for proximal and distal upper blade tissue, with some sites showing high values for blades bearing pneumatocysts. Both species form dense canopies on shallow reefs and there is significant shading of new tissue produced close to the meristem in the proximal area of thalli. However, in *P. comosa* lateral blades are usually quite long, and so the distal ends of lower blades coming off the central axis on the thallus often float relatively high in the water column due to water movement, intermittently exposing this part of the thallus to light levels comparable with those experienced by the upper blades. Moreover, in *P. comosa* blades which terminate in pneumatocysts (and thus have increased buoyancy) are often higher in the water column than other parts of the thallus, and are thus exposed to greater irradiance.

Investigation of different parts of the thallus in *M. pyrifera* showed consistently higher rETRmax and *Ek* values in measurements taken from blades near the surface. While this was anticipated given higher irradiances in surface waters than at mid-water and bottom depths, PAR values in shallow water in late spring and summer were far greater than the saturating irradiance of *M. pyrifera* (< 150 µmol photons m^{-2} s^{-1}), and thus some degree of summer photoinhibition is likely. It has previously been shown that *M. pyrifera* blades can respond to different environmental conditions at different depths, with surface blades presenting the highest concentration of UV-absorbing compounds, photoprotective carotenoids, and non-photochemical quenching (NPQ) capacity (Colombo-Pallotta et al., 2006). This supports our observations of lower values of α in surface blades which indicates downregulation of photosystem II and the induction of photoprotective mechanisms (Ralph, Gademann, 2005).

The higher values for photosynthetic capacity and saturating light intensity recorded at the Blackmans Bay site (Tasmania) are likely indicative of the close proximity to the *Blackmans Bay* wastewater

treatment plant (which provides secondary treatment only, i.e. does not strip nutrient from the effluent). *Macrocystis pyrifera* has limited capacity to store nitrogen, and growth is therefore strongly influenced by ambient nitrate availability (Jackson, 1982; Shivji, 1985; Wheeler, Srivastava, 1984; Zimmerman, Kremer, 1986). The increased levels of nutrients at this site would likely realise enhanced photosynthetic performance by enabling thalli to synthesise greater quantities of chlorophyll *a* and / or directly enhance of PSII functionality (Falkowski, Raven, 1997). The consistent values of both rETRmax and *Ek* across summer and winter is again likely indicative of seasonal photoadaptive responses to reduced irradiance (e.g. increased pigment synthesis), which may be augmented by the continuous input of nutrients from the outfall of wastewater treatment facility.

5.5.4 General recommendations for PAM fluorometry

Photosynthetic characteristics of *E. radiata, P. comosa* and *M. pyrifera* indicated by a diving PAM unit used *in situ* on attached algae were highly dependent on the time-of-day, depth, latitude/region, season, and part of the thallus from which measurements were taken. Patterns dependent on time-of-day, depth and thallus placement varied with season and/or geographic region, and the nature of these patterns varied between species. Recognition of this variability should help inform future research utilising PAM fluorometry to estimate performance of PS II (often interpreted as photosynthetic potential) in macroalgae. It also seems clear that PAM measurements may be sensitive to canopy shading, depth, and photoinhibitory and/or temperature-related stress responses, particularly at seasonal and range extremes.

Generally, all species at all depths consistently demonstrated highest activity of PSII during midday sampling, suggesting that comparative research between regions/sites should ensure that all measurements are taken at a standard time in the diurnal cycle. Most research is focused on maximum photosynthetic capacity (rETRmax), which is a reliable comparative measurement. However, for both *E. radiata* and *P. comosa*, in the northernmost latitudes (in WA and Tasmania) where summer seawater temperatures were most extreme, there was marked reduction in these values during midday sampling. This suggests that decisions of the most appropriate time of day for PAM measurements will depend on the ecological context of the study, since these measures are highly variable regionally and are likely to depend on local environmental conditions (e.g. temperature, irradiance, wave exposure, nutrient availability etc.).

For *M. pyrifera*, maximum photosynthetic capacity varied significantly with depth with a depth range between 0.5 m - ~30 m (different points of the plant in the water column), indicating the importance of standardising the depth at which measurements are made in comparative studies; PAM measurements made on one part of the thallus cannot be considered representative of all parts. Choice of thallus part for sampling will depend on the research objectives and will influence interpretation.

Measurements of this species (and other large macroalgae with thalli spanning the water column over a large depth range) must be made at multiple depths to adequately represent the photosynthetic potential of the entire individual.

Another important consideration is the choice of the position on the thallus from which the measurement is taken (independent of differences in depth). In contrast to previous research (Edwards, Kim, 2010), for all species examined our results showed that tissue age had little effect on photophysiology. Although measurements varied throughout different positions on a single thallus, they did not vary coincident with tissue age according to thallus position, suggesting that ambient irradiance levels may be relatively much more important. Therefore, the most important consideration for studies seeking to make comparative measurements is consistency in selecting the position on the thallus to be measured. The location on a thallus from which to obtain measurements for a given study will depend on the species and regional variation in species morphology. For example, at sites with high wave-action *E. radiata* has a smaller growth morphology with narrow laterals and blades (Wernberg, Thomsen, 2005), so that at exposed sites the effects of self-shading and shading by adjacent conspecifics may be less important than at more sheltered sites. Therefore, if the aim of the research is to compare photosynthetic parameters of individuals at an exposed site with those in an area with high levels of canopy shading then the most appropriate location for sampling will likely be on the upper blades of the thalli.

The similar patterns in photosynthetic potential indicated for both light- and dark-adapted RLCs show that, although absolute values may vary depending on which method is chosen, for the kind of comparative approach used in the present research, both are valid approaches. This supports earlier research on *E. radiata* and *P. comosa* that showed similar findings (Flukes, 2015). This research provides a unique investigation into the effects of sampling methodology on estimates of macroalgal productivity utilising PAM fluorometry, and these findings should be considered in methodological design for future research measuring photosynthetic potential of macroalgae using PAM fluorometry.

Acknowledgements

This work would not have been possible without the assistance of many volunteer divers, most notably Robert Perry and Pearse Buchanan from the University of Tasmania. The work was supported by an Australian Research Council (ARC) Discovery grant to Craig R Johnson and Jeffrey Wright, and Australian National Network in Marine Science (ANNiMS) grants to Jo Randall, Thomas Wernberg and Craig R. Johnson. Thomas Wernberg received funding from an ARC Future Fellowship.

Chapter 6

General Discussion: The impact of methodology on measurements of primary productivity in macroalgae

6.1 Summary

Macroalgal forests provide the ecological foundations of most temperate shallow marine reef systems. Ongoing climate change and other environmental change driven by anthropogenic activity poses an increasing threat to habitat-engineering seaweeds, and a central focus in ecological research is monitoring the way in which environmental change impacts on their functioning. Productivity is the usual proxy for macroalgal system functioning, but research on the productivity of macroalgal systems is generally conducted over small spatial scales using a variety of methods which measure different characteristics both individually and collectively. Interpreting these kinds of measurements requires a clear understanding of patterns of spatial and temporal variation in photosynthetic parameters, and of the relationships between the different methods. There is a critical need to not only develop new techniques for accurate measurement of productivity on both small and large spatial and temporal scales, but also to develop knowledge on how best to interpret and compare them. This chapter addresses the need for an overview that compares the most widely used methods for measuring productivity and photosynthetic potential in macroalgae. Because of the desire to estimate production of entire algal assemblages over large spatial scales, it includes the possible use of acoustics and ambient oxygen models.

Acoustics is an emerging technique which, in theory, allows measurement of productivity of entire macroalgal assemblages over large spatial scales in coastal areas providing that productivity is sufficiently high to produce microbubbles (i.e. in gaseous form). However, although our research shows that propagation models can detect void fractions of oxygen in the canopy layer, analysis of empirical acoustic data did not identify diurnal differences of the magnitude predicted by a bubble layer model for a small but ecologically significant void fraction. This suggests that, at least in some cases, oxygen production in some kelp forests is not so high as to produce microbubbles that can be detected with acoustics. Nonetheless, the method remains an area of interest for future study given the potential for very large scale measurements, and the possibility that productivity in some systems may

produce oxygen in the water column as microbubbles, which would not be detected when using traditional methods based on measuring dissolved oxygen.

We show that ambient oxygen models can provide a good fit to measurements of daily fluctuations in dissolved oxygen (DO) in the water column, and thus that the method can give a robust estimate of community-wide production over large spatial scales. Our findings suggest that estimates of total macroalgal production are about double that based on estimates of kelp only, despite that kelp accounts for most of the macroalgal biomass. Given development of more sophisticated models, this approach appears particularly promising for estimating total macroalgal production in relatively shallow waters with widespread macroalgal coverage where turnover rates of water masses is low.

Benthic oxygen exchange chambers allow capturing whole plant processes with accurate results, although, for those communities where biomasses are small (e.g. filamentous turfs on coral reefs) sometimes community assemblage measurements are possible. Often however, such as in canopy-forming macroalgal communities, they are only suitable for measuring photosynthetic performance of individual algae, and results cannot easily be scaled up to community level. PAM fluorescence techniques, which have the benefits of ease of use and ability to provide instantaneous measurements, only measure activity in PSII and thus need not equate to realised photosynthesis at all. Moreover, even as a proxy for potential photosynthesis, results relate only to the small area of tissue under analysis and not the physiology or metabolism elsewhere on the alga. It is recommended that PAM fluorometry be used in conjunction with other measurements, and with consideration given to small-scale variability associated with time-of-day, depth, and placement of the instrument on the thallus. While PAM fluorometry metrics cannot be seen as a proxy for photosynthesis, the Fv/Fm estimate provides a useful means to check for healthy PSII activity prior to subjecting individuals to measurement using other techniques.

We conclude that each method of measurement has distinct advantages and disadvantages. It is recommended that in planning research, it is important to consider that each method provides different kinds of estimates of production or proxies of actual or potential production, and that there needs to be considerable clarity in the question being tackled before selecting the most suitable technique. In many cases, using several of these techniques simultaneously will provide a more complete picture of macroalgal bed production.

6.2 Estimating and interpreting production in macroalgal beds

Appreciation and successful management of marine systems requires a comprehensive understanding of ecosystem processes. Suitable tools for monitoring system components in space and time are essential to this understanding. This is particularly important when considering ecosystem-

engineering species that play a vital role in regulating community structure and ecological processes. Macroalgal forests provide the ecological foundations of most temperate shallow marine reef ecosystems (Dayton, 1985; Steneck, Johnson, 2013). They modify the abiotic environment beneath the canopy, including flow, irradiance, scour, and sedimentation regimes, and provide a structurally complex habitat supporting high levels of biodiversity and endemism (Dayton, 1985; Steneck, Johnson, 2013). These communities tend to react strongly to short term environmental perturbations and often show low resistance to disturbance, but rapid recovery once disturbances are removed (Dayton, 1985; Kennelly, 1987; Tegner, Dayton, 1987). A change in productivity and functioning of macroalgae is likely to have large flow-on effects for associated organisms (Connell, 2007; Flukes et al., 2015a; Ling, 2008; Wernberg et al., 2013).

The south eastern Australian coastline contains some of the most productive macroalgal forests in the world (de Bettignies et al., 2014). Stronger and more frequent incursions of warm East Australian Current (EAC) water into south eastern Australia (particularly Tasmania; Ridgway, 2007) have caused warming of coastal waters in eastern Tasmania at a rate close to four times the global average (Johnson et al., 2011; Ridgway, 2007). In comparison to sub-Antarctic water masses that previously dominated waters off the east coast of Tasmania, the EAC water is nutrient-poor with nitrate levels often undetectable in summer (Coale et al., 2004). Hence, the canopy-forming macroalgal species that dominate this region (such as *Ecklonia radiata*, *Phyllospora comosa*, and *Macrocystis pyrifera*) are exposed to the confounding effects of elevated temperature and decreased nitrogen.

The predicted increase in temperature and decrease in nitrates for southeast Australian waters is likely to negatively impact the physiological performance of macroalgal species, and indeed this has been documented for *M. pyrifera* in eastern Tasmania (Johnson et al., 2011), while for *P. comosa* there are links between warmer temperatures and deleterious effects on photosynthetic efficiency, growth, and survival (Flukes et al., 2015b). There is now also evidence that, in some locations, macroalgal communities are retreating in a manner consistent with ocean warming (Johnson et al., 2011; Wernberg et al., 2011; Wernberg et al., 2016). Consequently, for successful management of these marine areas and mitigation of future climate change effects it is critical that effective tools are available to measure and compare productivity.

Research on the productivity of macroalgal systems is generally conducted over small spatial scales using any of a variety of methods. Generally, these methods measure different characteristics of individual algae and, in some cases, of algal assemblages (IMOS, 2017). Due to the diversity of measurement methods, estimates of primary productivity (GPP) for temperate reefs are numerous and variable (Schreiber, 2004a). In addition, interpreting these kinds of measurements requires a clear understanding of patterns of spatial and temporal variation in photosynthetic parameters (Urban et al., 2017). Despite the diversity of approaches to estimating production and space-time variability in

estimates, there has been little work to compare measurements and quantify differences in productivity estimates across the different techniques. This can lead to challenges for ecologists attempting to amalgamate research findings to facilitate long-term, broad-scale perspectives or compare short-term research between spatially separated communities or across different studies.

Measurements at small scales

Photosynthesis is a metabolic process that is routinely measured and used to estimate productivity in seaweeds. It is the basis of primary production and indicates the incorporation of carbon into organic compounds (Lobban, Harrison, 2000). A commonly-used method of estimating photosynthesis involves logging oxygen release in the light and dark as a proxy for both net photosynthesis (during the day) and respiration (at night). Oxygen exchange chambers have the advantage of being able to yield productivity values after a single 24 hour cycle. However, for larger macroalgae the method is usually restricted to measurement of a single individual, or partial individual, per chamber. Further challenges arise when considering size extremes; turf algae can be too small to be measured individually or even as a single species so that community rates must be measured (Atkinson, Grigg, 1984; Hackney, Sze, 1988), while large species such as *Macrocystis* must be sampled as tissue pieces, leading to issues such as wound respiration (Littler, 1979b).

Another widely used method to monitor the functional state of photosynthetic organisms is Pulse Amplitude Modulation (PAM) fluorometry, which measures chlorophyll (Chl) *a* fluorescence associated with photosystem II (Rosenqvist, van Kooten, 2003). Various photosynthetic parameters can be derived from the fluorescence measurements and collectively these parameters have been interpreted as a measure of *photosynthetic capacity*. Electron transport rate (ETR) has been found in some cases to relate closely to photosynthetic activity as measured by CO_2 uptake or oxygen evolution (Beer et al., 1998). Hence, PAM fluorometry is often interpreted as a method to measure potential photosynthetic performance, with the significant benefit of providing virtually instantaneous (90 second) measurements. However, PAM fluorometry measurements are strongly influenced by an individual's ambient light history, so measurements can vary greatly depending on cloud cover and/or the sun's position in the sky, canopy shading, depth, latitude and season. Consequently, appropriate interpretation of studies using PAM fluorometry must consider how these variables affect measurements.

Methods at large scales

Dissolved Oxygen (DO) models estimate gross primary productivity (GPP) from DO measurements in the open water column through time, factoring ecosystem respiration (estimated from night time changes in dissolved oxygen), exchange of O_2 from the atmosphere (typically modelled as a function

of the concentration gradient between water and atmosphere with a wind-derived coefficient), and vertical and horizontal advection (Staehr et al., 2010). Developments have made it easy to continuously measure DO concentrations and relevant physical and chemical parameters precisely over several days, allowing for detailed description of temporal variability and calculation of metabolism. Despite the obvious advantages and simplicity of obtaining relevant data (which is not to say that the underlying model is simple), questions remain about the extent to which free-water measurements actually represent whole-system metabolism (Coloso et al., 2008; Lauster et al., 2006; Van de Bogert et al., 2007). In particular, assumptions associated with advection, quantification of the air-water exchange and respiration estimates require consideration (Staehr et al., 2010).

The use of underwater acoustics also emerges as a potential technique to allow large-scale measurement of productivity in coastal areas. Measuring benthic production in shallow water marine environments using acoustics involves tracking changes of sound propagation characteristics over time with the ultimate goal of quantifying the volume of oxygen bubbles formed in the macroalgal canopy, although these measurements would also need to be complemented by measuring DO since sound speed is not appreciably affected by dissolved oxygen concentration. Variability in acoustic propagation is correlated with the diurnal productivity cycle, and can be mainly attributed to gas bubble production (Hermand, 2003; Hermand et al., 1998). Given the possibility that substantial proportions of the oxygen produced may be in gaseous form when saturation exceeds 100%, there is a risk that ecologists are underestimating productivity in coastal environments when using techniques based on measuring changes in DO. Successful development of this technique would allow non-intrusive measurements of productivity over multiple spatial scales simultaneously.

The development of ecologically sound estimates of primary production is difficult, regardless of whether it is based on short-term estimates of photosynthesis, long-term biomass yields, or large-scale community-level productivity. Nonetheless, it is an important and useful indicator of ecosystem functioning and thus useful to consider in assessing ecosystem performance. But clearly questions remain concerning comparability of techniques, and species/community- specific applicability, as well as a need for the development of methods that allow integrated large-scale measurements of total community production and metabolism.

Acoustic propagation modelling

The use of acoustic propagation modelling in seaweed communities has the potential to revolutionise measuring primary productivity in these systems depending on the extent to which photosynthesis produces microbubbles trapped in the macroalgal layer. Acoustics can potentially allow measurement of primary production aggregated across entire assemblages of algae and over ecologically meaningful spatial scales (10^0—10^5 m). One of the most interesting aspects of this technique is the

questions it raises over the validity of more traditional methods. Acoustics relies on super-saturation of oxygen in the water column and the formation of oxygen microbubbles. Macroalgal habitats are amongst the most highly productive ecosystems in the world (Cebrian, 1999; Mann, 1973b) and seaweed bed waters can readily become saturated with oxygen, suggesting that oxygen microbubbles may form through photosynthesis. It follows that methods that rely on measuring oxygen only in dissolved form could be underestimating productivity. The advantage of acoustic modelling is that even though it is only oxygen in bubble form that is measured, the dissolved oxygen portion could easily be quantified according to the environmental conditions at the time of measurement (since if microbubbles are present then the environment can be assumed to be saturated). Hence, acoustics could provide accurate estimates of total production of oxygen.

In the present research, propagation modelling was able to detect substantial void fractions of oxygen bubbles given environmental conditions as measured at Fortescue Bay during the empirical acoustics experiment. Indeed, the modelling suggests that acoustic detection would require only a relatively small proportion of oxygen production in bubble form. However, there was no acoustic detection of a void fraction in the inverse analysis of the empirical acoustic data, although we emphasise that this does not preclude successful future development of the technique. Experiments in seagrass communities reveal a distinct diurnal pattern in the acoustic signal, almost certainly due to production of oxygen bubbles within internal lacunae (Hermand, 2003). Various factors may have precluded this occurring in the present study, some of which are unavoidable in seaweed communities (e.g. the lack of internal lacunae in photosynthetic tissue in marine macroalgae, differences in mixing conditions in the water column between these habitats) and others that were specific to this site at the time of the experiment.

Further development of acoustic methods may see more favourable results, given several limitations of the model used in this study. Horizontal refraction, reflection from the shore (a horizontally stratified medium is assumed), and sound scattering due to other factors (e.g. fish schools, sea surface roughness without a “mirror-like” 180 degree phase shift reflection, bubble clouds just below the sea surface, the effect of seaweed in aggregations rather than individuals and oxygen bubbles) can have large effects on sound propagation, and cannot be predicted by the simplified ray/beam theory model used here. It is probable that dynamic vertical mixing at the Fortescue Bay site means that the environment does not meet the simplifying assumptions of the ray-based model used here, or of our analysis of the environmental acoustic data obtained at the site. It is possible that further work, particularly in highly productive environments and using a more complex analysis of the acoustic data, may prove acoustics to be a useful tool for estimating the productivity of some seaweed communities over meaningful spatial scales.

Modelling ambient dissolved oxygen

It is clear that for estimates of total community production holistic methods at a scale that encompasses a representative sample of the total community are necessary, and measuring and modelling diel change in dissolved oxygen can provide this approach in shallow water communities (Bott et al., 1978; Leclercq et al., 1999, Chapter 4). Some communities have characteristics which make them suitable candidates for scaling up of productivity estimates measured from other techniques. However, our results of diel models (Chapter 4) suggest that this might grossly underestimate community productivity in kelp forests by ignoring sub-canopy and understorey species, since we found that productivity estimates of the whole assemblage were approximately double that based on measurement of *E. radiata* alone from respirometry chambers and scaling by biomass density *in situ*.

The majority of research conducted using diel models has focussed on fresh water habitat (e.g. Bott et al., 1978; Odum, 1956; Staehr et al., 2010; Van Duin, Lijklema, 1989), although significant work has also occurred in coral reef systems (Leclercq et al., 1999; Odum, Odum, 1955; Suzuki et al., 1996). In kelp forest communities, the method has mostly been used to study productivity in giant kelp (*Macrocystis pyrifera*) with values of 1 mol m^{-2} s^{-1} reported by Jackson (1977), and similar results given by Towle and Pearse (1973). Although this value is ~2 times that estimated in this work for *E. radiata*, *M. pyrifera* is a much larger and faster growing species that spans the entire water column forming a dense surface canopy, so total biomass of photosynthetic tissue m^{-2} sea floor is typically much greater.

It cannot be known which of our two models most accurately represents oxygen production in the kelp bed as, to our knowledge, no research has previously used measurements of ambient DO to estimate productivity in *Ecklonia radiata* communities. It is envisaged that ultimately the preferred method for modelling the kelp bed system will be a hybrid of both approaches, i.e. where a relationship between O_2 production and PAR is defined and parameterised on the basis of fitting to observation and then applied to data from DO sensors in or close to the seaweed layer, and where Fourier components are fitted to data from surface sensors. It is also worth noting that the equation for O_2 diffusion at the surface was derived for open ocean environments, so more effort to modify this equation for much flatter water in confined bays is warranted.

It is important to note that the models presented are deliberately simplified. There are obvious limitations and future developments may well benefit by explicit numerical consideration of additional factors such as tide, wave action, and currents. However, in terms of experimental setup this method is extremely simple and cost effective, and continuous, long term measurements can be obtained with low effort. Therefore, even in systems where small scale estimates of productivity (i.e. respirometry chambers) have been shown to accurately scale to community level, taking an ambient oxygen modelling approach may be a more efficient means of measuring and integrated total

community production. It is most suited to sites supporting large continuous tracts of the community / habitat of interest where there is little or no horizontal flux of water masses. In kelp forests or communities dominated by large individuals but with well-developed sub-canopy or other understorey layers, ambient oxygen modelling may be the only means of obtaining accurate estimates of community-level metabolism.

Benthic chambers

As previously discussed, production per unit area of sea floor attributed to kelp (*Ecklonia radiata*) alone using the benthic chamber method (when scaled for biomass) is about half of the estimated gross production from modelling ambient DO. While other species undoubtedly account for a substantial amount of the difference, it is also possible that methods using respiration chambers underestimate ambient DO production. Longstaff et al. (2002) reported concerns with self-shading when using the oxygen exchange technique, and no doubt this is a factor to consider (as it is in nature) when interpreting production estimates using this method. While it is likely that dynamic self-shading occurs naturally, this shading effect is much more likely in relatively low volume chambers where the water is relatively still. Hence, projected surface area of the algae exposed to light is likely overestimated.

Additionally, processes such as photosynthesis and respiration in seaweeds are dependent on the flux of dissolved substances to and from the thallus surface (Hurd et al., 2014a). This, in turn, is dependent on the magnitude of water motion over the surface of the thallus which affects boundary layer properties and thus gas diffusion and nutrient uptake rates (Patterson et al., 1991). The saturating velocity for maximal rates of photosynthesis varies by species. For example, for photosynthesis and nutrient uptake by *M. pyrifera* the saturating velocity was 2–6 cm s^{-1} (Hurd et al., 1996; Wheeler, 1980), whereas for turf communities velocities of 20 cm s^{-1} were required for maximal rates (Carpenter et al., 1991).

Another drawback of the respirometry chamber method lies with the need for scaling to the biomass density of whatever is in the chamber. At one end of the spectrum, individual filaments of many species of turfing algae are too small and generally too entangled with others to be measured individually. At the other extreme, very large seaweeds, such as *Macrocystis pyrifera*, must be sampled using relatively small pieces of tissue, although large tent-like enclosures have also been used (Atkinson, Grigg, 1984; Hatcher, 1977). Cutting seaweed tissue has been shown to result in substantial underestimates of production (Hatcher, 1977), and there are also problems associated with crowding of thalli in chambers and physical injuries from compression (Flukes et al., 2015a). In addition, estimates of productivity will be dependent on the thallus portion sampled. Gradients in productivity and respiration from tip to base within individual blades have been found for, amongst

other species, *Macrocystis pyrifera* (Clendenning, 1971) and *Laminaria digitata* (King, Schramm, 1976; Küppers, Kremer, 1978). Consequently, care must be taken when extrapolating from measurements made on small segments of large/complex macroalgae to entire individuals or populations.

Despite its disadvantages, benthic oxygen exchange chambers can provide a precise estimate of productivity for individuals, single species, and communities comprised of small individuals. Oxygen production and respiration can be directly measured in chambers as they are a closed system, enabling minimisation of external variables and thus analysis is straightforward. Provided that potential limitations of the method are considered when interpreting results (e.g. self-shading and reduced water motion) this technique offers a robust method of assessing productivity over small spatial and temporal scales.

PAM fluorometry measurements

There has been a rapid rise in the use of physiological proxies for estimating photosynthetic capacity driven, in part, by advances in technology and falling costs of sophisticated equipment. In particular, the diving pulse-amplitude modulated (PAM) fluorometer (Diving-PAM, Walz, Germany) has permitted rapid growth and advances in seaweed ecophysiological research on plants and algae *in situ* (e.g. Falkowski, Raven, 1997; Flukes, 2015; Flukes et al., 2015b; Longstaff et al., 2002; Pedersen, Borum, 1997) by facilitating rapid and non-destructive sampling under natural conditions. PAM fluorometry parameters are often used as indicators of photosynthetic potential or 'health'. However, physiological proxies provide a snapshot in time that is typically only a description of a single physiological process, and therefore do not always accurately represent the multiple metabolic and biochemical processes which ultimately culminate in growth and productivity.

Electron transport rate in photosystem II often closely mirrors photosynthetic rate and productivity and growth (Beer et al. 2000, Longstaff et al. 2002). However, at saturating light intensities ETR values tend to overestimate O_2 evolution rates (Enríquez, Rodríguez-Román, 2006; Franklin, Badger, 2001). Chapter 4 shows a similar pattern in the relationship between rETRmax and PAR and the PI curve generated from the oxygen exchange chambers for *E. radiata*, however, this only indicates a pattern of maximum potential photosynthesis, rather than an actual photosynthetic rate. Fluorescence measurements yield estimates of photosynthetic potential but these do not factor alternative electron sinks which may consume O_2 (e.g. Mehler reaction and chlororespiration) (Consalvey et al., 2005).

Research suggests that photosynthetic capacity and efficiency appears to reflect only the health of photosystems at the immediate location of the measurement and are strongly influenced by tissue age, condition, and light history (including self-shading) (Enríquez, Borowitzka, 2010; Oláh et al., 2010).

In the present work we found that it is possible to obtain normal rapid light curves and Fv/Fm values from small areas of healthy tissue when >90% of an individual alga is necrotic, disintegrating, and appears to be senescing. Thus, it is important that individual measurements should not be used to predict organism-scale physiology, and applying one absorption factor to a multitude of situations is likely to result in over/under-estimation of ETR.

A second parameter, maximum quantum yield (*F*v/*F*m), or, for light- adapted RLCs, effective quantum yield (α) is proportional to the efficiency of light capture (Schreiber, 2004b). *F*v/*F*m is generally considered to be a sensitive measure of photosystem health as it gives a measure of the proportion of open reaction centres in PSII available for photosynthesis (i.e. the intrinsic potential quantum efficiency of PSII) (e.g. Jones et al., 2000; Macedo et al., 2008; Ralph, Short, 2002). However, recent work has demonstrated that relatively high values of *F*v/*F*m can be measured immediately adjacent to severely necrotic tissue (Flukes, 2015; Ralph, Short, 2002), and *F*v/*F*m (or α) is clearly not necessarily indicative of performance of the individual. Our work shows very little variation in effective quantum yield regardless of the irradiance (Chapter 4), and it is possible that this reflects the fact that conditions during the experiment were favourable for growth and the individuals that were sampled were healthy. However, high values of α do not necessarily indicate photosystem functionality because light energy transfer from reaction centres can be interrupted before PSI is reached. And even if absorbed light energy is used effectively to generate photosynthates, these may be used to synthesise cellular compounds such as pigments or proteins unrelated to growth (e.g. Cruces et al., 2012). Therefore, while low α indicates photosystem stress, high α does not necessarily translate to general 'health' of the alga or to growth or ecological capacity.

PAM fluorometry can undoubtedly give an indication of the health of photosystem II, and potential electron transport rate, with the clear advantage of being able to provide near-instantaneous measurements. However, PAM outputs are indications of potential, rather than an actual physiological processes, and they represent a snapshot in time from a single small area on an individual. Hence, they do not necessarily correspond to productivity and growth. Although PAM fluorometry can provide valuable information to researchers it is recommended that measurements be interpreted in conjunction with other measurements, such as growth and/or oxygen exchange.

Further considerations of PAM / methodology

Despite the limitations of PAM fluorometry measurements, it is without doubt that the technique can and does provide useful information for researchers. But because of the widespread use of PAM measurements to infer potential photosynthesis, to interpret these kinds of measures and compare values across different studies, it is necessary to understand factors that can underpin variability in

estimates. It is well known that fluorescence yield is dependent on the previous short-term light history. Energy can only be funnelled through PSII when the primary electron acceptor is open to accept electrons. When the amount of captured light increases, the possibility of being closed (not able to accept electrons) increases, and this results in a greater amount of fluorescence being emitted (Ralph, Gademann, 2005; White, Critchley, 1999). Hence, there are generally strong diurnal patterns in PAM-derived outputs in macroalgae (Colombo-Pallotta et al., 2006; Edwards, Kim, 2010, Chapter 5). However, this does not always translate as a trough in photosynthetic capacity over the midday period as there are a number of factors, including depth, latitude/region, and season, that can affect photophysiology, depending on the species.

While it is recommended that, in general, that fluorometry measurements should be taken during the midday period (i.e. typically between 11 am - 2 pm), in some situations this is not the case. The research presented here shows seaweeds in northern latitudes (NSW), where summer seawater temperatures are more extreme, show a marked reduction in these rETRmax values during midday sampling in summer, possibly a result of temperature and/or lack of canopy-shading enhancing photoinhibitory effects and photodamage. This suggests that decisions of the most appropriate time of day for PAM measurements will depend on the ecological context of the study, since these measures are highly variable regionally and are likely to depend on local environmental conditions (e.g. temperature, irradiance, wave exposure, nutrient availability etc).

Seasonal effects on PAM outputs are also dependent on the species and/or depth in the water column. For *M. pyrifera*, maximum photosynthetic capacity varies significantly with depth (different points of the plant in the water column), indicating the importance of standardising the depth at which measurements are made in comparative studies; PAM measurements made on one part of the thallus cannot be considered representative of all parts (Colombo-Pallotta et al., 2006; Edwards, Kim, 2010, Chapter 5). For *E. radiata*, considerably less diurnal variation in rETRmax is seen in deep water individuals compared to shallow water in winter; again, sampling from a single depth will not accurately represent the community. Choice of depth for sampling will depend on the research objectives and will influence interpretation. Measurements of *M. pyrifera* (and other large macroalgae with thalli spanning the water column over a large depth range) and species that cover a range of depths such as *E. radiata* must be made at multiple depths to adequately represent the photosynthetic potential of the entire individual or community.

Another important consideration is the choice of the position on the thallus from which the measurement is taken (independent of differences in depth). Photophysiology in macroalgae has been shown to vary according to tissue age (Edwards, Kim, 2010) and measurement position on the thallus. The location on a thallus from which to obtain measurements for a given study will depend on the species and regional variation in species morphology. For example, at sites with high wave-action *E.*

radiata has a smaller growth morphology with narrow laterals and blades (Wernberg, Thomsen, 2005), so that at exposed sites the effects of self-shading and shading by adjacent conspecifics may be less important than at more sheltered sites. Therefore, if the aim of the research is to compare photosynthetic parameters of individuals at an exposed site with those in an area with high levels of canopy shading then the most appropriate location for sampling will likely be on the upper blades of the thalli.

Similar patterns in photosynthetic potential have been found for both light- and dark-adapted RLCs conducted on *M. pyrifera*, *E. radiata* and *P. comosa*, although absolute values may vary depending on which method is chosen (Flukes, 2015, Chapter 5). Therefore, it seems that both are valid approaches for comparative research. The method chosen will likely vary according to research restrictions, for example, light- adapted RLCs are a more suitable approach when time is limited (e.g. *in situ* sampling underwater). However, the choice between light- and dark- adapted sampling is unlikely to influence research outcomes. Hence, the greatest priorities when planning PAM fluorometry research are consideration of latitude/region, season, and sampling depth when choosing time of day and thallus placement for measurements.

Future directions

There is a critical need to not only develop new techniques for accurate measurement of production in marine communities on both small and large spatial and temporal scales, but also to develop knowledge on how best to interpret and compare them. Advances in technology can lead to a 'rush' in development of scientific data and knowledge, but it is important to consider the accuracy of the estimates produced, and how they can be best interpreted alongside other methods. Of paramount importance when choosing a technique to measure oxygen production is both the nature of the question and scale (both temporally and spatially), and this should also always be considered when interpreting results.

Obtaining large scale community productivity estimates is difficult and options are limited. Ambient oxygen models can provide good fit to measurements of daily fluctuations in DO in the water column, and importantly, this approach provides estimates of oxygen production rates substantially higher than those estimated from incubation of single species sporophytes in benthic respirometry chambers. This suggests that the method can give a robust estimate of community-wide production. Further work would allow 'fine-tuning', however, the most suitable approach would likely depend on the study environment. Regardless, it is envisaged that ultimately the best method for modelling a kelp bed system would (i) be a (more complicated) hybrid where Fourier components are fitted for surface DO signals and for the kelp-bed layer a relationship between O_2 and PAR is defined; (ii) include explicit

numerical consideration of additional factors such as wave action, tides, and currents; and (iii) revisit and improve the equation for O_2 diffusion at the surface depending on wind.

Overall, this approach shows great promise. It is economically efficient, quick and relatively simple. This method would ideally be suited for monitoring of large scale communities in the face of a changing environment, in addition to being applicable to community comparisons across locations. Given the efficacy of the method, it is potentially ideally suited for monitoring kelp systems.

Underwater acoustics is an area that may have potential for large-scale measurements of community productivity. However, although modelling shows that acoustics can measure ecologically significant proportions of oxygen in gaseous form in the canopy layer, in an empirical study we found that acoustic data inversion was not able to detect diurnal differences in oxygen bubble concentration in the study environment. This does not preclude the successful use of acoustics to measure productivity in other macroalgae systems. It is possible that further work, particularly in highly productive environments and with more complex modelling and acoustic data analysis, may prove acoustics to be a useful tool for assisting in monitoring primary productivity in some seaweed communities.

The method remains an area of interest for future study given the potential for very large-scale sampling and possibility of oxygen in the water column present as gas microbubbles form (which is not measured at all by more traditional methods based on DO). However, given the results of this study it is unlikely that this method will be applicable in shallow water environments at the latitudes in question. With the high expense and difficulty of experimental setup, in addition to very complicated and time-consuming analyses, it is not envisaged at this time that acoustics will be a useful tool in measurement of productivity in kelp systems.

Benthic oxygen exchange chambers allow capturing whole plant processes with accurate results, and for those algal communities where biomasses are small (e.g. very small filamentous algae on coral reefs) sometimes measurement of community assemblages are possible (e.g. Klumpp, McKinnon, 1989). For kelp forests, measuring the production of canopy species only will clearly underestimate total photosynthesis rates per unit area of seafloor. There are additional considerations with respect to mixing and shading (see Chapter 4). However, benthic chamber measurements are able to provide a good "ground-truth" aspect to other large scale measurements. Although it is a small scale method, used in conjunction with large scale methods it holds great value for calibration and assessment of small scale variability in kelp environments.

PAM fluorescence techniques have the benefits of ease of use and ability to provide instantaneous measurements, but only measure activity in PSII and thus do not indicate realised photosynthesis. Moreover, even as a proxy for potential photosynthesis, results relate only to the small area of tissue under analysis which need not reflect the physiology or metabolism elsewhere in the alga. PAM

fluorometry can also provide other photosynthetic information relating to photochemical and non-photochemical quenching (Osmond et al., 1993; Schreiber, 2004b), however, consideration must be given to assumptions of light absorbance in addition to alternative electron sinks in PSII. It is clear that PAM measurements are sensitive to canopy shading, depth, and photoinhibitory and/or temperature-related stress responses, particularly at seasonal and range extremes. It is recommended that PAM fluorometry be used in conjunction with other measurements, and with consideration given to variability associated with time-of-day, depth, and thallus placement of the instrument.

Overall, the research shows that each method of measurement has distinct advantages and disadvantages. When planning future research or comparing results across different studies, it will be important to consider that each method provides different kinds of estimates of production or proxies of actual or potential production, and that there needs to be considerable clarity in the question being tackled before selecting a suitable measurement technique.

Appendices

Table 2A: Specifications of the ultrasonic probes used for sound speed measurements. Beam parameters are calculated for the sound speed of 1570 m s^{-1}.

Probe manufacturer	GS	GE	GE	Karl Deutsch	GE
Probe model	B2S(E)	MSW_QC_GAMMA	MSW_QC_GAMMA	S12 HB6	MSW_QC_GAMMA
Nominal frequency (MHz)	2	2.25	5	6	10
Transducer diameter (mm)	23.1	6.35	6.35	12.7	6.35
Beam diameter (mm)	5.9	1.6	1.6	3.3	1.6
Near field length (mm)	169.9	14.4	32.1	154.1	64.2
-6dB beam spread angle (⁹)	2.0	6.5	2.9	1.2	1.5

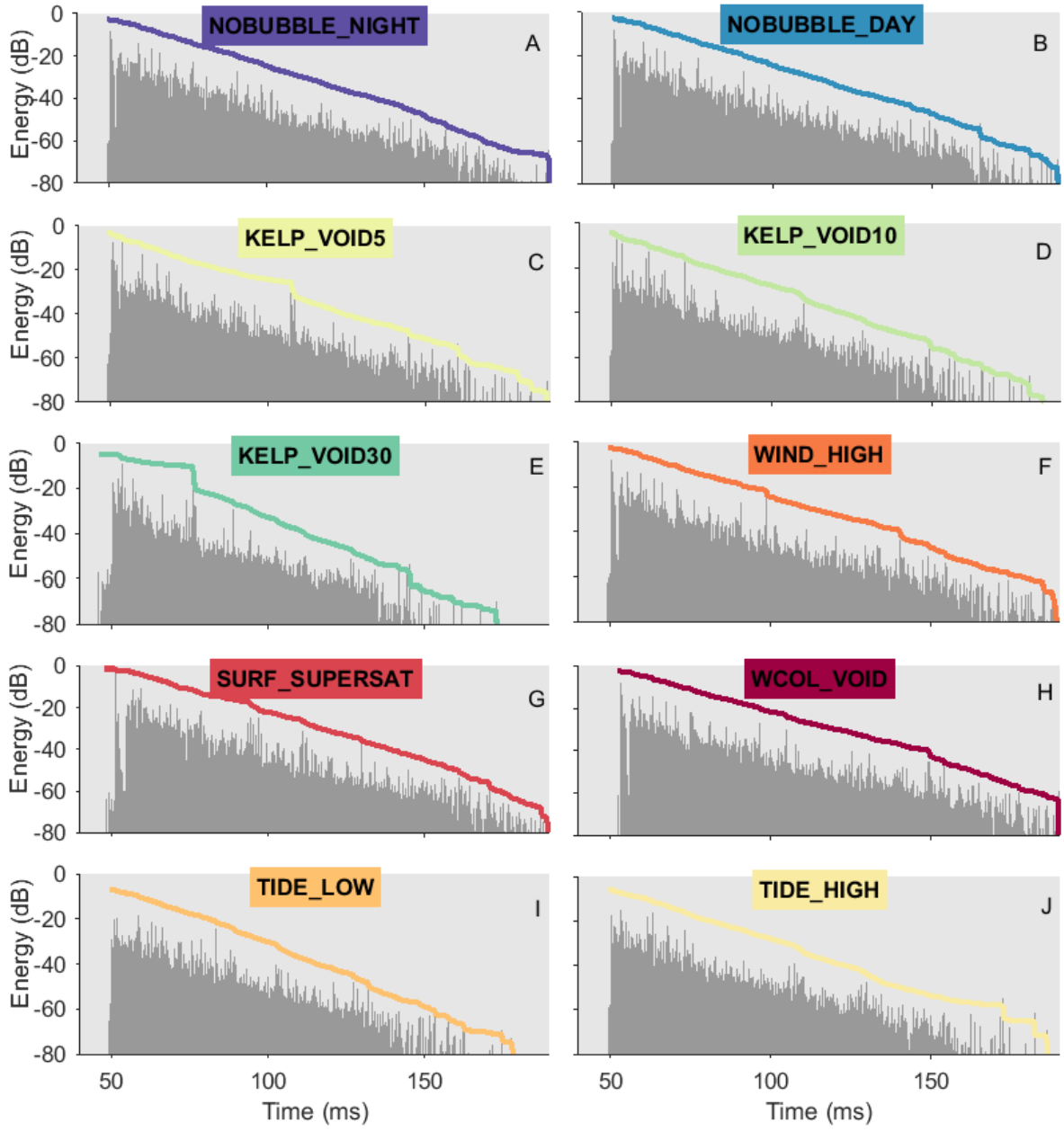

Figure 3A: Predicted time-energy spread of pulse received at Receiver1 within canopy hydrophone for (A) no oxygen void fraction for the day time period 15hr30 13th February, (B) no oxygen void fraction for the night time period 04hr45 14th February, (C) an oxygen void fraction of $4.6e^{-5}$ (5% oxygen in gaseous form), (D) an oxygen void fraction of $9.2e^{-5}$ (10% oxygen in gaseous form), (E) an oxygen void fraction of $2.8e^{-4}$ (30% oxygen in gaseous form), (F) a surface layer with an void fraction of $1.0e^{-6}$ (from wind), (G) a surface supersaturation layer with a void fraction of $1.1e^{-4}$ (30% oxygen in gaseous form) for the day time period, (H) water column void fraction of $1.4e^{-5}$ (30% oxygen in gaseous form) for the day time period, (I) high tide with a canopy layer with a void fraction $9.2e^{-5}$ (10% oxygen in gaseous form) for the day time period, and (J) low tide with a canopy layer with a void fraction $9.2e^{-5}$ (10% oxygen in gaseous form) for the day time period. These simulations were made with a Bellhop acoustic propagation model using 1600001 rays with a beam angle sector of −80 to 80 °.

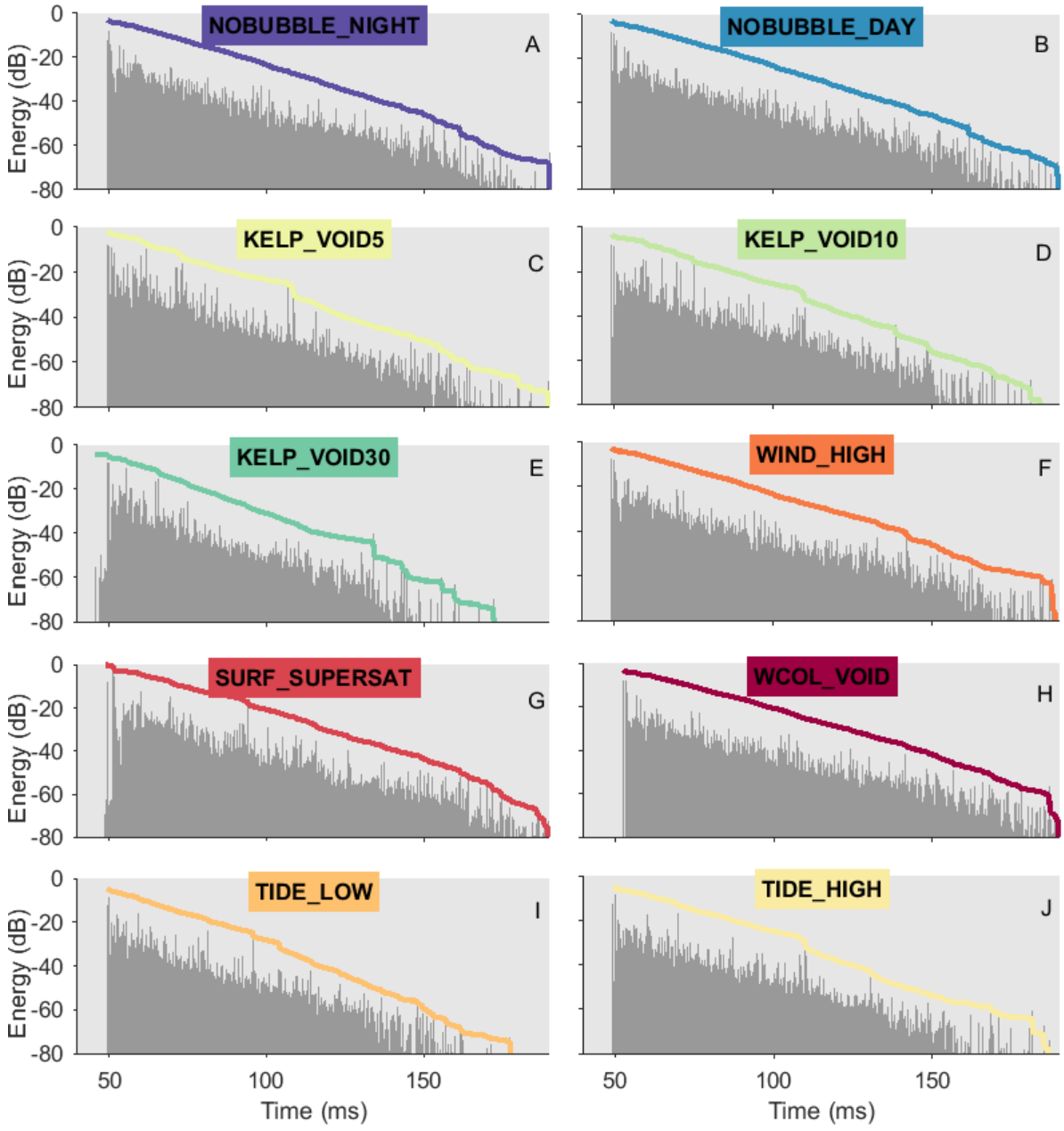

Figure 3B: Predicted time-energy spread of pulse received at Receiver1 above canopy hydrophone for (A) no oxygen void fraction for the day time period 15hr30 13th February, (B) no oxygen void fraction for the night time period 04hr45 14th February, (C) an oxygen void fraction of $4.6e^{-5}$ (5% oxygen in gaseous form), (D) an oxygen void fraction of $9.2e^{-5}$ (10% oxygen in gaseous form), (E) an oxygen void fraction of $2.8e^{-4}$ (30% oxygen in gaseous form), (F) a surface layer with an void fraction of $1.0e^{-6}$ (from wind), (G) a surface supersaturation layer with a void fraction of $1.1e^{-4}$ (30% oxygen in gaseous form) for the day time period, (H) water column void fraction of $1.4e^{-5}$ (30% oxygen in gaseous form) for the day time period, (I) high tide with a canopy layer with a void fraction $9.2e^{-5}$ (10% oxygen in gaseous form) for the day time period, and (J) low tide with a canopy layer with a void fraction $9.2e^{-5}$ (10% oxygen in gaseous form) for the day time period. These simulations were made with a Bellhop acoustic propagation model using 1600001 rays with a beam angle sector of −80 to 80 ˚.

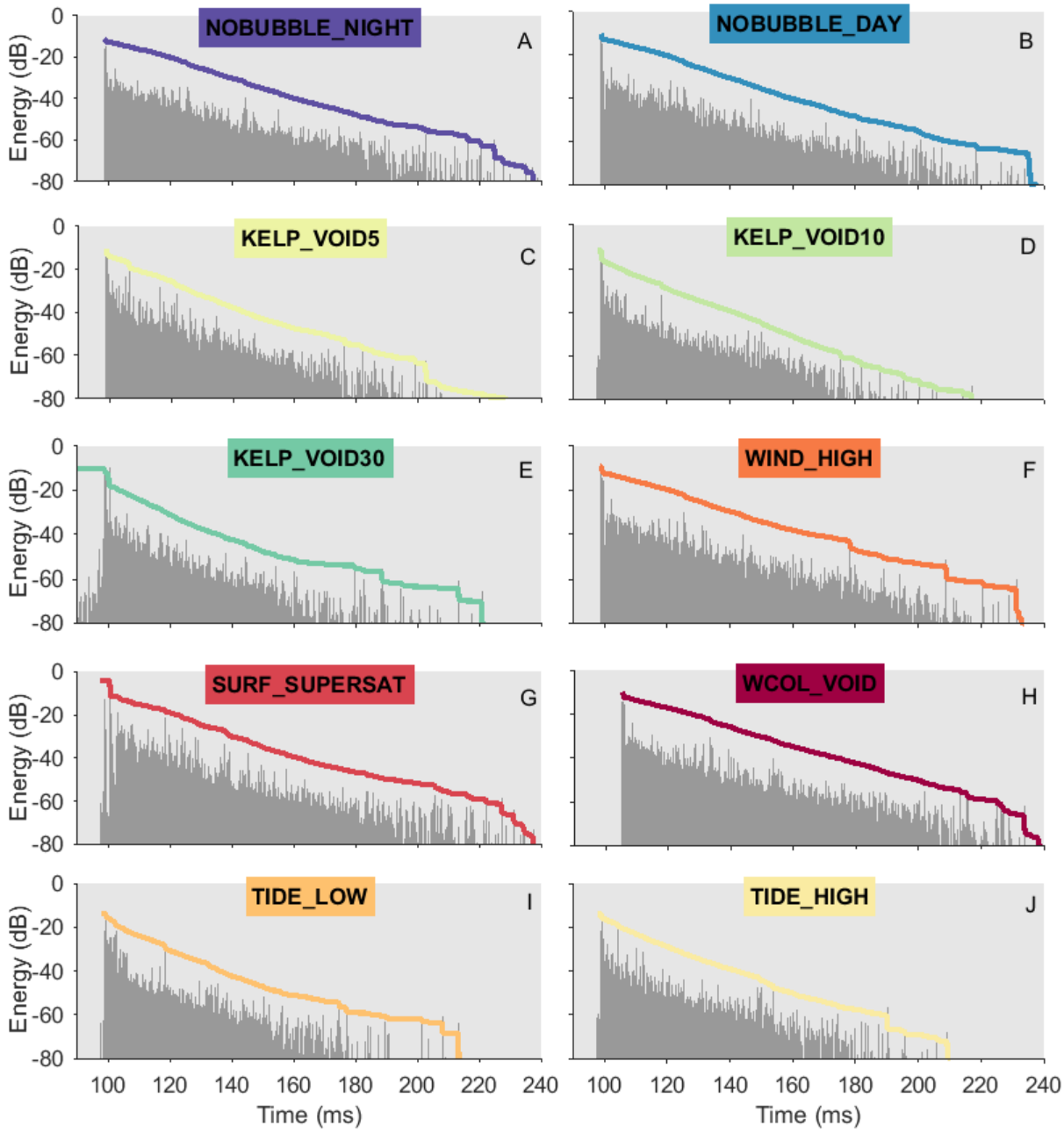

Figure 3C: Predicted time-energy spread of pulse received at Receiver 2 above canopy hydrophone for (A) no oxygen void fraction for the day time period 15hr30 13th February, (B) no oxygen void fraction for the night time period 04hr45 14th February, (C) an oxygen void fraction of $4.6e^{-5}$ (5% oxygen in gaseous form), (D) an oxygen void fraction of $9.2e^{-5}$ (10% oxygen in gaseous form), (E) an oxygen void fraction of $2.8e^{-4}$ (30% oxygen in gaseous form), (F) a surface layer with an void fraction of $1.0e^{-6}$ (from wind), (G) a surface supersaturation layer with a void fraction of $1.1e^{-4}$ (30% oxygen in gaseous form) for the day time period, (H) water column void fraction of $1.4e^{-5}$ (30% oxygen in gaseous form) for the day time period, (I) high tide with a canopy layer with a void fraction $9.2e^{-5}$ (10% oxygen in gaseous form) for the day time period, and (J) low tide with a canopy layer with a void fraction $9.2e^{-5}$ (10% oxygen in gaseous form) for the day time period. These simulations were made with a Bellhop acoustic propagation model using 1600001 rays with a beam angle sector of −80 to 80 °.

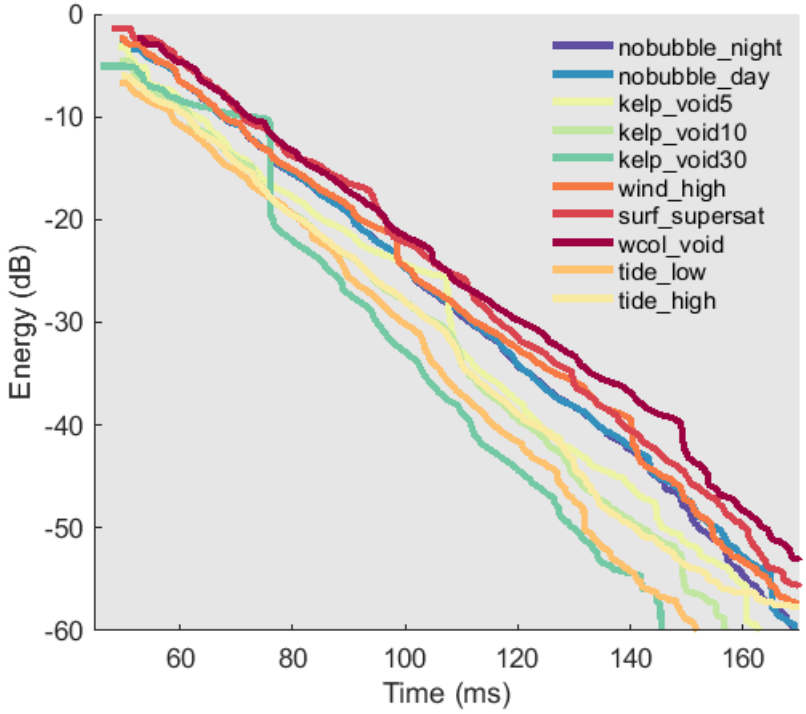

Figure 3D: Reversed time integration of the squared impulse response of pulse received for models of day time, night time, oxygen void fractions of $2.8e^{-4}$ (30% oxygen in gaseous form) $9.2e^{-5}$ (10% oxygen in gaseous form), $4.6e^{-5}$ (5% oxygen in gaseous form), surface supersaturation, high tide, low tide, water column void, and surface wind bubble layer at Receiver 1 within canopy hydrophone at 15hr30 13th February and 04hr45 14t^{h} February 2012. These simulations were made with Bellhop acoustic propagation using 1600001 rays with a beam angle sector of −80 to 80 °.

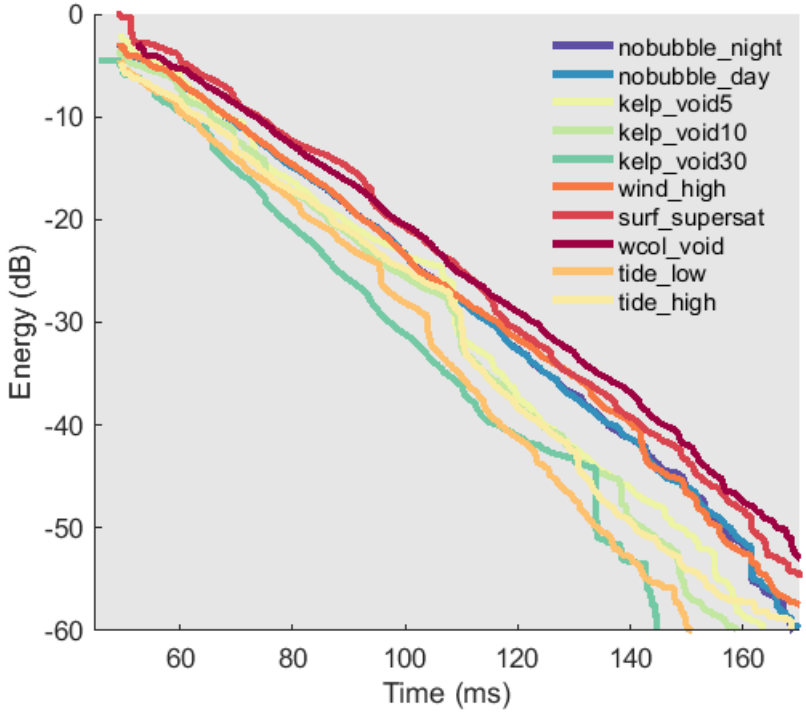

Figure 3E: Reversed time integration of the squared impulse response of pulse received for models of day time, night time, oxygen void fractions of $2.8e^{-4}$ (30% oxygen in gaseous form) $9.2e^{-5}$ (10% oxygen in gaseous form), $4.6e^{-5}$(5% oxygen in gaseous form), surface supersaturation, high tide, low tide, water column void, and surface wind bubble layer at Receiver 1 above canopy hydrophone at 15hr30 13th February and 04hr45 14t^{h} February 2012. These simulations were made with Bellhop acoustic propagation using 1600001 rays with a beam angle sector of −80 to 80 ˚.

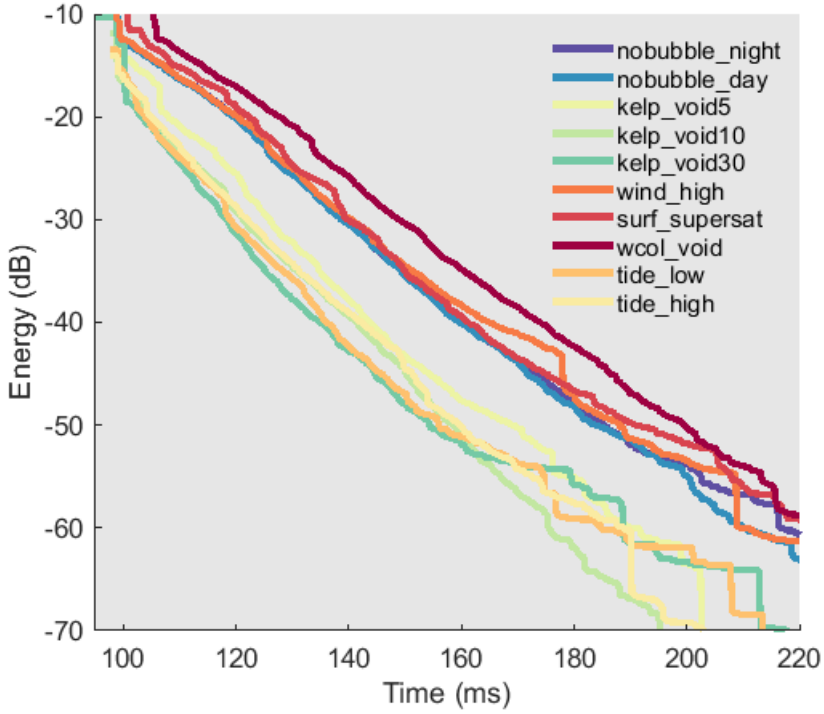

Figure 3F: Reversed time integration of the squared impulse response of pulse received for models of day time, night time, oxygen void fractions of $2.8e^{-4}$ (30% oxygen in gaseous form) $9.2e^{-5}$ (10% oxygen in gaseous form), $4.6e^{-5}$(5% oxygen in gaseous form), surface supersaturation, high tide, low tide, water column void, and surface wind bubble layer at Receiver 2 above canopy hydrophone at 15hr30 13th February and 04hr45 14t^{h} February 2012. These simulations were made with Bellhop acoustic propagation using 1600001 rays with a beam angle sector of −80 to 80 ˚.

References

Armstrong, W., 1979. Aeration in higher plants. In: Woolhouse, H. (Ed.), Advances in Botanical Research. Academic Press, London, pp. 225-332.

Atkinson, M.J., Grigg, R.W., 1984. Model of a coral reef ecosystem. Coral Reefs 3(1), 13-22.

Baird, M., Adams, M., Andrewartha, J., Cherukuru, N., Gustafsson, M., Hadley, S., Herzfeld, M., Jones, E., Margvelashvili, N., Mongin, M., 2014. CSIRO Environmental Modelling Suite: Scientific Description of the Optical, Carbon Chemistry and Biogeochemical Models Parameterised for the Great Barrier Reef. Commonwealth Scientific and Industrial Research Organisation Marine and Atmospheric Research, GPO Box.

Barrett, N.S., Sanderson, J., Lawler, M., Halley, V., Jordan, A., 2001. Mapping of inshore marine habitats in south-eastern Tasmania for marine protected area planning and marine management. Tasmanian Aquaculture and Fisheries Institute, Hobart.

Beer, S., Larsson, C., Poryan, O., Axelsson, L., 2000. Photosynthetic rates of Ulva (Chlorophyta) measured by pulse amplitude modulated (PAM) fluorometry. European Journal of Phycology 35(01), 69-74.

Beer, S., Vilenkin, B., Weil, A., Veste, M., Susel, L., Eshel, A., 1998. Measuring photosynthetic rates in seagrasses by pulse amplitude modulated (PAM) fluorometry. Marine Ecology-Progress Series 174, 293-300.

Belshe, E.F., Durako, M.J., Blum, J.E., 2007. Photosynthetic rapid light curves (RLC) of Thalassia testudinum exhibit diurnal variation. Journal of Experimental Marine Biology and Ecology 342(2), 253-268.

Bennett, S., Wernberg, T., Connell, S.D., Hobday, A.J., Johnson, C.R., Poloczanska, E.S., 2016. The 'Great Southern Reef': social, ecological and economic value of Australia's neglected kelp forests. Marine and Freshwater Research 67(1), 47-56.

Benson, B.B., Krause Jr, D., 1984. The concentration and isotopic fractionation of oxygen dissolved in freshwater and seawater in equilibrium with the atmosphere. Limnology and Oceanography 29(3), 620-632.

Berg, P., Huettel, M., 2008. Integrated benthic exchange dynamics. Oceanography 21(4), 164.

Berg, P., Røy, H., Janssen, F., Meyer, V., Jørgensen, B.B., Huettel, M., de Beer, D., 2003. Oxygen uptake by aquatic sediments measured with a novel non-invasive eddy-correlation technique. Marine Ecology Progress Series 261, 75-83.

BOM, A.G.B.o.M., 2011. Climate Data Online: Monthly Mean Daily Global Solar Exposure.

Bott, T., Brock, J., Cushing, C., Gregory, S., King, D., Petersen, R., 1978. A comparison of methods for measuring primary productivity and community respiration in streams. Hydrobiologia 60(1), 3-12.

Britton, D., Cornwall, C.E., Revill, A.T., Hurd, C.L., Johnson, C.R., 2016. Ocean acidification reverses the positive effects of seawater pH fluctuations on growth and photosynthesis of the habitat-forming kelp, Ecklonia radiata. Scientific Reports 6, 26036.

Brouwer, P.E., 1996. *In situ* photosynthesis and estimated annual production of the red macroalga *Myriogramme mangini* in relation to underwater irradiance at Signy Island (Antarctica). Antarctic Science 8(03), 245-252.

Bruno, J.F., Stachowicz, J.J., Bertness, M.D., 2003. Inclusion of facilitation into ecological theory. Trends in Ecology & Evolution 18(3), 119-125.

Campbell, A.H., Marzinelli, E.M., Verges, A., Coleman, M.A., Steinberg, P.D., 2014. Towards Restoration of Missing Underwater Forests. Plos One 9(1).

Carpenter, R.C., Hackney, J.M., Adey, W.H., 1991. Measurements of primary productivity and nitrogenase activity of coral reef algae in a chamber incorporating oscillatory flow. Limnology and Oceanography 36(1), 40-49.

Cebrian, J., 1999. Patterns in the fate of production in plant communities. The American Naturalist 154(4), 449-468.
Chalker, B., Carr, K., Gill, E., 1985. Measurement of primary production and irradiance in coral reef algal communities. Limnology and Oceanography 30, 784–793.
Cheshire, A., Westphalen, G., Wenden, A., Scriven, L., Rowland, B., 1996a. Photosynthesis and respiration of phaeophycean-dominated macroalgal communities in summer and winter. Aquatic Botany 55, 159-170.
Cheshire, A., Butler, A., Westphalen, G., Rowland, B., Stevenson, J., Wilkinson, C., 1995. Preliminary study of the distribution and photophysiology of the temperate phototrophic sponge *Cymbastela* sp. from South Australia. Marine and Freshwater Research 46(8), 1211-1216.
Cheshire, A.C., Wilkinson, C.R., Seddon, S., Westphalen, G., 1997. Bathymetric and seasonal changes in photosynthesis and respiration of the phototrophic sponge *Phyllospongia lamellosa* in comparison with respiration by the heterotrophic sponge *Ianthella basta* on Davies Reef, Great Barrier Reef. Marine and freshwater research 48(7), 589-599.
Cheshire, A.C., Westphalen, G., Wenden, A., Scriven, L.J., Rowland, B.C., 1996b. Photosynthesis and respiration of phaeophycean-dominated macroalgal communities in summer and winter. Aquatic Botany 55(3), 159-170.
Chu, D., Wiebe, P.H., 2005. Measurements of sound-speed and density contrasts of zooplankton in Antarctic waters. Ices Journal of Marine Science 62(4), 818-831.
Clendenning, K., 1971. Organic productivity in kelp areas. In: North, W. (Ed.), The biology of giant kelp beds (*Macrocystis*) in California. Cramer, pp. 257-263.
Coale, K.H., Johnson, K.S., Chavez, F.P., Buesseler, K.O., Barber, R.T., Brzezinski, M.A., Cochlan, W.P., Millero, F.J., Falkowski, P.G., Bauer, J.E., 2004. Southern Ocean iron enrichment experiment: carbon cycling in high-and low-Si waters. science 304(5669), 408-414.
Cole, J., Nina, J., Caraco, F., 1998. Atmospheric exchange of carbon dioxide in a low-wind oligotrophic lake measured by the addition of SF~ 6. Limnology and Oceanography 43, 647-656.
Colombo-Pallotta, M.F., García-Mendoza, E., Ladah, L.B., 2006. Photosynthetic performance, light absorbtion and pigment composition of *Macrocystid pyrifera* (Laminariales, Phaeophyceae) blades from different depths. Journal of Phycology 42(6), 1225-1234.
Coloso, J.J., Cole, J.J., Hanson, P.C., Pace, M.L., 2008. Depth-integrated, continuous estimates of metabolism in a clear-water lake. Canadian Journal of Fisheries and Aquatic Sciences 65(4), 712-722.
Connell, S.D., 2007. Water quality and the loss of coral reefs and kelp forests: alternative states and the influence of fishing. Marine ecology. Oxford University Press, Melbourne, 556-568.
Consalvey, M., Perkins, R.G., Paterson, D.M., Underwood, G.J.C., 2005. Pam fluorescence: A beginners guide for benthic diatomists. Diatom Research 20(1), 1-22.
Cordi, B., Depledge, M., Price, D., Salter, L., Donkin, M., 1997. Evaluation of chlorophyll fluorescence, *in vivo* spectrophotometric pigment absorption and ion leakage as biomarkers of UV-B exposure in marine macroalgae. Mar Biol 130, 41-49.
Costanza, R., d'Arge, R., de Groot, R., Farber, S., Grasso, M., Hannon, B., Limburg, K., Naeem, S., O'Neill, R.V., Paruelo, J., Raskin, R.G., Sutton, P., van den Belt, M., 1997. The value of the world's ecosystem services and natural capital. Nature 387(6630), 253-260.
Cruces, E., Huovinen, P., Gómez, I., 2012. Stress proteins and auxiliary anti-stress compounds in intertidal macroalgae/Proteínas de estrés y compuestos anti-estrés auxiliares en algas marinas intermareales. Latin American Journal of Aquatic Research 40(4), 822.
Davison, I., Davidson, J., 1987. The effect of growth temperature on enzyme activities in the brown alga *Laminaria saccharina*. British Phycological Journal 22, 77-87.
Davison, I.R., Davison, J.O., 1987. The effect of growth temperature on enzyme-activities in the brown alga *Laminaria saccharina*. British Phycological Journal 22(1), 77-87.

Dayton, P.K., 1985. Ecology of kelp communities. Annual review of ecology and systematics, 215-245.
de Bettignies, T., Wernberg, T., Scott Bennett, A.H., Russell, B.D., Peters, T., Wright, J.T., Steinberg, P.D., Johnson, C.R., Connell, S.D., Kendrick, G.A., 2014. Continental-scale patterns and environmental drivers of population ecology of a ubiquitous habitat-forming kelp.
Demes, K.W., Carrington, E., Gosline, J., Martone, P.T., 2011. Variation in anatomical and material properties explains differences in hydrodynamic performances of foliose red macroalgae (Rodophyta) Journal of Phycology 47(6), 1360-1367.
Demmig-Adams, B., Adams, W.W., 1996. The role of xanthophyll cycle carotenoids in the protection of photosynthesis. Trends in plant science 1(1), 21-26.
Draget, K.I., Skjåk-Bræk, G., Smidsrød, O., 1997. Alginate based new materials. International Journal of Biological Macromolecules 21(1–2), 47-55.
Draper, N.R., Smith, H., 1981. Applied Regression Analysis, John Wiley & Sons. New York 407.
Duarte, C.M., Losada, I.J., Hendriks, I.E., Mazarrasa, I., Marbà, N., 2013. The role of coastal plant communities for climate change mitigation and adaptation. Nature Climate Change 3(11), 961-968.
Dunton, K., Jodwalis, C., 1988. Photosynthetic performance of *Laminaria solidungula* measured in situ in the Alaskan High Arctic. Marine Biology 98(2), 277-285.
Dunton, K.H., 1996. Photosynthetic production and biomass of the subtropical seagrass *Halodule wrightii* along an estuarine gradient. Estuaries 19(2B), 436-447.
Edwards, M.S., Kim, K.Y., 2010. Diurnal variation in relative photosynthetic performance in giant kelp *Macrocystis pyrifera* (Phaeophyceae, Laminariales) at different depths as estimated using PAM fluorometry. Aquatic Botany 92(2), 119-128.
Eggert, A., Wiencke, C., 2000. Adaptation and acclimation of growth and photosynthesis of five Antarctic red algae to low temperatures. Polar Biology 23(9), 609-618.
Ekelund, N.G.A., Nygard, C.A., Nordstrom, R., Gylle, A.M., 2008. In situ study of relative electron transport rates in the marine macroalga *Fucus vesiculosus* in the Baltic Sea at different depths and times of year. Journal of Applied Phycology 20(5), 751-756.
Enenstein, G., Dolder, C., Wilson, P.S., Hermand, J.-P., 2013. Investigation of low-frequency acoustic tissue properties of seagrass, Proceedings of Meetings on Acoustics. Acoustical Society of America, pp. 005007.
Enríquez, S., Rodríguez-Román, A., 2006. Effect of water flow on the photosynthesis of three marine macrophytes from a fringing-reef lagoon. Marine Ecology Progress Series 323, 119-132.
Enríquez, S., Borowitzka, M.A., 2010. The use of the fluorescence signal in studies of seagrasses and macroalgae, Chlorophyll a fluorescence in aquatic sciences: methods and applications. Springer, pp. 187-208.
Enríquez, S., Agustí, S., Duarte, C.M., 1994. Light absorption by marine macrophytes. Oecologia 98(2), 121-129.
Etter, P.C., 2013. Underwater Acoustic Modeling and Simulation, 4th Edition, 1-492 pp.
Fairhead, V.A., Cheshire, A.C., 2004a. Seasonal and depth related variation in the photosynthesis–irradiance response of *Ecklonia radiata* (Phaeophyta, Laminariales) at West Island, South Australia. Mar Biol 145, 415-426.
Fairhead, V.A., Cheshire, A.C., 2004b. Rates of primary productivity and growth in *Ecklonia radiata* measured at different depths, over an annual cycle, at West Island, South Australia. Marine Biology 145(1), 41-50.
Falkowski, P., Raven, J., 1997. Aquatic Photosynthesis. Blackwell Science, Oxford.
Ferwerda, J.G., de Leeuw, J., Atzberger, C., Vekerdy, Z., 2007. Satellite-based monitoring of tropical seagrass vegetation: current techniques and future developments. Hydrobiologia 591, 59-71.
Fletcher, R.S., Pulich, W., Hardegree, B., 2009. A semiautomated approach for monitoring landscape changes in Texas seagrass beds from aerial photography. Journal of Coastal Research 25(2), 500-506.

Flores-Moya, A., Fernández, J.A., Xavier Niell, F., 1995. Seasonal variations of photosynthetic pigments, total C, N, and P content, and photosynthesis in *Phyllariopsis purpurascens*: (Phaeophyta) from the Strait of Gibraltar. Journal of Phycology 31(6), 867-874.

Flukes, E.B., 2015. Ecophysiology of habitat-forming seaweeds in a changing environment. University of Tasmania, Tasmania.

Flukes, E.B., Wright, J.T., Johnson, C.R., 2015a. Phenotypic plasticity and biogeographic variation in physiology of habitat-forming seaweed: response to temperature and nitrate. Journal of phycology 51(5), 896-909.

Flukes, E.B., Wright, J.T., Johnson, C.R., 2015b. Phenotypic plasticity and biogeographic variation in physiology of habitat-forming seaweed: response to temperature and nitrate. Journal of Phycology 51(5), 896-909.

Foote, K.G., 1990. Speed of sound in *Euphasia superba*. Journal of the Acoustical Society of America 87(4), 1405-1408.

Franklin, L.A., Badger, M.R., 2001. A comparison of photosynthetic electron transport rates in macroalgae measured by pulse amplitude modulated chlorophyll fluorometry and mass spectrometry. Journal of Phycology 37(5), 756-767.

Gao, K., Umezaki, I., 1988. Comparative photosynthetic capacities of the leaves of upper and lower parts of Sargassum plants. Botanica marina 31(3), 231-236.

Gattuso, J.-P.J., Pichon, M.M., Delesalle, B.B., Frankignoulle, M.M., 1993. Community metabolism and air-sea CO2 fluxes in a coral reef ecosystem (Moorea, French Polynesia). Marine Ecology Progress Series-pages: 96: 259-267.

Gelda, R.K., Effler, S.W., 2002. Metabolic rate estimates for a eutrophic lake from diel dissolved oxygen signals. Hydrobiologia 485(1-3), 51-66.

Gerard, V., 1986. Photosynthetic characteristics of giant kelp (*Macrocystis pyrifera*) determined in situ. Marine Biology 90(3), 473-482.

Gévaert, F., Créach, A., Davoult, D., Holl, A.C., Seuront, L., Lemoine, Y., 2002. Photo-inhibition and seasonal photosynthetic performance of the seaweed *Laminaria saccharina* during a simulated tidal cycle: chlorophyll fluorescence measurements and pigment analysis. Plant, Cell & Environment 25, 859-972.

Glud, R.N., Berg, P., Hume, A., Batty, P., Blicher, M.E., Lennert, K., Rysgaard, S., 2010. Benthic O2 exchange across hard-bottom substrates quantified by eddy correlation in a sub-Arctic fjord. Marine Ecology Progress Series 417, 1-12.

Golléty, C., Migné, A., Davoult, D., 2008. Benthic metabolism on a sheltered rocky shore: role of the canopy in the carbon budget. Journal of Phycology 44(5), 1146-1153.

Greenlaw, C.F., Johnson, R.K., 1982. Physical and acoustical properties of zooplankton. The Journal of the Acoustical Society of America 72(6), 1706-1710.

Hackney, J., Sze, P., 1988. Photorespiration and productivity rates of a coral reef algal turf assemblage. Marine Biology 98(4), 483-492.

Häder, D.-P., Herrmann, H., Schäfer, J., Santas, R., 1997. Photosynthetic fluorescence induction and oxygen production in two Mediterranean Cladophora species measured on site. Aquatic Botany 56(3), 253-264.

Hanelt, D., Nultsch, W., 1991. The role of chromatophore arrangement in protecting the chromatophores of the brown alga Dictyota dichotoma against photodamage. Journal of plant physiology 138(4), 470-475.

Hanelt, D., Melchersmann, B., Wiencke, C., Nultsch, W., 1997. Effects of high light stress on photosynthesis of polar macroalgae in relation to depth distribution. Marine Ecology-Progress Series 149(1-3), 255-266.

Hanson, P.C., Bade, D.L., Carpenter, S.R., Kratz, T.K., 2003. Lake metabolism: Relationships with dissolved organic carbon and phosphorus. Limnology and Oceanography 48(3), 1112-1119.

Hatcher, B., 1977. An apparatus for measuring photosynthesis and respiration of intact large marine algae and comparison of results with those from experiments with tissue segments. Marine Biology 43(4), 381-385.
Hatcher, B.G., Chapman, A.R.O., Mann, K.H., 1977. An annual carbon budget for the kelp *Laminaria longicruris*. Marine Biology 44(1), 85-96.
Heiss, W.M., Smith, A.M., Probert, P.K., 2000. Influence of the small intertidal seagrass *Zostera novazelandica* on linear water flow and sediment texture. New Zealand Journal of Marine and Freshwater Research 34(4), 689-694.
Heldt, H.-W., 2005. Plant BiochemistryElsevier Academic Press, CA, USA.
Henley, W.J., 1993. Measurement and interpretation of photosynthetic light-response curves in algae in the context of photoinhibition and diel changes. Journal of Phycology 29(6), 729-739.
Hermand, J.-P., 2003. Acoustic remote sensing of photosynthetic activity in seagrass beds. In: Seuront, L., Strutten, P. (Eds.), Scaling Methods in Aquatic Ecology: Measurement, analysis, simulation. CRC Press, USA, pp. 66-94.
Hermand, J.-P., 2016a. Modelling macroalgae scattering (*Ecklonia radiata*). The Journal of the Acoustical Society of America 140(4), 3305-3305.
Hermand, J.-P., Randall, J., 2015. A Monte Carlo experiment for measuring acoustic properties of macroalgae living tissue. The Journal of the Acoustical Society of America 137(4), EL314-EL319.
Hermand, J.-P., Nascetti, P., Cinelli, F., 1998. Inversion of acoustic waveguide propagation features to measure oxygen synthesis by *Posidonia oceanica*, Oceans'98 IEEE/OES. IEEE, Europe, pp. 919-926.
Hermand, J.-P., Randall, J., Ross, J., Johnson, C.R., 2013. Acoustics of *Ecklonia radiata* kelp forest: MARIA 11-FORTES 12, Unpublished data.
Hermand, J.-P., Guo, L., Randall, J., Brehmer, P., 2014. Non-destructive optical holographic imaging of microorganisms in situ off the Senegalese coast, OCEANS 2014-TAIPEI. IEEE, pp. 1-4.
Hermand, J.P., 2016b. Bubbles in a bed of *Cymodocea nodosa* (Western Crete)
Hirose, M., Mukai, T., Hwang, D., Iida, K., 2009. The acoustic characteristics of three jellyfish species: Nemopilema nomurai, Cyanea nozakii, and Aurelia aurita. ICES Journal of Marine Science: Journal du Conseil.
Hoegh-Guldberg, O., Jones, R.J., 1999. Photoinhibition and photoprotection in symbiotic dinoflagellates from reef-building corals. Marine Ecology Progress Series 183, 73-86.
Horn, S.J., 2000. Bioenergy from brown seaweeds, Department of Biotechnology. Norwegian University of Science and Technology, Norway, pp. 82.
Hurd, C., Harrison, P., Druehl, L., 1996. Effect of seawater velocity on inorganic nitrogen uptake by morphologically distinct forms of *Macrocystis integrifolia* from wave-sheltered and exposed sites. Marine Biology 126(2), 205-214.
Hurd, C.L., Harrison, P.J., Bischof, K., Lobban, C.S., 2014a. Seaweed ecology and physiology. Cambridge University Press.
Hurd, C.L., Harrison, P.J., Bischof, K., Lobban, C.S., 2014b. Seaweed Ecology and PhysiologyCambridge University Press, United Kingdom.
IMOS, 2017. IMOS - SRS Satellite - SST L3S - 1 month composite - night time.
Jackson, G., 1982. Nutrients and production of giant kelp, *Macrocystis pyrifera* off southern California. Limnology and Oceanography 22, 979-995.
Jackson, G.A., 1977. Nutrients and production of giant kelp, *Macrocystis pyrifera*, off southern California1. OCEANOGRAPHY 22(6).
Jackson, J.B.C., Sala, E., 2001. Unnatural oceans. Scientia Marina 65, 273-281.
Jensen, F.B., Kuperman, W.A., Porter, M.B., Schmidt, H., 2000. Computational ocean acousticsSpringer Science & Business Media.

Johnson, C.R., Banks, S.C., Barrett, N.S., Cazassus, F., Dunstan, P.K., Edgar, G.J., Frusher, S.D., Gardner, C., Haddon, M., Helidoniotis, F., Hill, K.L., Holbrook, N.J., Hosie, G.W., Last, P.R., Ling, S.D., Melbourne-Thomas, J., Miller, K., Pecl, G.T., Richardson, A.J., Ridgway, K.R., Rintoul, S.R., Ritz, D.A., Ross, D.J., Sanderson, J.C., Shepherd, S.A., Slotwinski, A., Swadling, K.M., Taw, N., 2011. Climate change cascades: Shifts in oceanography, species' ranges and subtidal marine community dynamics in eastern Tasmania. Journal of Experimental Marine Biology and Ecology 400(1–2), 17-32.

Johnston, A.M., Maberly, S.C., Raven, J.A., 1992. The aquisition of inorganic carbon by 4 red macroalgae. Oecologia 92(3), 317-326.

Jones, C.G., Lawton, J.H., Shachak, M., 1996. Organisms as ecosystem engineers, Ecosystem Management. Springer, pp. 130-147.

Jones, R.J., Ward, S., Amri, A.Y., Hoegh-Guldberg, O., 2000. Changes in quantum efficiency of Photosystem II of symbiotic dinoflagellates of corals after heat stress, and of bleached corals sampled after the 1998 Great Barrier Reef mass bleaching event. Marine and Freshwater Research 51(1), 63-71.

Kargl, S., 2002. Effective medium approach to linear acoustics in bubbly liquids. The Journal of the Acoustical Society of America 111(1), 168-173.

Kemp, W., Boynton, W., 1980. Influence of biological and physical processes on dissolved oxygen dynamics in an estuarine system: Implications for measurement of community metabolism. Estuarine and Coastal Marine Science 11(4), 407-431.

Kennelly, S., 1987. Physical disturbances in an Australian kelp. Mar. Ecol. Prog. Ser 40, 145-153.

Kim, K.Y., Garbary, D.J., 2006. Fluorescence responses of photosynthesis to extremes of hyposalinity, freezing and desiccation in the intertidal crust *Hildenbrandia rubra* (Hildenbrandiales, Rhodophyta). Phycologia 45(6), 680-686.

Kim, K.Y., Choi, T.S., Kim, J.H., Han, T., Shin, H.W., Garbary, D.J., 2004. Physiological ecology and seasonality of Ulva pertusa on a temperate rocky shore. Phycologia 43(4), 483-492.

King, R.J., Schramm, W., 1976. Determination of photosynthetic rates for the marine algae Fucus vesiculosus and Laminaria digitata. Marine Biology 37(3), 209-213.

Kirkman, H., 1981. The first year in the life history and the survival of the juvenile marine macrophyte, *Ecklonia radiata* (Turn.) J. Agardh. Journal of experimental marine biology and ecology 55(2), 243-254.

Klemenz, A., Schwinger, C., Brandt, J., Kressler, J., 2003. Investigation of elasto-mechanical properties of alginate microcapsules by scanning acoustic microscopy. Journal of Biomedical Materials Research Part A 65A(2), 237-243.

Klumpp, D., McKinnon, A., 1989. Temporal and spatial patterns in primary production of a coral-reef epilithic algal community. Journal of Experimental Marine Biology and Ecology 131(1), 1-22.

Koch, E., Gust, G., 1999. Water flow in tide-and wave-dominated beds of the seagrass *Thalassia testudinum*. Marine Ecology Progress Series 184(1), 63-72.

Komatsu, T., Igararashi, C., Tatsukawa, K., Nakaoka, M., Hiraishi, T., Taira, A., 2002. Mapping of seagrass and seaweed beds using hydro-acoustic methods. Fisheries Science 68, 580-583.

Komatsu, T., Igarashi, C., Tatsukawa, K., Sultana, S., Matsuoka, Y., Harada, S., 2003. Use of multi-beam sonar to map seagrass beds in Otsuchi Bay on the Sanriku Coast of Japan. Aquatic Living Resources 16(3), 223-230.

Krause, G.H., 1988. Photoinhibition of photosynthesis. An evaluation of damaging and protective mechanisms. Physiologia Plantarum 74(3), 566-574.

Krumhansl, K.A., Okamoto, D.K., Rassweiler, A., Novak, M., Bolton, J.J., Cavanaugh, K.C., Connell, S.D., Johnson, C.R., Konar, B., Ling, S.D., 2016. Global patterns of kelp forest change over the past half-century. Proceedings of the National Academy of Sciences 113(48), 13785-13790.

Kubler, J.E., Johnston, A.M., Raven, J.A., 1999. The effects of reduced and elevated CO2 and O-2 on the seaweed *Lomentaria articulata*. Plant Cell and Environment 22(10), 1303-1310.

Küppers, U., Kremer, B.P., 1978. Longitudinal profiles of carbon dioxide fixation capacities in marine macroalgae. Plant Physiology 62(1), 49-53.
Lamarre, E., Melville, W., 1994. Sound-speed measurements near the ocean surface. The Journal of the Acoustical Society of America 96(6), 3605-3616.
Larkum, A.W.D., Orth, R.R., Duarte, C.M., 2006. Seagrasses: Biology, Ecology and Conservation. Springer, Dordrecht, The Netherlands, pp.
Lassen, C., Bebout, L., Paerl, H., Jørgensen, B., 1994. Microsensor studies of oxygen and light distribution in the green macroalga *Codium fragile*. Journal of Phycology 30(3), 381-386.
Lauster, G.H., Hanson, P.C., Kratz, T.K., 2006. Gross primary production and respiration differences among littoral and pelagic habitats in northern Wisconsin lakes. Canadian Journal of Fisheries and Aquatic Sciences 63(5), 1130-1141.
Leclercq, N., Gattuso, J.-P., Jaubert, J., 1999. Measurement of oxygen metabolism in open-top aquatic mesocosms: application to a coral reef community. Marine Ecology Progress Series 177, 299-304.
Lewis, E.R., Schwartz, S.E., 2004. Sea salt aerosol production: mechanisms, methods, measurements, and models-A critical review. American Geophysical Union.
Lin, Y.-T., Lynch, J., 2017. Three-dimensional sound propagation and scattering in an ocean with surface and internal waves over range-dependent seafloor. The Journal of the Acoustical Society of America 141(5), 3753-3753.
Ling, S., 2008. Range expansion of a habitat-modifying species leads to loss of taxonomic diversity: a new and impoverished reef state. Oecologia 156(4), 883-894.
Littler, M., 1979a. The effects of bottle volume, thallus weight, oxygen saturation levels, and water movement on apparent photosynthetic rates in marine algae. Aquatic Botany 7(0), 21-34.
Littler, M.M., 1979b. The effects of bottle volume, thallus weight, oxygen saturation levels, and water movement on apparent photosynthetic rates in marine algae. Aquatic Botany 7, 21-34.
Lobban, C., Harrison, P., 1994. Seaweed Ecology and Physiology, Cambridge University Press, New York.
Lobban, C., Harrison, P., 2000. Seaweed Ecology and PhysiologyCambridge University Press, Cambridge.
Lofqvist, T., Niemi, J., Aitomaki, Y., IEEE, 2007. Ultrasonic methods in determining elastic material properties of fibres in suspension, 2007 IEEE Ultrasonics Symposium Proceedings, Vols 1-6, pp. 46-49.
Long, M.H., Berg, P., McGlathery, K.J., Zieman, J.C., 2015. Sub-tropical seagrass ecosystem metabolism measured by eddy covariance.
Longstaff, B.J., Kildea, T., Runcie, J.W., Cheshire, A., Dennison, W.C., Hurd, C., Kana, T., Raven, J.A., Larkum, A.W.D., 2002. An in situ study of photosynthetic oxygen exchange and electron transport rate in the marine macroalga *Ulva lactuca* (Chlorophyta). Photosynthesis Research 74(3), 281-293.
Lough, J., 2009. Temperature. In: Polaczanska, E., Hobday, A., Richardson, A. (Eds.), Marine Climate Change for Australia: Impacts and Adaptation Responses. NCCARF, Queensland, Australia.
Lucieer, V.L., 2008. Object-oriented classification of sidescan sonar data for mapping benthic marine habitats. International Journal of Remote Sensing 29(3), 905-921.
Lüder, U., Knoetzel, J., Wiencke, C., 2002. Acclimation of photosynthesis and pigments to seasonally changing light conditions in the endemic Antarctic red macroalga *Palmaria decipiens*. In: Arntz, W., Clarke, A. (Eds.), Ecological Studies in the Antarctic Sea Ice Zone. Springer Berlin Heidelberg, pp. 231-236.
Macedo, R., Lombardi, A., Omachi, C., Rörig, L., 2008. Effects of the herbicide bentazon on growth and photosystem II maximum quantum yield of the marine diatom *Skeletonema costatum*. Toxicology in Vitro 22(3), 716-722.

Mann, K., 1972. Ecological energetics of the sea-weed zone in a marine bay on the Atlantic coast of Canada. II. Productivity of the seaweeds. Marine Biology 14(3), 199-209.
Mann, K., 1973a. Seaweeds: their productivity and strategy for growth. Science 182, 975-981.
Mann, K.H., 1973b. Seaweeds: Their Productivity and Strategy for Growth. Science 182(4116), 975-981.
Marszalek, D.S., 1982. The role of heavy skeletons in vertical movements of non-motile zooplankton. Marine Behaviour and Physiology 8(4), 295-303.
Marzani, A., Bocchini, P., Viola, E., Bartoli, I., Coccia, S., Salamone, S., Lanza di Scalea, F., 2009. A software for the computation of acoustic waves in cylindrical, plate and arbitrary cross-section waveguides, attidella 13a Congresso Nazionale sulle prove non distruttive Monitoraggio e diagnostica AIPnD, Roma, Italia, pp. 1-9.
Marzinelli, E.M., Williams, S.B., Babcock, R.C., Barrett, N.S., Johnson, C.R., Jordan, A., Kendrick, G.A., Pizarro, O.R., Smale, D.A., Steinberg, P.D., 2015. Large-Scale Geographic Variation in Distribution and Abundance of Australian Deep-Water Kelp Forests. PLoS ONE 10(2), e0118390.
McDougal, T.J., Barker, P.M., 2011. Getting started with the TEOS-10 and the Gibbs Seawater (GSW) Oceanographic Toolbox. SCOR/IAPSO WG 127, pp. 28.
McGinnis, D., Cherednichenko, S., Sommer, S., Berg, P., Rovelli, L., Schwarz, R., Glud, R.N., Linke, P., 2011. Simple, robust eddy correlation amplifier for aquatic dissolved oxygen and hydrogen sulfide flux measurements. Limnology and Oceanography: Methods 9, 340-347.
McKee, J., Kavalieris, L., Brasch, D., Brown, M., Melton, L., 1992. Alginate content and composition of Macrocystis pyrifera from New Zealand. Journal of Applied Phycology 4(4), 357-369.
Mount, R., 2005. Acquisition of through-water aerial survey images: Surface effects and the prediction of sun glitter and subsurface illumination. Photogrammetric Engineering and Remote Sensing 71(12), 1407-1415.
Nielsen, H.D., Nielsen, S.L., 2008. Evaluation of imaging and conventional PAM as a measure of photosynthesis in thin-and thick-leaved marine macroalgae. Aquat Biol 3, 121-131.
Nielsen, K.J., Blanchette, C.A., Menge, B.A., Lubchenco, J., 2006. Physiological snapshots reflect ecological performance of the sea palm *Postelsia palmaeformis* (Paeophycaea) across intertidal elevation and exposure gradients. Journal of Phycology 42(3), 548-559.
Odum, H.T., 1956. Primary production in flowing waters. Limnol. Oceanogr 1(2), 102-117.
Odum, H.T., 1957. Trophic structure and productivity of Silver Springs, Florida. Ecological monographs 27(1), 55-112.
Odum, H.T., Odum, E.P., 1955. Trophic structure and productivity of a windward coral reef community on Eniwetok Atoll. Ecological Monographs 25(3), 291-320.
Oláh, V., Lakatos, G., Bertók, C., Kanalas, P., Szőllősi, E., Kis, J., Mészáros, I., 2010. Short-term chromium (VI) stress induces different photosynthetic responses in two duckweed species, *Lemna gibba* L. and *Lemna minor* L. Photosynthetica 48(4), 513-520.
Oliveira, F.G.R.d., Candian, M., Lucchette, F.F., Salgon, J.L., Sales, A., 2005. Moisture content effect on ultrasonic velocity in Goupia glabra. Materials Research 8, 11-14.
Oliver, J., 1957. Elastic wave dispersion in a cylindrical rod by a wide-band short-duration pulse technique. The Journal of the Acoustical Society of America 29, 189-194.
Osmond, C., Ramus, J., Levavasseur, G., Franklin, L., Henley, W., 1993. Fluorescence quenching during photosynthesis and photoinhibition of *Ulva rotundata* blid. Planta 190(1), 97-106.
Patterson, M.R., Sebens, K.P., Olson, R.R., 1991. In situ measurements of flow effects on primary production and dark respiration in reef corals. Limnology and Oceanography 36(5), 936-948.
Pedersen, M.F., Borum, J., 1997. Nutrient control of estuarine macroalgae: growth strategy and the balance between nitrogen requirements and uptake. Marine Ecology Progress Series 161, 155-163.
Percival, E., 1979. The polysaccharides of green, red and brown seaweeds: Their basic structure, biosynthesis and function. British Phycological Journal 14(2), 103-117.

Platt, T., C, G., Harrison, W., 1980. Photoinhibition of photosynthesis in natural assemblages of marine phytoplankton. Journal of Marine Research 38, 687-701.
Porter, M., 2011. BELLHOP gaussian beam/finite element beam code.
Povey, M.J., 1997. Ultrasonic Techniques for Fluids CharacterizationAcademic Press, San Diego.
Ralph, P.J., Burchett, M.D., 1995. Photosynthetic responses of the seagrass *Halophila ovalis* (R. Br.) Hook. f. to high irradiance stress, using chlorophyll a fluorescence. Aquatic Botany 51(1), 55-66.
Ralph, P.J., Short, F.T., 2002. Impact of the wasting disease pathogen, Labyrinthula zosterae, on the photobiology of eelgrass *Zostera marina*. Marine Ecology Progress Series 226, 265-271.
Ralph, P.J., Gademann, R., 2005. Rapid light curves: a powerful tool to assess photosynthetic activity. Aquatic Botany 82(3), 222-237.
Ramsey, W., 1962. Dissolved oxygen in shallow near-shore water and its relation to possible bubble formation. Limnology and Oceanography 7(4), 453-461.
Randall, J., Hermand, J.-P., Ernould, M.-E., Ross, J., Johnson, C., 2014. Measurement of acoustic material properties of macroalgae (Ecklonia radiata). Journal of Experimental Marine Biology and Ecology 461(0), 430-440.
Randall, J., Flukes, E., Wernberg, T., De Bettignies, T., Johnson, C.R., In review. Space-time variability in *in situ* PAM fluorometry measures three key habitat-forming macroalgae Manuscript submitted for publication.
Rascher, U., Liebig, M., Lüttge, U., 2000. Evaluation of instant light-response curves of chlorophyll fluorescence parameters obtained with a portable chlorophyll fluorometer on site in the field. Plant, Cell & Environment 23(12), 1397-1405.
Raven, J.A., Geider, R.J., 2003. Adaptation, acclimation and regulation in algal photosynthesis. In: AWD, L., SE, D., JA, R. (Eds.), Photosynthesis in algae. Springer, pp. 385-412.
Raybaud, V., Beaugrand, G., Goberville, E., Delebecq, G., Destombe, C., Valero, M., Davoult, D., Morin, P., Gevaert, F., 2013. Decline in kelp in west Europe and climate. Plos One 8(6).
Richards, S., Brown, N., Leighton, T., 1998. Characterisation of propagation parameters for high frequency sonar in turbid coastal waters. In: Alippi, A., Cannelli, G. (Eds.), Fourth European Conference on Underwater Acoustics, Rome, pp. 709-714.
Richardson, A.J., Poloczanska, E.S., 2008. Ocean science - Under-resourced, under threat. Science 320(5881), 1294-1295.
Ridgway, K.R., 2007. Long-term trend and decadal variability of the southward penetration of the East Australian Current. Geophysical Research Letters 34(13).
Robeldo, D., Freile-Pelegrin, Y., 2005. Seasonal variation in photosynthesis and biochemical composition of *Caulerpa* spp. (Bryopsidales, Chlorophyta) from the Gulf of Mexico. Phycologia 44(3), 312-319.
Rosenberg, C., Ramus, J., 1982. Ecological growth strategies in the seaweeds *Gracilaria foliifera* (Rhodophyceae) and *Ulva* sp. (Chlorophyceae): Photosynthesis and antenna composition Mar Biol 8, 233-241.
Rosenberg, G., Littler, D.S., Littler, M.M., Oliveira, E.C., 1995. Primary production and photosynthetic quotients of seaweeds from Sao Paulo State, Brazil. Botanica Marina 38(1-6), 369-378.
Rosenqvist, E., van Kooten, O., 2003. Chlorophyll fluorescence: a general description and nomenclature. In: DeEll, J., Toivonen, P. (Eds.), Practical Applications of Chlorophyll Fluorescence in Plant Biology. Kluwer Academic Publ, Dordrecht/Boston/London, pp. 31-77.
Ross, K.A., Pyrak-Nolte, L.J., Campanella, O.H., 2006. The effect of mixing conditions on the material properties of an agar gel - microstructural and macrostructural considerations. Food Hydrocolloids 20(1), 79-87.
Russell, B.D., Connell, S.D., 2005. A novel interaction between nutrients and grazers alters relative dominance of marine habitats. Marine Ecology Progress Series 289, 5-11.

Russell, B.D., Thompson, J.-a.I., Falkenberg, L.J., Connell, S.D., 2009. Synergistic effects of climate change and local stressors: CO2 and nutrient-driven change in subtidal rocky habitats. Global Change Biology 15(9), 2153-2162.
Sakanishi, Y., Yokohama, Y., Aruga, Y., 1989. Seasonal changes of photosynthetic activity of a brown alga *Ecklonia cava* Kjellman. Bot. Mag. Tokyo 102(1), 37-51.
Sakanishi, Y., Yokohama, Y., Aruga, Y., 1991. Photosynthetic capacity of various parts of the blade of *Laminaria longissima Miyabe* (Phaeophyta). Jap. J. Phycol 39, 239-243.
Sargent, M.C., Austin, T.S., 1949. Organic productivity of an atoll. Eos, Transactions American Geophysical Union 30(2), 245-249.
Saroussi, S., Beer, S., 2007a. Acclimations of macroalgae as reflected in photosynthetic parameters derived from PAM fluorometry, and possible implications for abundance patterns. Marine Ecology 28(3), 377-383.
Saroussi, S., Beer, S., 2007b. Alpha and quantum yield of aquatic plants derived from PAM fluorometry: Uses and misuses. Aquatic Botany 86(1), 89-92.
Schafer, M.E., 2000. Ultrasound for defect detection and grading in wood and lumber, Ultrasonics Symposium, 2000 IEEE, pp. 771-778 vol.771.
Schreiber, U., 2004a. Pulse-Amplitude-Modulation (PAM) Fluorometry and Saturation Pulse Method: An Overview. In: Papageorgiou, G.C., Govindjee (Eds.), Chlorophyll a Fluorescence: A Signature of Photosynthesis. Springer Netherlands, Dordrecht, pp. 279-319.
Schreiber, U., Gademann, R., Ralph, P., Larkum, A., 1997. Assessment of photosynthetic performance of Prochloron in *Lissoclinum patella* in hospite by chlorophyll fluorescence measurements. Plant and Cell Physiology 38(8), 945-951.
Schroeder, M.R., 1965. New method of measuring reverberation time. The Journal of the Acoustical Society of America 37(3), 409-412.
Seaman, R., Finkbeiner, M., Worthy, L.D., 2000. Application of single-beam acoustics to macro-algae bloom management, 1703-1705 pp.
Sharon, Y., Beer, S., 2008. Diurnal movements of chloroplasts in *Halophila stipulacea* and their effect on PAM fluorometric measurements of photosynthetic rates. Aquatic Botany 88(4), 273-276.
Shepherd, S., 2013. Ecology of Australian temperate reefs: the unique South. CSIRO publishing.
Shivji, M.S., 1985. Interactive effects of light and nitrogen on growth and chemical composition of juvenile *Macrocystis pyrifera* (L.) C. Ag.(Phaeophyta) sporophytes. Journal of Experimental Marine Biology and Ecology 89(1), 81-96.
Silva, J., Santos, R., Serôdio, J., Melo, R.A., 1998. Light response curves for *Gelidium sesquipedale* from different depths, determined by two methods: O2 evolution and chlorophyll fluorescence. Journal of Applied Phycology 10(3), 295-301.
Sloane, D., 1991. Some physical properties of dolerite. In: Resources, D.o.M.a.M. (Ed.). Tasmania Department of Resources and Energy, Tasmania.
Smith, G.D., 1985. Numerical solution of partial differential equations: finite difference methods. Oxford university press.
Smith, J.N., Ressler, P.H., Warren, J.D., 2010. Material properties of euphausiids and other zooplankton from the Bering Sea. The Journal of the Acoustical Society of America 128(5), 2664-2680.
Smith, R.G., Wheeler, W.N., Srivastava, L.M., 1983. Seasonal photosynthetic performance of *Macrocystis integrifolia* (Phaeophyceae). Journal of Phycology 19(3), 352-359.
Smith, S., Key, G., 1975. Carbon dioxide and metabolism in marine environments. Limnology and Oceanography 20(3), 493-495.
Spilling, K., Titelman, J., Greve, T., Kühl, M., 2010. Microsensor measurements of the external and internal microenvironment of *Fucus vesiculosus* (Phaeophyceae). Journal of Phycology 46(6), 1350-1355.
Staehr, P.A., Sand-Jensen, K., Raun, A.L., Nilsson, B., Kidmose, J., 2010. Drivers of metabolism and net heterotrophy in contrasting lakes. Limnology and Oceanography 55(2), 817.

Steinberg, P., Kendrick, G., 1999. Kelp Forests. In: Andrew, N. (Ed.), Under Southern Seas. University of New South Wales Press, Sydney. The University of New South Wales Press Ltd, NSW, pp. 50-57.

Steneck, R., Graham, M., Bourque, B., Corbett, D., Erlandson, J., Estes, J., Tegner, M., 2002. Kelp forest ecosystems: biodiversity, stability, resilience and future. Environmental Conservation 29(04), 436-459.

Steneck, R.S., Johnson, C.R., 2013. Dynamic patterns, processes and feedbacks. In: Bertness, M., Bruno, J., Silliman, B., Stachowicz, J. (Eds.), Marine Community Ecology. Sinauer Assoc., pp. 315-336.

Stirbet, A., 2011. On the relation between the Kautsky effect (chlorophyll *a* fluorescence induction) and photosystem II: basics and applications of the OJIP fluorescence transient. Journal of Photochemistry and Photobiology B: Biology 104(1), 236-257.

Suggett, D.J., Oxborough, K., Baker, N.R., MacIntyre, H.L., Kana, T.M., Geider, R.J., 2003. Fast repetition rate and pulse amplitude modulation chlorophyll a fluorescence measurements for assessment of photosynthetic electron transport in marine phytoplankton. European Journal of Phycology 38(4), 371-384.

Suzuki, Y., Yamada, K., Komiyama, H., 1996. Separating biological and physical changes in dissolved oxygen concentration in a coral reef.

Tegner, M., Dayton, P.K., 1987. El Nino effects on southern California kelp forest communities. Advances in Ecological Research 17, 243-279.

Towle, D.W., Pearse, J.S., 1973. Production of the giant kelp, *Macrocystis*, estimated by in situ incorporation of 14C in polyethylene bags. Limnology and Oceanography 18(1), 155-159.

Tu, L.Y., Brennan, J.N., Sauer, J.A., 1955. Dispersion of ultrasonic pulse velocity in cylindrical rods. The Journal of the Acoustical Society of America 27, 550-555.

Tyberghein, L., Verbruggen, H., Pauly, K., Troupin, C., Mineur, F., De Clerck, O., 2012. Bio-ORACLE: a global environmental dataset for marine species distribution modelling. Global Ecology and Biogeography 21(2), 272-281.

Urban, P., Köser, K., Greinert, J., 2017. Processing of multibeam water column image data for automated bubble/seep detection and repeated mapping. Limnology and Oceanography: Methods 15(1), 1-21.

Urick, 1947. A sound velocity method for determining the compressibility of finely divided substances. Journal of Applied Physics 18(11), 983–987.

Van de Bogert, M.C., Carpenter, S.R., Cole, J.J., Pace, M.L., 2007. Assessing pelagic and benthic metabolism using free water measurements. Limnol Oceanogr Methods 5, 145-155.

Van Duin, E., Lijklema, L., 1989. Modelling photosynthesis and oxygen in a shallow, hypertrophic lake. Ecological modelling 45(4), 243-260.

van Rein, H., Brown, C.J., Quinn, R., Breen, J., Schoeman, D., 2011. An evaluation of acoustic seabed classification techniques for marine biotope monitoring over broad-scales (>1 km2) and meso-scales (10 m2–1 km2). Estuarine, Coastal and Shelf Science 93(4), 336-349.

Wanninkhof, R., 1992. Relationship between wind speed and gas exchange over the ocean. Journal of Geophysical Research: Oceans 97(C5), 7373-7382.

Warren, J.D., Smith, J.N., 2007. Density and sound speed of two gelatinous zooplankton: Ctenophore (*Mnemiopsis leidyi*) and lion's mane jellyfish (*Cyanea capillata*). Journal of the Acoustical Society of America 122(1), 574-580.

Wernberg, T., Thomsen, M.S., 2005. The effect of wave exposure on the morphology of *Ecklonia radiata*. Aquatic Botany 83(1), 61-70.

Wernberg, T., Kendrick, G.A., Phillips, J.C., 2003a. Regional differences in kelp-associated algal assemblages on temperate limestone reefs in south-western Australia. Diversity and Distributions 9(6), 427-441.

Wernberg, T., Coleman, M., Fairhead, A., Miller, S., Thomsen, M., 2003b. Morphology of *Ecklonia radiata* (Phaeophyta: Laminarales) along its geographic distribution in south-western Australia and Australasia. Marine Biology 143(1), 47-55.

Wernberg, T., Thomsen, M.S., Tuya, F., Kendrick, G.A., Staehr, P.A., Toohey, B.D., 2010. Decreasing resilience of kelp beds along a latitudinal temperature gradient: potential implications for a warmer future. Ecology Letters 13(6), 685-694.

Wernberg, T., Russell, B.D., Thomsen, M.S., Gurgel, C.F.D., Bradshaw, C.J.A., Poloczanska, E.S., Connell, S.D., 2011. Seaweed communities in retreat from ocean warming. Current Biology 21(21), 1828-1832.

Wernberg, T., Smale, D.A., Tuya, F., Thomsen, M.S., Langlois, T.J., De Bettignies, T., Bennett, S., Rousseaux, C.S., 2013. An extreme climatic event alters marine ecosystem structure in a global biodiversity hotspot. Nature Climate Change 3(1), 78-82.

Wernberg, T., Bennett, S., Babcock, R.C., de Bettignies, T., Cure, K., Depczynski, M., Dufois, F., Fromont, J., Fulton, C.J., Hovey, R.K., 2016. Climate-driven regime shift of a temperate marine ecosystem. Science 353(6295), 169-172.

Westphalen, G., Cheshire, A.C., 1997. Quantum efficiency and photosynthetic production of a temperate turf algal community. Australian Journal of Botany 45(2), 343-349.

Weykam, G., Wiencke, C., 1996. Seasonal photosynthetic performance of the endemic antarctic red alga *Palmaria decipiens* (Reinsch) Ricker. Polar Biology 16(5), 357-361.

Wheeler, W., 1980. Effect of boundary layer transport on the fixation of carbon by the giant kelp *Macrocystis pyrifera*. Marine Biology 56(2), 103-110.

Wheeler, W., Srivastava, L., 1984. Seasonal nitrate physiology of *Macrocystis integrifolia* Bory. J Exp Mar Biol Ecol 76, 35-50.

White, A.J., Critchley, C., 1999. Rapid light curves: a new fluorescence method to assess the state of the photosynthetic apparatus. Photosynthesis research 59(1), 63-72.

Wiebe, P.H., Chu, D.Z., Kaartvedt, S., Hundt, A., Melle, W., Ona, E., Batta-Lona, P., 2010. The acoustic properties of Salpa thompsoni. ICES Journal of Marine Science 67(3), 583-593.

Wilson, C.J., Wilson, P.S., Dunton, K.H., 2013. Assessing the low frequency acoustic characteristics of *Macrocystis pyrifera*, *Egregia menziessi*, and *Laminaria solidungula*. Journal of the Acoustical Society of America 133(6), 3819-3826.

Wilson, C.J., Wilson, P.S., Greene, C.A., Dunton, K.H., 2010. Seagrass leaves in 3-D: Using computed tomography and low-frequency acoustics to investigate the material properties of seagrass tissue. Journal of Experimental Marine Biology and Ecology 395(1-2), 128-134.

Wilson, P.S., Dunton, K.H., 2009. Laboratory investigation of the acoustic response of seagrass tissue in the frequency band 0.5-2.5 kHz. Journal of the Acoustical Society of America 125(4), 1951-1959.

Wood, A.B., 1932. A Textbook of Sound. G. Bell and Sons Ltd, London, England.

Zimmerman, R.C., Kremer, J.N., 1986. *In situ* growth and chemical composition of the giant kelp, *Macrocystis pyrifera*: response to emporal changes in ambient nutrient availability. Marine Ecology Progress Series 27, 277-285.